Journal of Systematic Palaeontology **4** (4): 359–395
doi:10.1017/S1477201906001933 Printed in the United Kingdom

Issued 6 November 2006

A Ceratopsian dinosaur *Psittacosaurus sibiricus* from the Early Cretaceous of West Siberia, Russia and its phylogenetic relationships

Alexander O. Averianov
Zoological Institute, Russian Academy of Sciences, Universitetskaya nab. 1, Saint Petersburg 199034, Russia

Alexei V. Voronkevich
Tomsk State University, Prospekt Lenina 36, Tomsk 634050, Russia

Sergei V. Leshchinskiy
Tomsk State University, Prospekt Lenina 36, Tomsk 634050, Russia

Alexei V. Fayngertz
Tomsk State University, Prospekt Lenina 36, Tomsk 634050, Russia

SYNOPSIS *Psittacosaurus sibiricus* from the Aptian–Albian Ilek Formation at Shestakovo, Kemerovo Province, West Siberia, is represented by two almost complete adult skeletons, several associated groups of bones and numerous isolated bones of individuals ranging from post-hatchling to fully grown animals. *Psittacosaurus sibiricus* differs from nine other species of the genus by a unique combination of 32 diagnostic characters, six of which are autapomorphies of the species: small infratemporal fenestra, anteroposteriorly short premaxilla, short medial process of postorbital, deep cleft for qaudratojugal on jugal, extending to the posterior side of jugal horn, angular with prominent tuber and 23 presacrals. *Psittacosaurus sibiricus* is the sister species of *P. sinensis*, with which it shares the prominent pyramidal laterally projecting jugal horn, but more derived than the latter in having more developed palpebral and postorbital horns. The three lateral foramina on the exoccipital/opisthotic are interpreted as exits for cranial nerves X+XI, XII_{1+2} and XII_3, in contrast with previous interpretations. Cranial nerve IX exits the brain cavity through the metotic fissure. Most *Psittacosaurus* localities are confined to lacustrine deposits and this animal undoubtedly inhabited areas around the great lakes widely distributed in Central Asia during the Early Cretaceous. The age of the *Psittacosaurus* biochron is estimated as Hauterivian–Albian.

KEY WORDS vertebrate palaeontology, Ceratopsia, anatomy, phylogeny

Contents

INTRODUCTION

The archaic ceratopsian *Psittacosaurus* is the most abundant and characteristic member of the Early Cretaceous terrestrial vertebrate faunas of Asia. The genus comprises nine currently recognised species found in Mongolia, China, Russia, Japan and Thailand (Osborn 1923, 1924; Young 1931, 1958; Colbert 1945; Rozhdestvensky 1955*a*, *b*, 1960; Chao 1962; Coombs 1980, 1982; Cheng 1983; Suslov 1983; Sereno & Chao 1988; Sereno *et al.* 1988; Buffetaut *et al.* 1989; Sereno 1990*a*, *b*, 1997, 2000; Manabe & Hasegawa 1991; Buffetaut & Suteethorn 1992, 2002; Russell & Zhao 1996; Xu 1997; Ji & Bo 1998; Voronkevich 1998; Xu & Wang 1998; Alifanov *et al.* 1999; Erickson & Tumanova 2000; Leshchinskiy *et al.* 2000; Brinkman *et al.* 2001; Buffetaut 2001; Mayr *et al.* 2002). It is one of the few dinosaurian genera known from more than 100 skeletons or skeletal fragments (Sereno 1990*b*; Russell & Zhao 1996).

In Russia there are only three *Psittacosaurus* localities: the Barremian–Aptian Mogoito locality in Transbaikalia and the ?Hauterivian–Barremian Bol'shoi Kemchug and Aptian–Albian Shestakovo localities in Western Siberia. Bol'shoi Kemchug is the northernmost record of the genus. In Mogoito, a few isolated psittacosaur teeth were found during screen washing (Averianov & Skutschas 2000; Averianov *et al.* 2003*b*). In Bol'shoi Kemchug a few fragmentary remains of *Psittacosaurus* sp., including teeth, were recently recovered by underwater screening (Leshchinskiy *et al.* 2003; Averianov *et al.* 2003*a*). In Shestakovo, fortunately, *Psittacosaurus* is represented by two reasonably complete skeletons, skeletal fragments and disarticulated bones displaying superb preservation, which provides a rare opportunity to study the skeletal anatomy in detail.

The Shestakovo complex of vertebrate localities, consisting of three sites (Shestakovo 1, 2, and 3; Fig. 1), is located around the Shestakovo settlement in the Chebula District of Kemerovo Province in West Siberia, eastern Russia. Geologist A. A. Mossakovsky found the first psittacosaur remains (a skeletal fragment, PIN 2860/1) at Shestakovo 1 in 1953, at the water level of the Kiya River. Later the same year I. V. Lebedev found a skull and forelimb of another psittacosaur specimen at Shestakovo 1. In 1954 A. K. Rozhdestvensky explored the locality but did not find dinosaur remains, due to the higher water level of the Kiya River that year (Rozhdestvensky 1955*a*, 1960). In the early 1960s the remains of a distinctly larger dinosaur were found at Shestakovo 1 (Bulynnikova & Trushkova 1967), but the fate of this material is unknown. The next palaeontological discoveries at Shestakovo 1 were made only in 1994, when E. N. Maschenko found a tritylodontid tooth and a sauropod phalanx (Tatarinov & Maschenko 1999; Averianov *et al.* 2002). In 1995, he also found a dentary fragment of *Gobiconodon borissiaki* there, the first Mesozoic mammal discovered in Russia (Maschenko & Lopatin 1998). In 1995, V. I. Saev and S. V. Leshchinskiy found localities Shestakovo 2 and 3. Since 1996 the palaeontological team from the Tomsk State University, led by Leshchinskiy, has carried out extensive excavations at Shestakovo 3, producing new articulated specimens of *Psittacosaurus* and other vertebrates (Leshchinskiy *et al.* 1997). In 1997 the palaeontological team from the Moscow Paleontological Institute, led by V. R. Alifanov, found a psittacosaur skeleton at Shestakovo 1, referred to as *P. mongoliensis* by tooth morphology (Alifanov *et al.* 1999). Alifanov *et al.* (1999) also noted the presence of another psittacosaur species, similar in its tooth morphology to *P. xinjiangensis*, at Shestakovo 3 (based on materials from the Tomsk collection). *Psittacosaurus* material from Shestakovo, housed in the Moscow Paleontological Institute, remain unpublished. The Tomsk *Psittacosaurus* collection was treated in a preliminary note by A. V. Voronkevich (1998),

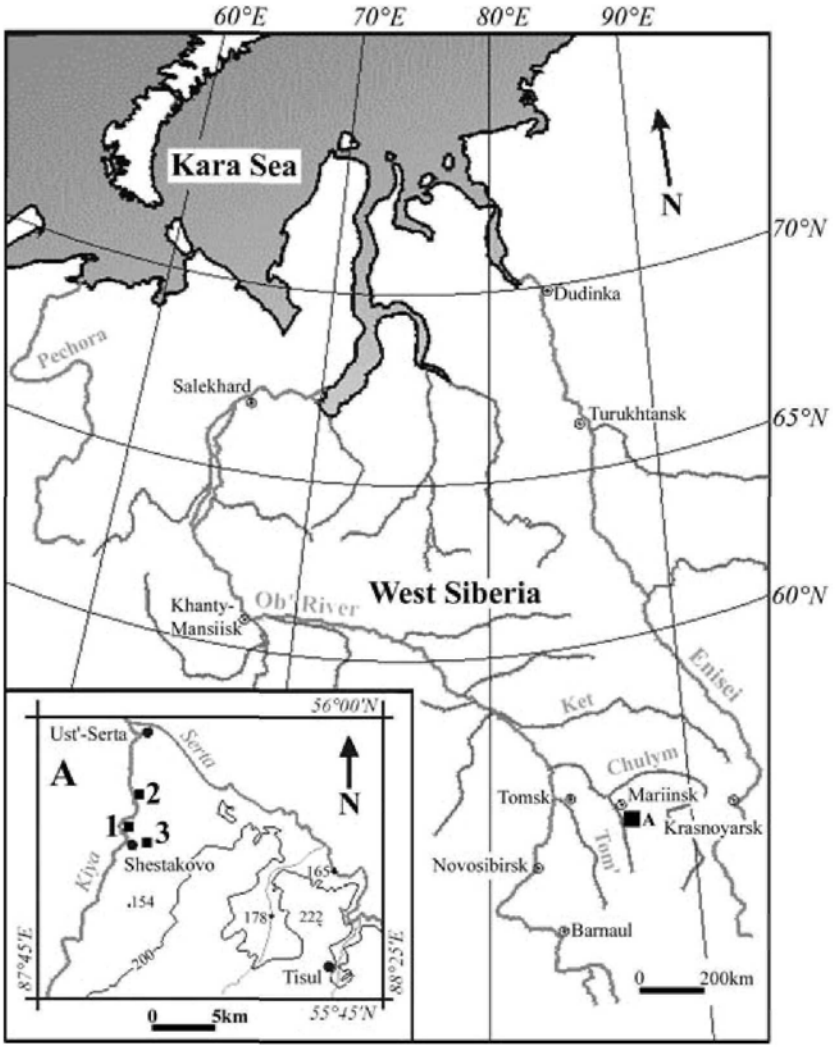

Figure 1 Geographical position of Shestakovo (A) and (inset) the localities Shestakovo 1 (N 55° 54′, E 87° 56′), Shestakovo 2 (N 55° 56′, E 87° 59′) and Shestakovo 3 (N 55° 53′, E 87° 59′).

who noted the relatively large size of the Shestakovo psittacosaur, referred to as *Psittacosaurus* aff. *mongoliensis*.

Our investigation of all the Tomsk psittacosaur material led us to the conclusion that there is only one psittacosaur species in the Shestakovo sites, ultimately described as *Psittacosaurus sibiricus* Voronkevich & Averianov, 2000 (Leshchinskiy *et al.* 2000). The PIN 2860/1 specimen is about half the size of the holotype of *P. sibiricus* and, apparently, lacks some features (e.g. well developed jugal, postorbital and palpebral horns), characteristic of the fully-grown individuals. This specimen was also considered to be subadult by Sereno (1990*a*: 203). This may explain earlier identifications of the Shestakovo psittacosaur as *P. mongoliensis*.

The Shestakovo vertebrate fauna consists of some 25 taxa (Table 1) and is the most important Mesozoic vertebrate locality in Siberia. Two *Gobiconodon* species found at Shestakovo are also known from the Aptian–Albian Khoboor fauna of Mongolia (Kielan-Jaworowska *et al.* 2000 and references therein). This and other geological and palaeontological data discussed by Leshchinskiy *et al.* (2000, 2001), indicate that the age of the Shestakovo fauna is Aptian–Albian, more probably Albian.

Up to now, very little has been published on Siberian *Psittacosaurus*. Unfamiliarity by western authors with the Russian literature and geography led to two mistakes surrounding these findings. Firstly, the Shestakovo locality was often erroneously placed in 'Gorno-Altayaskaya [=Altaiskaya] Avtonomnaya Oblast' (Weishampel 1990: 104, fig. 3.21 and some subsequent authors), instead of Kemerovo Province. Secondly, almost universally the paper by Rozhdestvensky (1955*b*) was cited in reference to the Siberian *Psittacosaurus*. In fact, this paper only marginally mentioned it and is devoted to description of *P. mongoliensis* from the Ulan Osh locality in Mongolia.

The aim of this paper is to give a full description of *P. sibiricus* and to determine its phylogenetic position within the genus.

Institutional abbreviations

AMNH, American Museum of Natural History, New York, USA; **PIN**, Paleontological Institute, Russian Academy of Sciences, Moscow, Russia; **PM TGU**, Paleontological Museum, Tomsk State University, Tomsk, Russia.

Table 1 Vertebrates from Shestakovo localities 1 and 3.

Osteichthyes	Palaeonisciformes indet.
	Sinamiidae indet.
Amphibia: Caudata	*Kiyatriton leshchinskiyi*
Testudinata: Macrobaeinidae	*Kirgizemys* sp.
Squamata:Gekkota	*Kiyasaura oblongata*
Scincomorpha, Paramacellodidae	*Ilekia sibirica*
	Saurillodon tschebulensis
Anguimorpha: Xenosauridae	*Shestakovia voronkevichi*
Crocodylomorpha: Protosuchia	*Tagarosuchus kulemzini*
Shartegosuchidae	*Kyasuchus saevi*
Pterosauria	Pterodactyloidea indet.
Dinosauria: Theropoda	Troodontidae indet.
	Dromaeosauridae indet.
Sauropoda	Titanosauriformes indet.
Stegosauria	Stegosauridae indet.
Ornithopoda	Hypsilophodontidae indet.
Ceratopsia	*Psittacosaurus sibiricus*
Aves	Aves indet.
Therapsida	*Xenocretosuchus sibiricus*
Mammalia: 'Triconodonta'	Amphilestinae gen. et sp. nov.
	Gobiconodon borissiaki
	Gobiconodon hoburensis
	Gobiconodon sp. nov.
Docodonta	*Sibirotherium rossicus*
'Symmetrodonta'	*Yermakia domitor*
Peramura	*Kiyatherium cardiodens*

Anatomical abbreviations

ac, acetabulum; **acn**, anterior condyle; **ap**, anterior process; **AS**, astragalus; **at**, angular tuber; **atr**, anterior trochanter; **BO**, basioccipital; **bof**, facet for basioccipital; **bpt**, basipterygoid process of basisphenoid; **bptf**, facet for basipterygoid process of basisphenoid; **BS**, basisphenoid; **bt**, basal tuber; **c**, canal; **CA**, calcaneum; **ca1–ca4**, caudals 1–4; **cap**, capitulum; **cc**, cnemial crest; **cf**, head of femur; **ch**, head of humerus; **clf**, facet for clavicle; **cof**, facet for coracoid; **cofor**, coracoid foramen; **cop**, coronoid process; **cri**, crista interfenestralis; **D**, dentary; **di**, diapophysis; **dp**, dorsal process; **dpc**, deltopectoral crest; **dph**, dorsal postorbital horn; **EX**, exoccipital/opisthotic; **exf**, facet for exoccipital/opisthotic; **f**, foramen; **fgr**, flexor groove; **FI**, fibula; **fm**, foramen magnum; **fo**, fenestra ovalis; **ftr**, fourth trochanter; **gl**, glenoid; **gtr**, greater trochanter; **ica**, opening for internal carotid artery; **ins**, internasal suture; **ilpd**, iliac peduncle; **ispd**, ischiadic peduncle; **itf**, infratemporal fenestra; **iptf**, interpterygoid facet; **J**, jugal; **jf**, facet for jugal; **jh**, jugal horn; **lc**, lateral condyle; **lp**, lateral process; **lvs**, diverticulum for longitudinal venous sinus; **mc**, medial condyle; **mcI–mcIV**, metacarpals I–IV; **mcl**, median cleft; **mdt**, medial distal tarsal; **mf**, metotic fissure; **mp**, medial process; **mph**, middle postorbital horn; **mr**, mandibular ramus of pterygoid; **ms**, mandibular symphysis; **mst**, metotic strut; **mtI–mtV**, metatarsals I–V; **mxf**, facet for maxilla; **mxr**, maxillary recess; **N**, nasal; **nf**, facet for nasal; **no**, nasal opening; **ns**, neural spine; **oc**, occipital condyle; **of**, obturator foramen; **or**, orbit; **P**, parietal; **pa**, parapophysis; **palp**, palatal process; **pap**, paraoccipital process; **parf**, facet for paroccipital process of exoccipital/opisthotic; **pc**, posterior condyle; **PD**, predentary; **pdf**, facet for predentary; **pf**, pituitary fossa; **plf**, facet for palatine; **plr**, palatine ramus of pterygoid; **plp**, posterolateral process; **PM**, premaxilla; **pmf**, facet for premaxilla; **pmp**, posteromedial process; **PO**, postorbital; **pp**, posterior process; **ppd**, pubic peduncle; **pph**, palpebral horn; **ppmg**, groove for posterior process of maxilla; **ppr**, postpubic rod; **pr**, parasphenoid rostrum; **prf**, facet for prootic; **prap**, preacetabular process; **PRO**, prootic; **prp**, prepubic process; **prz**, prezygapophysis; **PT**, pterygoid; **ptap**, postacetabular process; **ptf**, facet for pterygoid; **ptr**, pterygoid ramus of quadrate; **ptz**, postzygapophysis; **qc**, quadrate condyle; **qf**, facet for quadrate; **qh**, quadrate head; **QJ**, quadratojugal; **qjf**, facet for quadratojugal; **qr**, quadrate ramus of pterygoid; **qs**, quadrate shaft; **R**, rostral; **replf**, replacement foramina; **rf**, facet for rostral; **rt**, replacing tooth; **rvp**, rostroventral process; **s1–s6**, sacrals 1–6; **sc**, sagittal crest; **scf**, facet for scapula; **SO**, supraoccipital; **spf**, splenial facet; **SQ**, squamosal; **sqg**, groove for squamosal; **sr**, sacral rib; **stf**, supratemporal fenestra; **TI**, tibia; **tub**, tuberculum; **vcl**, opening for lateral head vein; **vf**, ventral flange; **vp**, ventral process; **vpl**, ventral plate; **vph**, ventral postorbital horn; **VII**, opening for facial cranial nerve; **IX**, opening for glossopharyngeal cranial nerve; **X**, opening for vagus cranial nerve; **XI**, opening for accessorius cranial nerve; **XII**, opening for hypoglossal cranial nerve.

SYSTEMATIC PALAEONTOLOGY

ORNITHISCHIA Seeley, 1888

CERATOPSIA Marsh, 1890

PSITTACOSAURIDAE Osborn, 1923

PSITTACOSAURUS Osborn, 1923

Psittacosaurus sibiricus Voronkevich & Averianov *in* Leshchinskiy *et al.* 2000 (Figs 2–23, 24D)

1955*b* *Psittacosaurus* [sp.] Rozhdestvensky: 118.
1960 *Psittacosaurus* [sp.] Rozhdestvensky: 165.
1967 *Psittacosaurus* [sp.] Rozhdestvensky & Khozatsky: 84.
1973 *Psittacosaurus mongoliensis* Rozhdestvensky: 96.
1974 *Psittacosaurus mongoliensis* Rozhdestvensky: 122.
1977 *Psittacosaurus mongoliensis* Rozhdestvensky: 106.
1995 *Psittacosaurus mongoliensis* Nessov: 87.
1998 *Psittacosaurus* aff. *mongoliensis* Voronkevich: 191, figs 2–4.
1999 *Psittacosaurus mongoliensis* Alifanov *et al.*: 492.
1999 [cf.] *Psittacosaurus xinjiangensis* Alifanov *et al.*: 492.
2000 *Psittacosaurus sibiricus*: Leshchinskiy *et al.*: 364, fig. 3.

TYPES. Holotype PM TGU 16/4-20, an articulated almost complete adult skeleton including the skull.

TYPE LOCALITY AND HORIZON. Shestakovo 3, approximately 40 km south of Mariinsk city, Chebula District, Kemerovo Province, Russia; Ilek Formation, Lower Cretaceous, Aptian–Albian.

DIAGNOSIS. The species can be diagnosed by a combination of the following primitive (−), derived (+) and uncertain

polarity (?) characters (the polarity of the characters is determined according to comparison with outgroups as defined in the phylogenetic analysis section, below): 1, skull rectangular in lateral view, with vertical anterior face (?); 2, skull width exceeds skull length (+); 3, jugal, palpebral and postorbital horns well developed in adults (+; possible sexually correlated character); 4, maximum height of infratemporal fenestra 25% of skull length (+); 5, posterior part of skull not lower than preorbital region (?); 6, premaxilla–jugal contact present (+); 7, premaxilla maximum length to height ratio less than 60% (+); 8, ventral margin of premaxilla–maxilla contact straight (?); 9, 'maxillary process' of maxilla lacking (−); 10, secondary maxillary depression lacking (+); 11, postorbital bar vertical (?); 12, postorbital with short medial process, having no contribution to the orbit margin (+); 13, postorbital with ventral horn (+); 14, squamosal with anterior ramus extending anteriorly to anterior end of supratemporal fossa (−); 15, jugal with deep cleft for quadratojugal extending to posterior face of jugal horn (+); 16, palpebral with medial edge subequal in length to anterior edge (+); 17, quadrate shaft with deeply excavated posterior margin (+); 18, external mandibular fenestra absent (+); 19, ventral flange of mandible present (+); 20, mandibular ventral flange expands considerably on to angular (+); 21, angular with prominent angular tuber (+); 22, maxillary and dentary tooth rows laterally concave (−); 23, primary ridge on maxillary teeth weakly developed (−); 24, denticle number on maxillary teeth less than 14 (−); 25, 23 presacrals (+); 26, nine cervicals (+); 27, ossified epaxial tendons extend posteriorly to the anterior caudals in adults (+; ontogenetically controlled character); 28, scapula with prominent acromion (+); 29, scapula with distally expanded scapular blade (+); 30, coracoid with flat ventral edge (?); 31, ischium longer than femur (−); 32, ischium with distal end unexpanded (−); 33, metatarsal I is about 70% of metatarsal III length (?).

DIFFERENTIAL DIAGNOSIS. Characters 4, 7, 12, 15, 21 and 25 are autapomorphies of *P. sibiricus*. In addition, *P. sibiricus* differs from *P. mongoliensis* Osborn, 1923 in characters 2, 3, 6, 8–11, 13, 17, 18, 22, 26, 30 and 31; from *P. xinjiangensis* Sereno & Chao, 1988 in characters 9, 13, 16, 17, 22, 24, and 27; from *P. meileyingensis* Sereno, Chao, Cheng & Rao, 1988 in characters 1–3, 5, 6, 8, 9, 13, 16, 18, 20, 23, 27 and 30; from *P. neimongoliensis* Russell & Zhao, 1996 in characters 1–3, 6, 13, 14, 17, 19, 20, 26 and 32; from *P. ordosensis* Russell & Zhao, 1996 in characters 1, 8, 17, 18 and 22; from *P. sinensis* Young, 1958 in characters 1, 5, 8, 11, 16, 19, 20, 27–31 and 33; from *P. mazongshanensis* Xu, 1997 in characters 2, 6, 9, 11, 13, 17 and 22–24; and from *P. sattayaraki* Buffetaut & Suteethorn, 1992 in character 22.

REMARKS. *Psittacosaurus sibiricus* is one of the largest species of the genus with a skull length of ~21 cm and a skeletal length of 170–185 cm in adults.

Sereno (2000: 492) considered *P. sattayaraki* as Ceratopsia *incertae sedis*, not belonging to *Psittacosaurus*, and *P. mazongshanensis* as a *nomen dubium*, questioning the bulbous nature of the primary ridge in the teeth of *P. sattayaraki*. However, more detailed figures of its teeth (Buffetaut & Suteethorn 2002: fig. 1) clearly show a bulbous primary ridge typical for psittacosaurs, a symmetrical crown and lack of a basal cingulid. In neoceratopsians from the Early Cretaceous of North America (e.g. Chinnery *et al.* 1998: figs 1–3) the crown is asymmetrical, with the primary ridge shifted to one side and with depressed crown areas between the primary ridge and basal cingulum. In the oldest neoceratopsian, *Liaoceratops*, from the Early Cretaceous of China (Xu *et al.* 2002) there is no basal cingulum, but the primary ridge is offset. Sereno (2000: 492) also cited the low position of the predentary attachment surface (on the lateral side of the dentary) relative to the tooth row as an unusual feature of *P. sattayaraki*. On isolated dentaries of *Psittacosaurus* (e.g. Osborn 1923: fig. 4A and below) the predentary attachment surface on the lateral side is very smooth and does not differ from the rest of the dentary in sculpture. In basal neoceratopsians this attachment surface bears characteristic ornamentation of longitudinal undulating very faint ridges (e.g. Ryan & Currie 1998: fig. 3A and *Asiaceratops salsopaludalis* Nessov & Kaznyshkina, 1989). Although *P. sattayaraki* is similar to basal neoceratopsians in having at least a partially sculptured lateral predentary attachment surface, it lacks the deep socket-like articulation for the lateral process of the predentary on the dorsal side of the dentary, seen in some basal neoceratopsians. We consider *P. sattayaraki* to be a valid species. It differs from *P. sibiricus* in the straight (mediolaterally) dentary tooth row, greatly convex (dorsoventrally) upper margin of the dentary and less developed mandibular ventral flange.

Although only a preliminary description of *P. mazongshanensis* has been published, it is certainly a distinct taxon which differs from other species, including *P. sibiricus*, in its proportionately longer rostral region and Y-shaped lower jaw with anterior and posterior parts of the mandibular symphysis almost equal in transverse width. *Psittacosaurus mazongshanensis*, in addition, differs from *P. sibiricus* in having bulbous primary ridges on its maxillary teeth and prominent 'maxillary process' on the maxilla.

REFERRED SPECIMENS. See Appendix 1 for the list of referred specimens.

OSTEOLOGICAL DESCRIPTION

Skull

The skull of *P. sibiricus* is large (the length is ~21 cm in adult individuals: Table 2), subrectangular in profile, relatively lower than in *P. meileyingensis* and intermediate in proportions between *P. mongoliensis* and *P. sinensis*, more approximating the latter in its very well developed jugal horns (Fig. 2). The palpebral and two smaller dorsal postorbital horns are better developed than in any other psittacosaur species. The skull roof is almost flat (concave at the middle) and the parrot-like rostrum has an almost vertical anterior face, forming a nearly right angle between the anterior and dorsal skull surfaces. The infratemporal fenestra is distinctly smaller than in other psittacosaurs (its maximum height is 25% of the skull length, 31–38% in other species). The orbit is more oval-shaped (more subtriangular in other species), horizontally orientated, with gentle dorsal and ventral arcs. No sclerotic ossifications are preserved within the orbit. The posterodorsal corner of the skull in lateral view is relatively elevated, level with or higher than the preorbital region (as

Table 2 Measurements of PM TGU 16/4-20, the holotype of *Psittacosaurus sibiricus*.

Skull
Skull, length, premaxilla to quadratomandibular articulation = 207 mm
External naris, maximum diameter = 22 mm
Orbit, width = 55 mm
Orbit, height = 34 mm
Infratemporal fenestra, width = 40 mm
Infratemporal fenestra, height = 52 mm
Preorbital skull, length = 70 mm
Lower jaw, length = 201 mm
Quadrate, height = 72 mm

Axial skeleton
Cervicals, length = 234 mm
Dorsals, length = 338 mm
Sacrals, length = 171 mm
Caudals, length = 903 mm

Appendicular skeleton
Scapula, distal width = 80 mm
Radius, length = 106 mm
Ulna, length = 123 mm
Metacarpal II, length = 31 mm
Metacarpal III, length = 36 mm
Metacarpal IV, length = 25 mm
Phalanx II-1, length = 16 mm
Phalanx II-2, length = 11 mm
Phalanx II-3, length = 14 mm
Phalanx III-1, length = 14 mm
Phalanx III-2, length = 10 mm
Phalanx III-3, length = 9 mm
Phalanx III-4, length = 15
Ilium, length = 270 mm
Ilium, anterior end to middle of acetabulum = 125 mm
Ilium, middle of acetabulum to posterior end = 145
Ilium, height above acetabulum = 34 mm
Femur, length = 223 mm
Femur, proximal end to fourth trochanter = 109 mm
Tibia–astragalus, length = 205 mm
Metatarsal I, length = 69 mm
Metatarsal II, length = 94 mm
Metatarsal III, length = 95 mm
Metatarsal IV, length = 83 mm
Phalanx I-1, length = 30 mm
Phalanx I-2, length = 29 mm
Phalanx II-2, length = 24 mm
Phalanx II-3, length = 32 mm
Phalanx III-1, length = 24 mm
Phalanx III-2, length = 22 mm
Phalanx III-3, length = 20 mm
Phalanx III-4, length = 33 mm
Phalanx IV-1, length = 24 mm
Phalanx IV-2, length = 19 mm
Phalanx IV-3, length = 18 mm
Phalanx IV-4, length = 13 mm†
Phalanx IV-5, length = 28 mm†

†Measured on imprints.

in *P. mongoliensis*, depressed in *P. sinensis* and *P. meileyingensis*); the squamosal is positioned level with the top of the postorbital. In dorsal view the difference in width between the preorbital and postorbital segments is less marked compared with other psittacosaurs, because of the more obtuse rostrum (Figs 2C, D).

Dermal skull roof

The rostral is preserved in the holotype, in PM TGU 16/4-21 and as a ventral portion of one isolated bone (Figs 2A, B & 3A–C). It is a tall bone forming about a half of the rostrum height. The rostral is broad ventrally and tapers dorsally; the dorsal portion is slightly wedged between the ventral tips of the nasals. The bone surface is relatively smooth, with few pits and grooves.

The nasal (Figs 2A, B & 3D, E) consists of three parts, the dorsal, rostroventral and lateral processes. The rostroventral process is a thin, rod-like, vertically orientated structure, lying in front of the rostrum and contacting the rostral ventrally. It forms the entire anterior rim of the naris. On the posterolateral side of its distal edge there is a facet for the premaxilla. The lateral process is a short thin plate, which borders most of the posterior side of the nasal opening. The lateral process would be at least partially covered by the premaxilla from the lateral side. The dorsal process is deflected posteromedially at ~130° to the rest of the bone. It is a thin plate tapering posteriorly, which forms an anterior portion of the dorsal skull roof. The nasal–prefrontal and nasal–frontal contacts are hardly detected on the holotype skull and are not preserved in PM TGU 16/1-294, but appear similar to other psittacosaurs in position. The internasal suture occupies about half of the length of the nasals and apparently dorsally and ventrally the nasals were separated by wedged frontals and the rostral. The nasal opening is oval in shape, with its long axis vertically orientated and placed between the nasal and the premaxilla at the top of the latter.

The premaxilla is known in the two skulls and from four disarticulated specimens (Figs 2A, B, 3F-M); it is relatively shorter anteroposteriorly than in other species, with a relatively unexpanded posterolateral process. As in other psittacosaurs, the premaxilla contacts the rostral, nasal, prefrontal, lacrimal and maxilla. The premaxilla–jugal contact (a diagnostic character of *P. sinensis*) is not visible in the skulls, because both specimens represent aged animals with the majority of sutures obliterated. However, two associated blocks of premaxilla and maxilla (PM TGU 16/1-46–16/1-73 and PM TGU 16/1-204–16/1-206: Fig. 3L) show that the premaxilla considerably overhangs the maxilla dorsally, which undoubtedly eliminates the possibility of a maxilla–lacrimal contact. The maxillary suture is present in PM TGU 16/1-204 and 16/1-46 (Figs 3I, L & M); it is orientated nearly subparallel to the nasal suture. A horny bill covered only the anteroventral portion of the premaxilla and, possibly, only the most anterior portion of the maxilla. Sculptured rugose surfaces mark the horny sheath area (Figs 3I, L & M) and have a similar distribution to those in *P. mongoliensis* (Sereno *et al.* 1988: fig. 5). At the premaxilla–rostral contact there is a small depression leading to a short canal, possibly for a blood vessel (Fig. 3M). A similar depression is seen in *P. meileyingensis* (Sereno *et al.* 1988: fig. 2A), but apparently not in other species. From the medial side of the premaxilla there is a short subhorizontal process, lying approximately level with the rostral–nasal contact (Figs 3G, H, J & K). This process contacts the anterior process of the maxilla and corresponds to the palatal process (=ventral

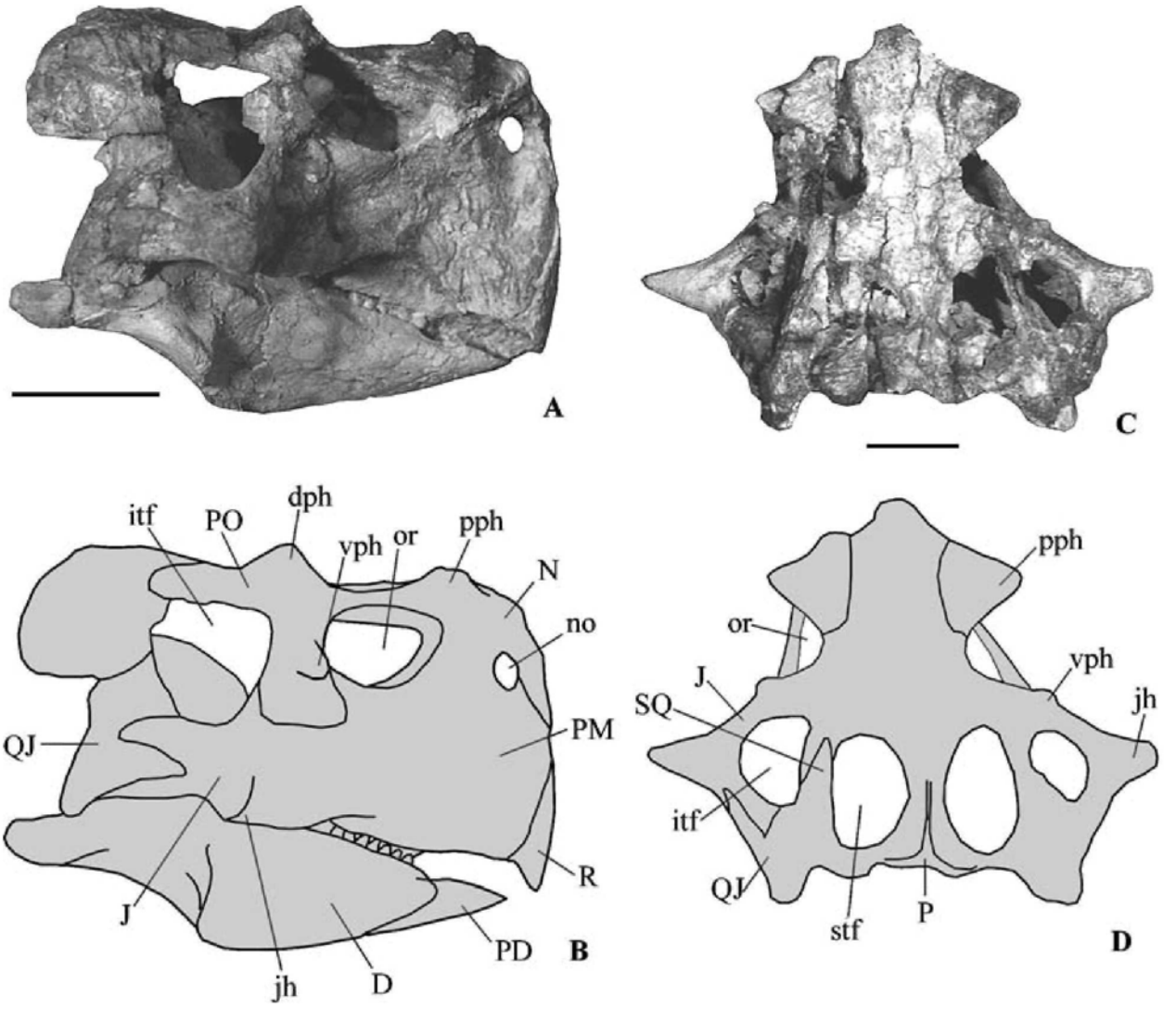

Figure 2 *Psittacosaurus sibiricus*, PM TGU 16/4-20, holotype, skull in lateral (**A, B**) and dorsal (**C, D**) views. See the text for abbreviations. Scale bar = 5 cm.

sheet) of the premaxilla in other ornithischians. Medially the palatal process apparently contacted the corresponding structure on the opposite premaxilla and roofed a strongly vaulted premaxillary palatal surface. In psittacosaurs and other marginocephalians the palatal process of the premaxilla does not contact the vomer and does not participate in the formation of the internal naris margin (Sereno 1990*b*). The premaxilla is thickest anteriorly, above the medial process. The ventral margin of the premaxilla and maxilla is almost straight at their junction, not deeply incised as in *P. sinensis* and *P. meileyingensis* (Chao 1962: fig. 1; Sereno *et al.* 1988: figs 1A & D). At the anterodorsal corner of PM TGU 16/1-204 the ventral border of the nasal opening is preserved (Figs 3I, J & L).

The maxilla (Figs 3L & 4) is a stout vertically orientated bone with four processes, bearing nine tooth positions (possibly the maximum maxillary tooth count reached). The lateral maxillary surface is subdivided by a horizontal semicircular rim, projecting posteriorly into the relatively long posterior process. There is no protuberance ('maxillary process' of Sereno *et al.* 1988) on this rim, characteristic for *P. mongoliensis*, *P. xinjiangensis* and, especially, for *P. mazongshanensis* and *P. meileyingensis* (Sereno *et al.* 1988: figs 2A & 5). Immediately below this rim, there are five foramina, two of which (the fourth and fifth from the anterior) are confluent and lead to a maxillary recess between the posterior process and the main body of the maxilla (Fig. 4A). Medial to this recess, the maxilla contacts the palatine (Fig. 4B), so this recess corresponds to the extensive opening between the maxilla and palatine in basal neoceratopsians and *Psittacosaurus* described by Osmólska (1986: 152). This recess is possibly homologous with the 'intermaxillary sinus' of basal neoceratospians (Osmólska 1986; and see Discussion, below). The tooth row is slightly concave laterally and inset from the lateral surface of the maxilla by a labial emargination. On the medial side, dorsal to the tooth row, there is a row of replacement foramina. A posteromedial process, projecting posteromedially posterior to the tooth row, is short, but possibly not complete in PM TGU 16/1-73 (and broken in other specimens). The dorsal process is a thin plate,

Figure 3 *Psittacosaurus sibiricus*. **A–C**, PM TGU 16/1-216, ventral portion of rostral in anterior (**A**), lateral (**B**) and ventral (**C**) views; **D**, **E**, PM TGU 16/1-294, right nasal in lateral (**D**) and ventromedial (**E**) views; **F–H**, PM TGU 16/1-133, juvenile right premaxilla in lateral (**F**), anterodorsal (**G**) and medial (**H**) views; **I–K**, PM TGU 16/1-204, right premaxilla, in lateral (**I**), medial (**J**) and anterodorsal (**K**) views; **L**, PM TGU 16/1-206, right maxilla with missing anteroventral portion and PM TGU 16/1-204, right premaxilla of the same individual in anatomical position, lateral view; **M**, PM TGU 16/1-46, right premaxilla in lateral view; **N**, **O**, PM TGU 16/1-135, juvenile right quadrate in anterior (**N**) and medial (**O**) views. See the text for abbreviations. Scale bars = 1 cm.

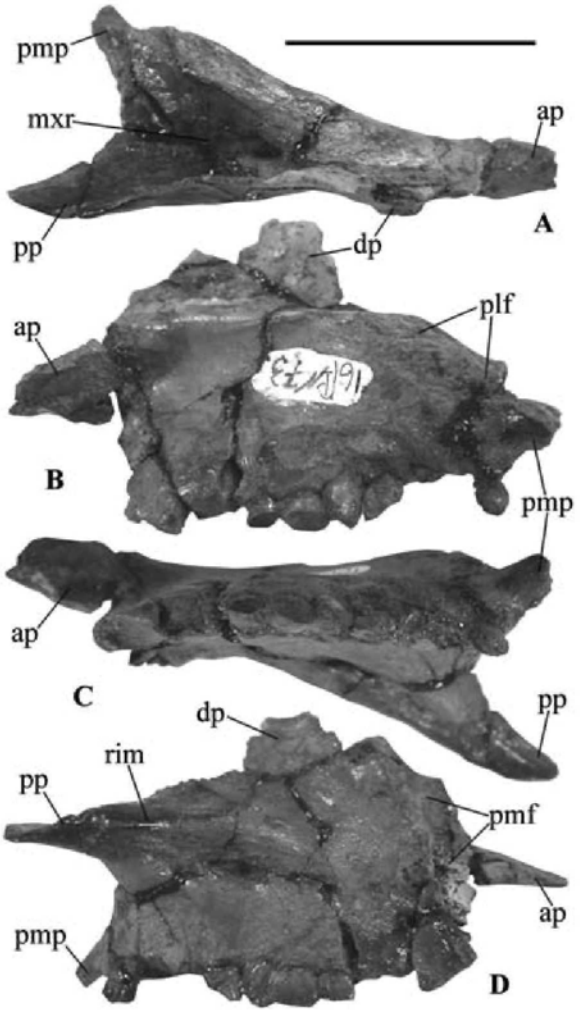

Figure 4 *Psittacosaurus sibiricus*, PM TGU 16/1-73, right maxilla in dorsal (**A**), medial (**B**), ventral (**C**) and lateral (**D**) views. See the text for abbreviations. Scale bar = 3 cm.

directed dorsally and, apparently, did not contact the lacrimal (its dorsal tip is incomplete in all specimens but was apparently overhung by the premaxilla). The secondary maxillary depression (='antorbital fossa' in some previous descriptions; see Discussion, below) is indistinct in all isolated specimens, as in *P. sinensis*. In the holotype, representing a somewhat older individual, the secondary maxillary depression is also lacking, but its place is occupied by a noticeable rugosity, formed by small tubercles, possibly indicating a muscle attachment. The anterior process is a subhorizontal lamina, contacting the palatal process of the premaxilla (and possibly the vomer: Sereno *et al.* 1988: 372). On the anterior part of the maxillary lateral surface there is a distinct subvertical ridge, marking the posterior margin of the premaxilla articular surface. The posterior process is likely to be relatively longer than in other psittacosaur species, but in most published figures it is obscured by the overhanging jugal and its exact length is difficult to estimate. Its dorsal surface bears a distinct groove for reception of the jugal ventral margin and its medial edge fits into a deep groove on the lateral process of the ectopterygoid.

The lacrimal cannot be distinguished in the skulls and is not present among the isolated bones. Similarly, the lacrimal canal cannot be detected on the skulls. Apparently, the walls of the lacrimal canal were fully ossified in contrast to other psittacosaur species (Sereno 2000).

The prefrontal, exposed on the dorsal cranial surface, is a rather narrow bone surrounding the big palpebral horn. The prefrontal is dorsally flat and lacking the raised lateral edge characteristic of *P. mongoliensis*.

The frontal can be confidently delimited on the holotype, except for its contact with the postorbital. The anterior portion of the frontal is wedged between the nasals. The frontal, as in the majority of psittacosaurs and in contrast to *P. sinensis* (Sereno *et al.* 1988: 370) does not participate in the formation of the supratemporal fenestra.

The parietal (Figs 2D & 5A) is relatively long, some 36% of the dorsal skull length (~37% in *P. mongoliensis*, ~35% in *P. neimongoliensis*, ~32% in *P. sinensis* and ~25% in *P. meileyingensis*). The sagittal crest is low but distinct. The parietal frill is relatively long, about 30–35 mm in length (15–18% of the skull length, ~11% in *P. meileyingensis*: Sereno *et al.* 1988: 370), incised posterior to the sagittal crest and overhanging the occiput as a horizontal shelf, as in *P. mongoliensis* and *P. sinensis* and in contrast to *P. meileyingensis* (Sereno *et al.* 1988).

The postorbital (Figs 2 & 5B–H) in *P. sibiricus* differs in a number of details from that bone in some other psittacosaur species. Firstly, its posterior and ventral processes are set at almost a right angle, ~95° (as in *P. meileyingensis*; ~110° in *P. mongoliensis* and *P. sinensis*), giving a more vertical orientation to the postorbital bar. Secondly, the medial process is very abbreviated, its insertion into the frontal is very limited, its contribution to the dorsal margin of the orbit is almost lacking and it is transformed into a dorsal horn, projecting dorsally beyond the skull roof. Thirdly, the ventral portion of the postorbital body projects as a horn-like structure, directed ventrolaterally (ventral postorbital horn). The lateral surface of the central body of the postorbital bears only a very small, horn-like rugosity in its dorsal portion (middle postorbital horn, somewhat better developed in the holotype and in PM TGU 16/1-58: Figs 5G & H). The specimen PM TGU 16/1-166 belongs to a somewhat larger individual than the holotype and it bears a more developed dorsal horn (Figs 5B–F), directed anteriorly and having deep grooves on the anterior surface and a marked rugosity on the medial surface. In total, the postorbital bears three horns, consisting of well-developed ventral and dorsal horns and a much smaller middle horn. In *P. sinensis* there is a distinct ventral horn (='a prominent tuber' of Sereno *et al.* 1988: 371) and a weaker dorsal horn on the postorbital. The ventral horn on the postorbital is a very distinctive feature of *P. sibiricus*, present even on the smallest postorbital in the collection (PM TGU 16/0-10). Psittacosaur species other than *P. sinensis* and *P. sibiricus* lack postorbital horns altogether (the postorbital is not known for *Psittacosaurus* sp. from Yixian Formation and *P. ordosensis*), but have a rugosity or low ridge approximately in the place of the intermediate horn of *P. sibiricus* (Sereno *et al.* 1988: 370). The posterior process is transversely thin, tapers posteriorly and bears a distinct groove for the squamosal along its dorsal side (Fig. 5B). The distal end of the ventral process is slightly anteroposteriorly expanded and is very thin, as in other psittacosaurs. On the posterior surface of the postorbital bar, there is a deep triangular

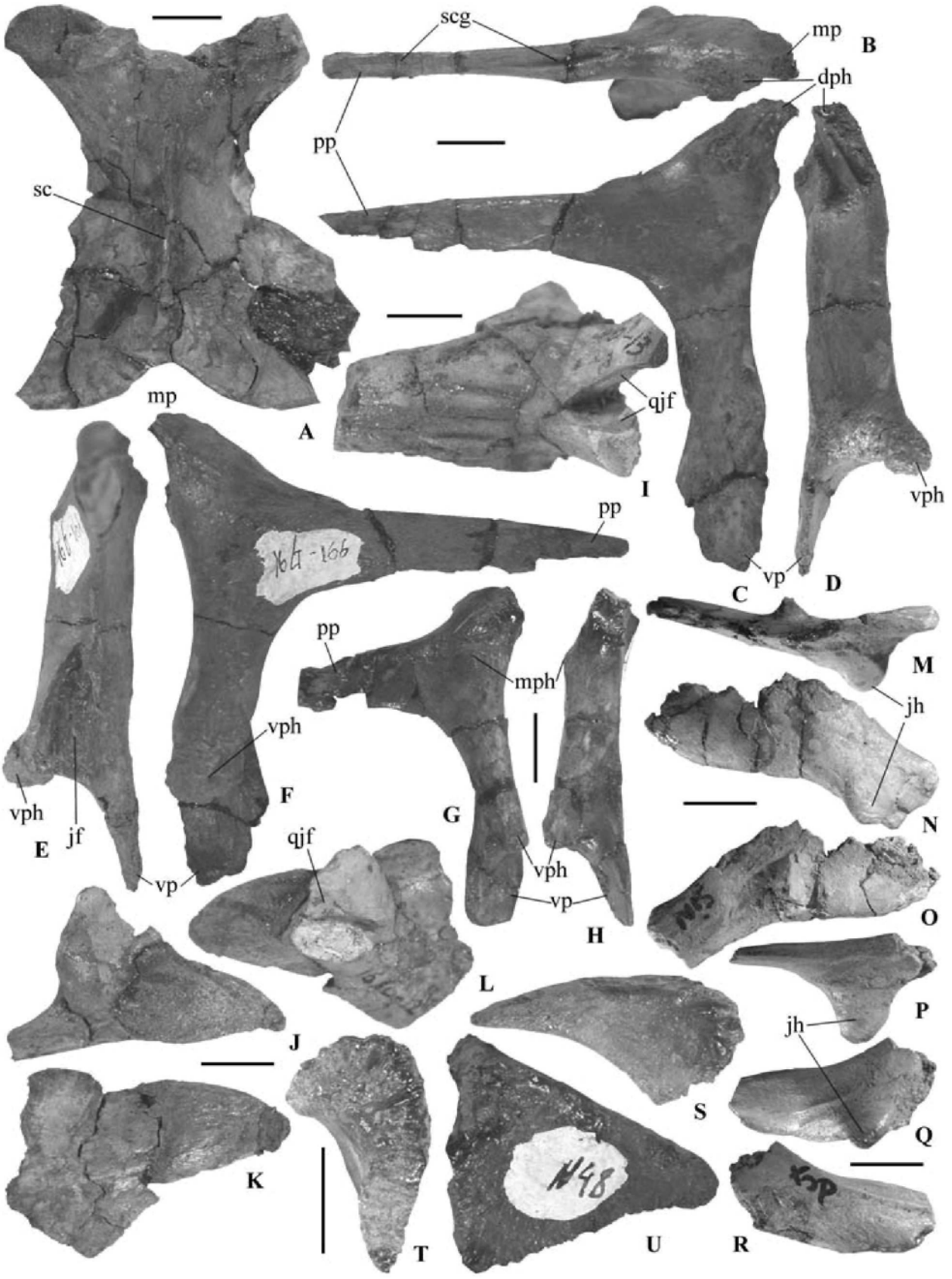

Figure 5 *Psittacosaurus sibiricus*: **A**, PM TGU 16/1-283, fused incomplete parietals in dorsal view; **B–F**, PM TGU 16/1-166, left postorbital in dorsal (**B**), medial (**C**), anterior (**D**), posterior (**E**) and lateral (**F**) views; **G**, **H**, PM TGU 16/1-58, right postorbital in lateral (**G**) and anterior (**H**) views; **I**, PM TGU 16/0-13, left jugal horn in posterior view; **J–L**, PM TGU 16/0-12, left jugal horn in dorsal (**J**), anterior (**K**) and posterior (**L**) views; **M–O**, PM TGU 16/1-292, juvenile left jugal lacking posterior end in dorsal (**M**), lateral (**N**) and medial (**O**) views; **P–R**, PM TGU 16/1-293, posterior end of juvenile right jugal in dorsal (**P**), lateral (**Q**) and medial (**R**) vies; **S–U**, PM TGU 16/1-48, right palpebral in anterior (**S**), medial (**T**) and dorsal (**U**) views. See the text for abbreviations. Scale bars = 1 cm.

pocket, placed between the ventral horn and the ventral process, which served for insertion of the jugal (Fig. 5E).

The squamosal can be seen only in the holotype skull, but it is inadequately preserved. The long anterior ramus tapers anteriorly and fits in a special groove along the dorsal surface of the posterior process of the postorbital. It extends anteriorly as far as the anterior wall of the supratemporal fenestra, as in other psittacosaur species except *P. neimongoliensis*. The medial process of the squamosal overlaps the lateral parietal frill. The posterior process of the squamosal does not separate the quadrate head from the paroccipital process, as in *P. xinjiangensis*, *P. meileyingensis* and *P. sinensis* (Sereno *et al.* 1988: 371).

The jugal is preserved on the skulls (Fig. 2), where its sutural contacts are obliterated, as well as in four isolated fragments (jugal horns). Judging from the isolated premaxillae (see above), the jugal most probably had a broad contact with this bone, as in *P. sinensis* (Sereno 1990*a*, *b*). The most distinctive character of the jugal in *P. sibiricus* is a well-developed pyramidal jugal horn, projecting laterally (Figs 2C, D & 5I–L). Among psittacosaurs, only *P. sinensis* and *Psittacosaurus* sp. from Yixian Formation (Mayr *et al.* 2002) have similarly exaggerated jugal horns. In the holotype of *P. sibiricus* the tips of the jugal horns are inclined ventrally, whereas in *P. sinensis* they are directed laterally (Young 1958: fig. 51). There is some variation in the structure of jugal horns. In isolated specimens the horn is relatively short with a flat anterior surface and a greatly convex and rugose posterior surface, sometimes with several longitudinal, deep grooves and ridges (Fig. 5I). The jugal horns on the holotype are longer, with a less flattened anterior surface and a less convex posterior surface bearing much weaker sculpturing (longitudinal grooves). This variation may arise from sexual dimorphism or ontogenetic change. The jugal horns were apparently covered by a horny sheath, extending anterodorsally to contact the postorbital at least. The margin of the horny sheath is clear in the holotype; it follows posteriorly a low rounded ridge that joins the jugal horn and the postorbital bar and divides the lateral jugal surface into two planes. The second distinctive character of the jugal in *P. sibiricus* is the division of its posterior portion by a deep cleft for the insertion of the quadratojugal, reaching anteriorly to the very posterior surface of the jugal horn (Figs 5I & L). In other psittacosaur species the quadratojugal is only inserted distally in the jugal, in its posterior third. The juvenile jugal fragments (Figs 5M–R) are very similar in structure to the adult jugal morphology in *P. mongoliensis* (Sereno *et al.* 1988: fig. 5), with a relatively subtle flexure across the bone from the postorbital bar to the tip of a weak and mostly ventrally projecting jugal horn. On the medial side, there is a prominent vertical ridge at the middle of the bone. This ridge possibly delimits the posterior contact area for the lateral process of the palatine. There is no quadratojugal notch posterior to the jugal horn and the contact with the quadratojugal is far from this horn.

The quadratojugal is exposed on the skulls (Fig. 2B). The quadratojugal forms the posteroventral corner of the infratemporal fenestra and is laterally overlain by two long spine-like posterior projections of the jugal. As a result, the jugal and the quadrate are separated in lateral view by only a very narrow band of the quadratojugal. The anterior portion of the quadratojugal is exposed between these projections of the jugal, extending further anteriorly than in any other psittacosaur species, up to the jugal horn posterior surface and along the majority of the infratemporal fenestra ventral margin (see also description of jugal, above). The posterior portion of the quadratojugal covers the quadrate, but the overlap is not complete and the quadrate is visible in lateral view, as in *P. meileyingensis* (Sereno *et al.* 1988: figs 2A & D). The quadratojugal of *P. sibiricus* lacks a rugose prominence, characteristic for *P. meileyingensis*.

The palpebral is a subtriangular bone loosely articulating with the prefrontal in the anterodorsal corner of the orbit (Figs 2C, D & 5S–U). The bone consists of two planes, a horizontal one and an anterior vertical one, both tapering distally. In the holotype the palpebrals are very large and robust, forming laterally projecting palpebral horns. The palpebral surface is sculptured on the holotype, especially on the anterior face, bearing prominent longitudinal grooves and was undoubtedly covered by a horny cap. In other psittacosaur species the palpebral horns are somewhat smaller and directed posterolaterally, not laterally as in *P. sibiricus*. Possibly, the state of development of the palpebral bones was correlated with sex or ontogeny: they are extremely developed on the holotype which is presumably an adult male, whereas five disarticulated palpebrals (Fig. 5S-U) are much finer and may pertain to females or subadult animals. In *P. sibiricus* the medial edge of the palpebral is subequal in length to the anterior (='external') edge, as in *P. mongoliensis*; in *P. xinjiangensis*, *P. meileyingensis* and *P. sinensis* it is noticeably shorter (Sereno *et al.* 1988: 371).

Palate

The palate in psittacosaurs is known for *P. mongoliensis*, but only briefly described (Sereno 1990*b*). In particular, the palatal view of a psittacosaur skull has only been published for a juvenile specimen (Coombs 1982: pl. 14, figs 3, 4). There are some descriptions and pictures of isolated palatal bones in other psittacosaur species (Sereno *et al.* 1988; Russell & Zhao 1996). In *P. sibiricus* the palatal region on both known skulls is not yet fully prepared, but several isolated palatal elements and one articulated complex of the quadrate fragment, pterygoids, ectopterygoid, basioccipital and basisphenoid allow us to supplement descriptions of this morphological complex in psittacosaurs.

The quadrate is exposed on the skulls and also represented by two isolated almost complete elements (Fig. 6A–E), a quadrate condyle and a juvenile quadrate fragment (Figs 3N & O). In lateral view, the dorsal half of the quadrate shaft arches posteriorly to a greater extent than in other psittacosaurs and its head is rounded and slightly narrowed, as in *P. neimongoliensis* (Russell & Zhao 1996: fig. 1) (expanded in *P. meileyingensis*). The posterior surface of the quadrate shaft is greatly concave. The shaft is relatively vertically orientated, at an angle of ~65° to the sagittal plane (45° in *P. meileyingensis*: Sereno *et al.* 1988: 372). The broadened condylar surface is orientated at an angle of ~80° from the anteroposterior axis of the skull (~60° in *P. meileyingensis*, ~90° in *P. mongoliensis* and *P. sinensis*: Sereno *et al.* 1988: 372). The ventral half of the lateral surface of the quadrate shaft is occupied by a well delimited facet for the quadratojugal. Dorsal to the latter facet along the anterior margin of the quadrate shaft there is a strip-like tuberosity continuing towards the quadrate head. At the posterodorsal end of the quadrate shaft there is a facet for articulation with the

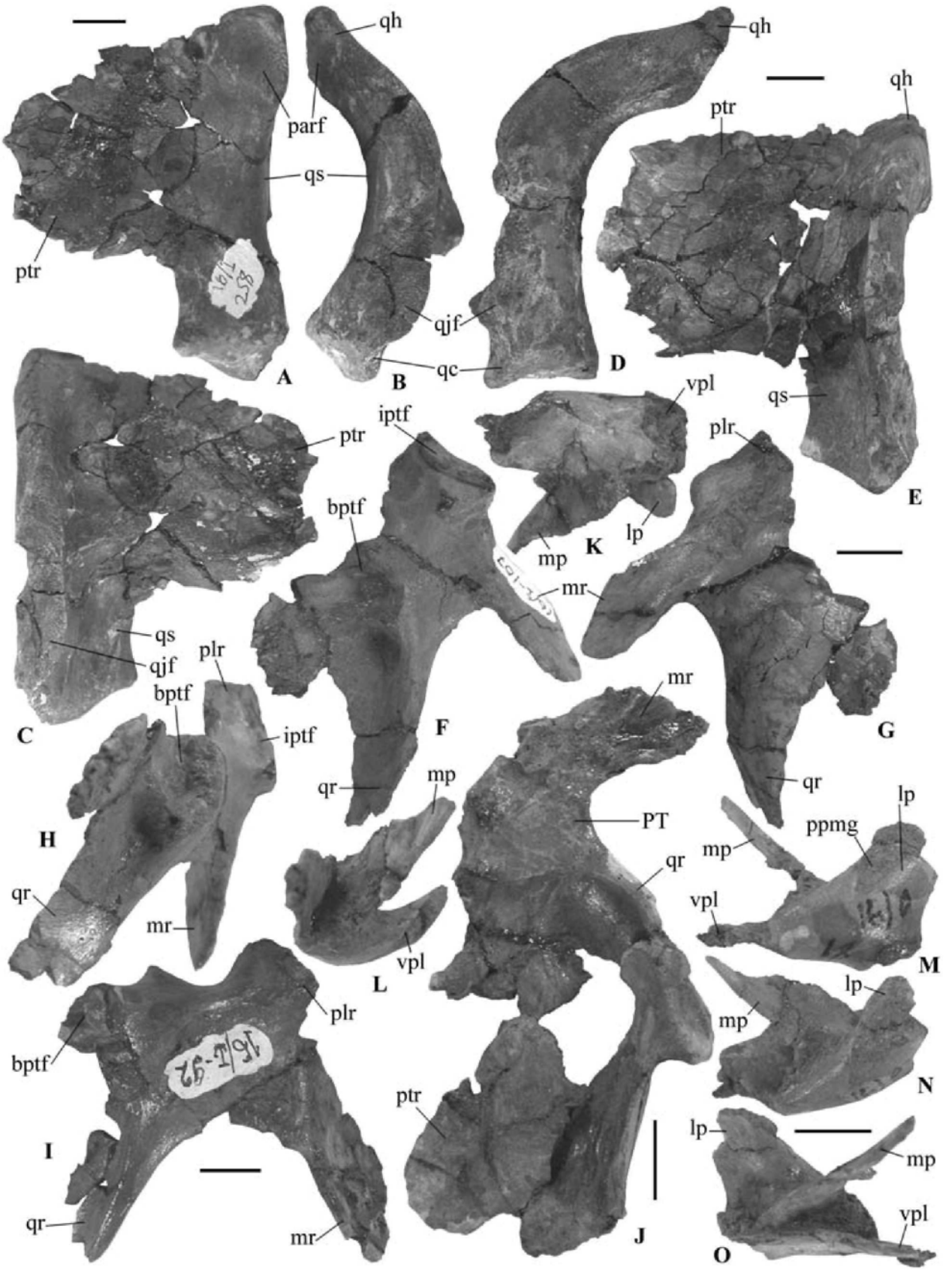

Figure 6 *Psittacosaurus sibiricus*: **A–C**, PM TGU 16/1-258, right quadrate in posteromedial (**A**), posterior (**B**) and anteromedial (**C**) views; **D, E**, PM TGU 16/1-202, left quadrate in posterior (**D**) and anterolateral (**E**) views; **F–H**, PM TGU 16/1-107, left pterygoid in medial (**F**), lateral (**G**) and dorsal (**H**) views; **I**, PM TGU 16/1-92, left pterygoid in medial view; **J**, PM TGU 16/0-17, left pterygoid and part of quadrate in medial view; **K–O**, PM TGU 16/0-18, left ectopterygoid in ventromedial (**K**), anterior (**L**), ventrolateral (**M**), dorsolateral (**N**) and dorsomedial (**O**) views. See the text for abbreviations. Scale bars = 1 cm.

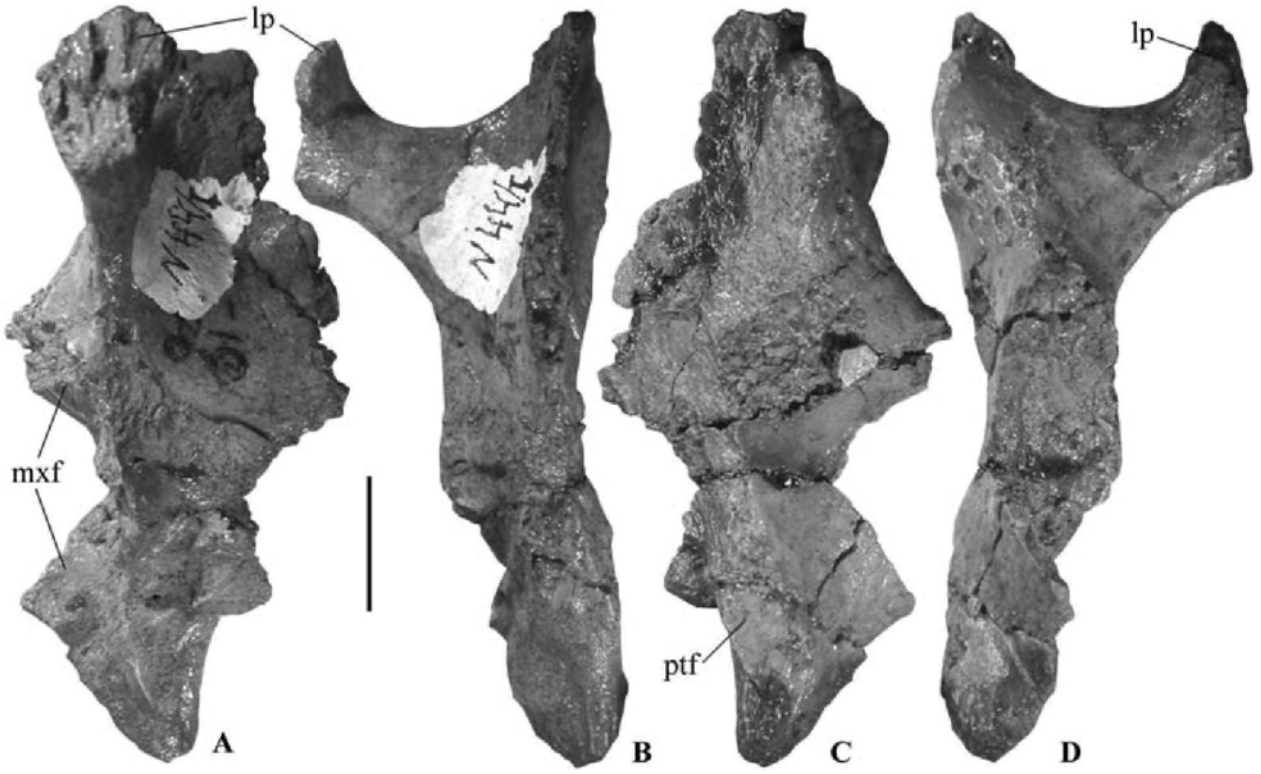

Figure 7 *Psittacosaurus sibiricus*, PM TGU 16/1-44, left palatine in lateral (**A**), dorsal (**B**), medial (**C**) and ventral (**D**) views. See the text for abbreviations. Scale bar = 1 cm.

paroccipital process of the exoccipital/opisthotic. The pterygoid ramus of the quadrate is seen on the skull and isolated quadrates (Figs 6A, C & E). It is an expanded very thin plate that is bent according to the curvature of the quadrate shaft. The most distal end of the pterygoid ramus, contacting the quadrate ramus of the pterygoid, is preserved in PM TGU 16/0-17 (Fig. 6J).

The pterygoid (Figs 6F–J) is represented by three more or less complete specimens, one disarticulated fragment and another fragment articulated with the pterygoid ramus of the quadrate. The posterolaterally directed quadrate ramus of the pterygoid is a thin, obliquely orientated plate, divided from the medial surface by a subvertical ridge into two unequal depressions. The smaller anterior depression is a socket for the basipterygoid process of the basisphenoid. Some movement might have been possible in the basipterygoid contact, in contrast to *P. neimongoliensis* (Russell & Zhao 1996: 639). The dorsal margin of the pterygoid quadrate ramus is subdivided by an incision into posterior and anterior branches; the latter is shorter and wider compared to the posterior branch and the anterior branch in *P. neimongoliensis* (Russell & Zhao 1996: fig. 2C). The mandibular ramus of the pterygoid is a thin plate of triangular shape, joined laterally by the ectopterygoid. The palatine ramus of the pterygoid is distinctly shorter and narrower dorsoventrally than in *P. neimongoliensis* (Russell & Zhao 1996: fig. 2C) and the sutural surface for the opposite pterygoid extends nearly towards the anterior end of the bone.

The ectopterygoid (Figs 6K–O), represented by two nearly complete disarticulated specimens, is a complex triradiate bone. The thin ventral plate, which attaches to the dorsal surface of the pterygoid mandibular ramus, tapers anteriorly. Above it, there is a thin medial process that is directed and tapers anterodorsally and is adjacent to the lateral surface of the pterygoid quadrate ramus. The ventral plate and the medial process border a cleft-like opening ventrally, laterally and dorsally, which is bordered medially by the lateral pterygoid surface. The triangular lateral process is the thickest portion of the bone. It curves gently posterolaterally and bears a cleft-like socket for the insertion of the posterior process of the maxilla on its lateral surface (Fig. 6N).

The palatine is known from two fragmented and isolated bones (Fig. 7). The bone is a rhomboid vertical plate with a robust lateral process at the anterior end. The lateral process is dorsoventrally flat and expanded distally, where it contacts the jugal and lacrimal. Posterior to the lateral process there is an extensive attachment area for the maxilla, which is placed ventral to the level of the lateral process. The medial bone side is slightly concave. Its dorsal margin is occupied by a continuous strip-like facet. The posterior part of this facet articulates with the pterygoid, the anterior part possibly with the vomer.

Braincase

The occiput is broad transversely and low dorsoventrally. The foramen magnum is oval-shaped, with a long horizontal axis and is surrounded by the supraoccipital basioccipital and the exoccipitals. The foramen magnum is equal in width to the occipital condyle.

The supraoccipital sutural boundaries are obliterated. There is a low supraoccipital crest, going from the foramen

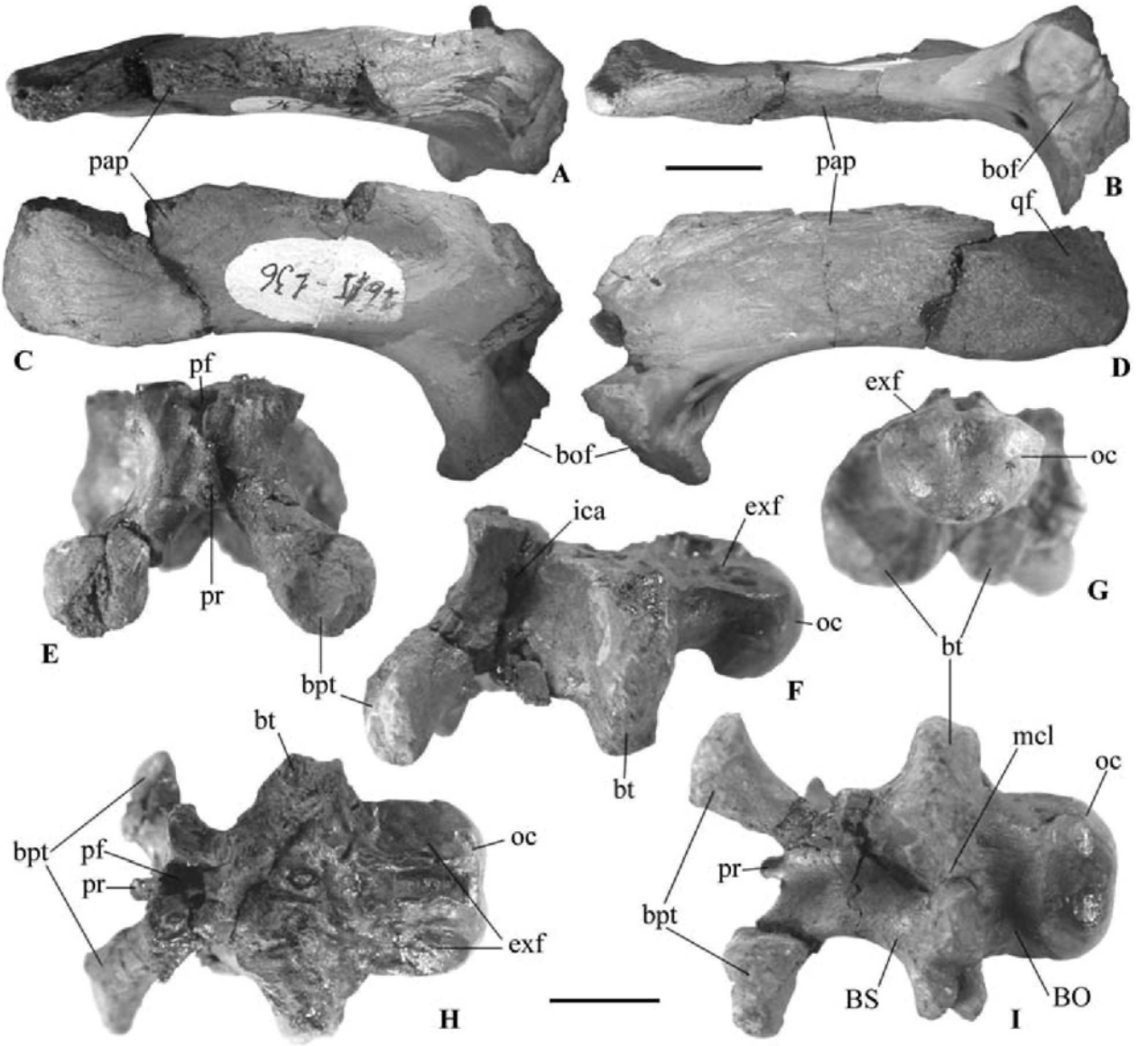

Figure 8 *Psittacosaurus sibiricus*: **A–D**, PM TGU 16/1-136, left exoccipital/opisthotic in dorsal (**A**), ventral (**B**), posterior (**C**), and anterior (**D**) views; **E–I**, PM TGU 16/o-15, basioccipital/basisphenoid in anterior (**E**), lateral (**F**), posterior (**G**), dorsal (**H**) and ventral (**I**) views. See the text for abbreviations. Scale bars = 1 cm.

magnum towards the parietal shelf along the supraoccipital midline. Lateral to the supraoccipital crest, the supraoccipital (and parietal?) surface is deeply depressed.

The basioccipital can be seen on the holotype and is represented by two complete disarticulated specimens of about half the size, one of which is fused with the basisphenoid (Figs 8E–I) and the other is associated with the atlas intercentrum. The occipital condyle is oval-shaped, with a longer horizontal axis and is formed mostly by the basioccipital. The basioccipital forms only a narrow portion of the ventral floor of the foramen magnum and neurocranial cavity. The basal tubera have rounded ventral outlines, are separated by a median cleft and extend ventrally slightly beyond the level of the occipital condyle. Along the basal tubera the basioccipital–basisphenoid suture can be detected; both bones contribute approximately equally to the composition of the tubera.

The exoccipital/opisthotic is known from two almost complete disarticulated specimens and several isolated fragments (Figs 8A–D & 9) and can be seen on the holotype. It has an anteroposteriorly expanded peduncle with a ventral sutural surface for articulation with the basioccipital. The opposite exoccipitals do not meet at the midline, leaving a narrow space between them for the basioccipital which contributes to the ventral floor of the foramen magnum. The exoccipital/opisthotic peduncle forms the lateral side of the foramen magnum and is pierced by three foramina for cranial nerves. The posteriormost portion of this peduncle forms a small, but distinctly delimited, articular surface of the occipital condyle, separated from the rest of the peduncle by a constricted neck. The cranial nerve foramina open on the lateral side posterior to the oblique ridge (metotic strut), continuing from the anterolateral corner of the peduncle towards the ventral margin of the paroccipital process and possibly delimiting the border between the exoccipital and the opisthotic. These foramina are interpreted as exits for the cranial nerves XII_3 (posterior), XII_{1+2} (anterior) and X-XI (dorsal:

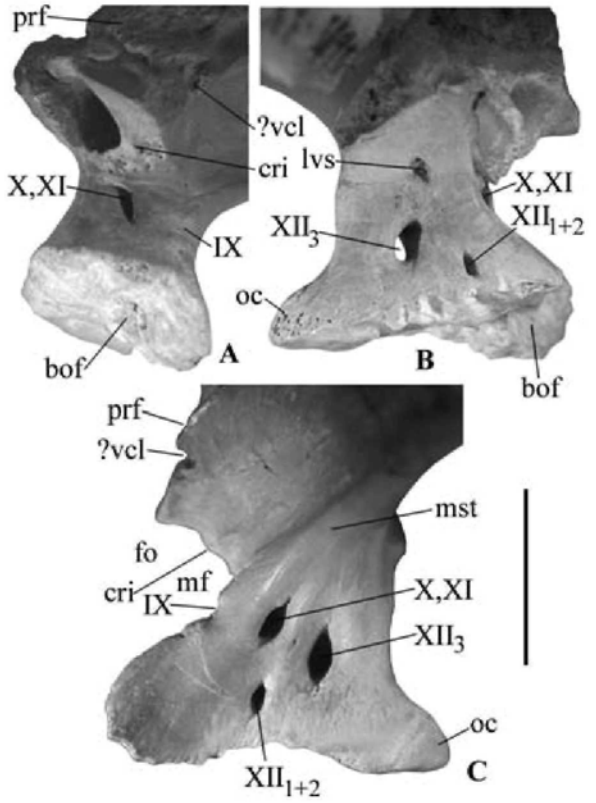

Figure 9 *Psittacosaurus sibiricus*, PM TGU 16/1-136, left exoccipital/opisthotic peduncle in anteroventromedial (**A**), medial (**B**) and lateral (**C**) views. See the text for abbreviations. Scale bar = 1 cm.

see Discussion, below and Fig. 9). The posterior hypoglossal (XII_3) foramen is the largest and is situated close to the foramen magnum. It opens medially to a similarly sized and placed foramen. The anterior hypoglossal foramen (XII_{1+2}) is smaller and situated anteriorly and ventrally to the former. It opens medially into an even smaller slit placed in a somewhat more anterior position at the exoccipital/basioccipital suture. The dorsal vagus foramen (for X and XI cranial nerves) is only slightly smaller than the posterior hypoglossal foramen and is placed somewhat dorsal to the latter. It leads to the jugular channel, which opens by a slit-like aperture on the anterior wall of the metotic strut (Fig. 9A). The metotic fissure (= jugular foramen) is confluent with the fenestra ovalis; both openings were probably separated by a cartilaginous lamina whose attachment rugosity is visible on the posterodorsal ceiling of their common chamber (Figs 9A & C). In *Protoceratops* and *Bagaceratops* these structures are separated by a thin bony bridge (Maryańska & Osmólska 1975: 152). On the posterior wall of the metotic fissure there is a distinct furrow, which is interpreted here as indicating the course of the IX cranial nerve and jugular vein (Figs 9A & C; see Discussion, below). This furrow is placed at the level of the vagus foramen and along the wall of the jugular channel. On the dorsal wall of the fenestra ovalis there is a deep recess. The contact with the prootic is made by two dorsal sutural surfaces meeting at an angle of ~120° and possibly by a smaller sutural surface ventral to the fenestra ovalis + metotic fissure opening. On the medial side of the exoccipital/opisthotic peduncle dorsal to the posterior hypoglossal (XII_3) foramen there is a small blind recess (Fig. 9B). This recess (='foramen') is present in *Hypsilophodon* (Galton 1974: 105, fig. 9B), where it is interpreted as a foramen for the vena cerebralis posterior and in dromaeosaurid theropods, where it is interpreted once as an opening for the endolymphatic duct (Kurzanov 1976; Currie 1995). It is more likely that this is the opening for a diverticulum of the longitudinal venous sinus (Hopson 1979; Sues 1997). Along the lateral edge of the dorsal sutural surface there is a distinct foramen, possibly an opening for the vena capitis lateralis (see Sereno *et al.* 1988: 372).

Most of the exoccipital/opisthotic is formed by the long posterolaterally projecting paroccipital process. It has a concave posterior surface and an anterior surface divided by a longitudinal ridge into a concave ventral surface and a dorsal surface bearing rugose sutural facets for articulation with the supraoccipital and squamosal and a smoother triangular facet for the quadrate, occupying the most distal part of the process (Fig. 8D).

The basisphenoid is best seen on an isolated specimen (Figs 8E, F, H & I). The basipterygoid processes are transversely compressed proximally but transversely expanded at their distal ends. The basipterygoid processes are anterolaterally directed, with their distal tips slightly ventrally inclined. Posteriorly the basipterygoid processes are continuous with parasagittal ridges that cross the ventral surface of the basisphenoid to the respective basal tubera. Dorsal to the median cleft separating the basal tubera, the ventral basisphenoid surface has a marked depression. On the lateral surface of the basisphenoid, just posterior to the base of the basipterygoid process, there is a foramen for the internal carotid artery, leading to the pituitary fossa (Fig. 8F). This foramen is placed relatively higher and further anteriorly than in *P. neimongoliensis* (Russell & Zhao 1996: fig. 2B). The dorsal surface of the basisphenoid, including the sella turcica, is not preserved. Only the base of the parasphenoid rostrum is preserved. It is transversely compressed and dorsoventrally high, as in *P. neimongoliensis* (Russell & Zhao 1996: fig. 2B).

Lower jaw

The lower jaw (Figs 2A & B) is present in both skulls (the ventral side is cleaned only in PM TGU 16/4-21) and as some disarticulated bones, among which the dentary is the most common. The external mandibular fenestra is absent, as in *P. neimongoliensis* and *P. sinensis* (derived feature). The mandibular rami are laterally concave (laterally convex in *P. sinensis*, straight in *P. mongoliensis* and *P. neimongoliensis*), set at an angle of ~35° (~45° in *P. meileyingensis*, ~55° in *P. sinensis*).

The predentary is preserved in both skulls (Figs 2A & B). The predentary in *P. sibiricus* is relatively anteroposteriorly long and dorsoventrally very low, unlike the much shorter and taller predentary in *P. meileyingensis P. neimongoliensis*, and *P. sinensis*. In its proportions, it is closer to that of *P. mongoliensis*, but still lower (Figs 2A & B). As can be judged from the isolated dentaries, the predentary has a lateral process, which extends along the anterior dentary margin posterolaterally beyond the level of the tooth row. The predentary lateral surface is relatively smooth, with few nutrient pits. The occlusal edge of the predentary is very sharp, dorsolaterally projected and would have sheared inside that of the rostrum.

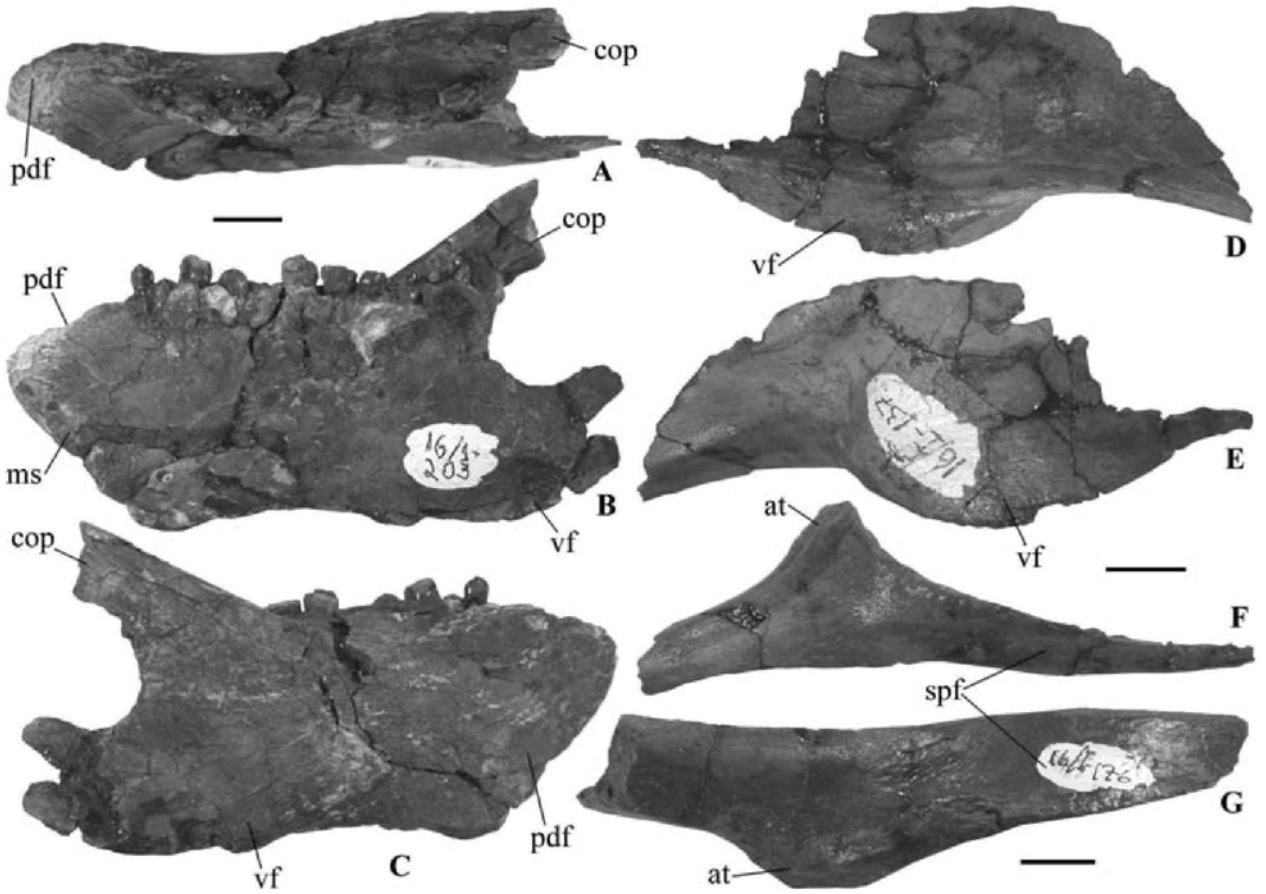

Figure 10 *Psittacosaurus sibiricus*: **A–C**, PM TGU 16/1-230, right dentary in dorsal (**A**), medial (**B**) and lateral (**C**) views; **D–F**, PM TGU 16/1-137, right angular in medial (**D**), lateral (**E**) and ventral (**F**) views; **G**, PM TGU 16/1-176, left angular in ventral view. See the text for abbreviations. Scale bars = 1 cm.

The dentary (Figs 2A, B & 10A-C) is seen in the skulls and is represented by six disarticulated bones of different sizes. Even the largest isolated dentaries are not firmly attached to the predentary. Only in the holotype does the predentary appear to be attached to the dentary (Figs 2A & B). The tooth count varies from seven to 11 and apparently does not correlate with the size of the bone: two dentaries of similar size have different number of teeth, seven (PM TGU 16/1-174) or 10 (PM TGU 16/0-20). In PM TGU 16/1-203 the 11th tooth is distinctly smaller than the 10th tooth and set almost transversely to the tooth row (Fig. 11E). The tooth row is laterally concave and inset from the lateral surface of the dentary by a labial emargination. On the medial side, just ventral to the tooth row, there is a line of relatively big replacement foramina. The symphysis is relatively long and obliquely orientated. A distinct facet for the predentary occupies the anterior margin. It is rugose with a shallow longitudinal groove in the centre, but without a deep socket for the predentary lateral process as in neoceratopsians. On the lateral face, the attachment area for the predentary extends parallel to the dentary symphysis (Fig. 10C). Its surface is flat and not sculptured and set at a slightly different angle to the rest of the dentary lateral surface. The splenial attachment surface occupies the ventral half of the bone on the medial side and comes very close to the dentary symphysis. The posterodorsal portion of the dentary forms a very deep socket for the anterior portion of the surangular. The dentary forms the tip of the coronoid process. The posteroventral portion of the dentary, forming the ventral flange, is a very thin plate. The ventral flange (Fig. 10C) starts in a more posterior position than in *P. mongoliensis* (Sereno *et al.* 1988: fig. 5), closer to the posterior end of the tooth row and projects ventrally (ventrolaterally in *P. meileyingensis*: Sereno *et al.* 1988: 373). The ventral flange is present in *P. meileyingensis* *P. mongoliensis* and *P. ordosensis* and is evidently lacking in *P. sinensis* and *P. neimongoliensis* (Sereno *et al.* 1988: 373; Russell & Zhao 1996: 641, 645). The lateral dentary surface bears no rounded prominence between the coronoid process and the ventral flange, in marked contrast to *P. meileyingensis* and to a lesser extent in *P. mongoliensis* (Sereno *et al.* 1988: 373).

The angular (Figs 10D–G) is visible in the skulls and is also represented by two incomplete specimens. The anterior portion of the angular lateral surface, adjacent to the dentary, is flat and bordered ventrally by a prominent subcircular ridge. This ridge is a continuation of the mandibular ventral flange, which in *P. meileyingensis* only 'dissipates' on the angular (Sereno *et al.* 1988: 373, fig. 2A) and in other species apparently avoids the angular. So, the ventral flange in *P. sibiricus* is more extensively developed than in other psittacosaur species. The ventral flange extends dorsally as a less prominent vertical ridge, bordering the flat anterior surface of the bone posteriorly. At the meeting of these two ridges the bone projects strongly laterally, forming a prominent

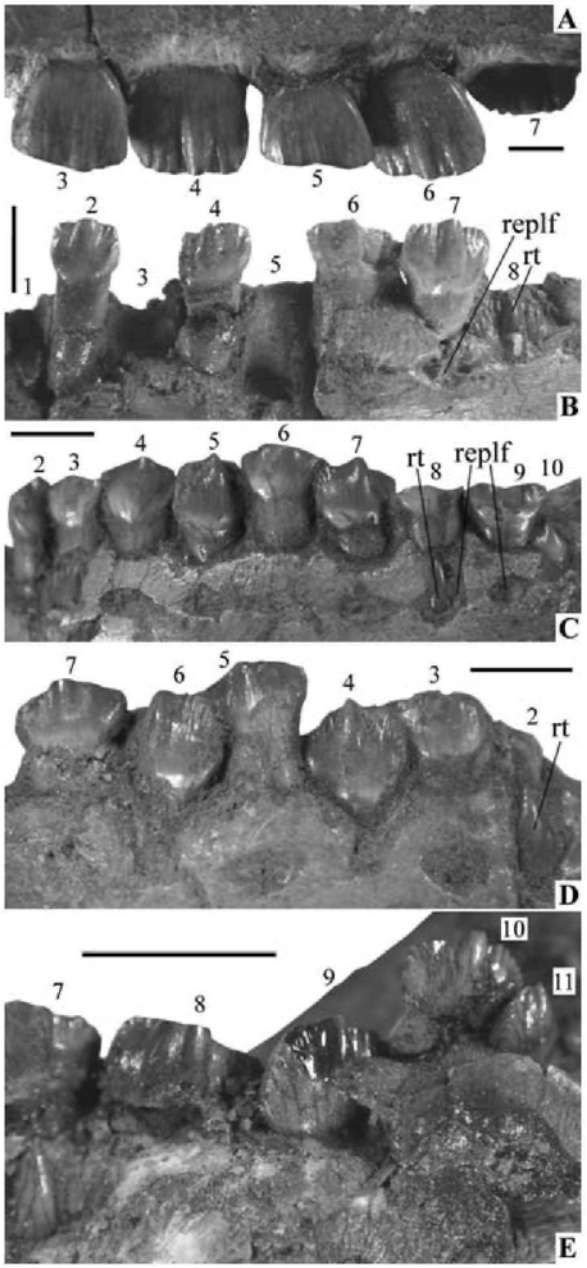

Figure 11 *Psittacosaurus sibiricus*: **A**, PM TGU 16/1-284, left maxillary teeth in labial view; **B**, PM TGU 16/0-20, right dentary teeth in lingual view; **C**, PM TGU 16/1-175, right dentary teeth in lingual view; **D**, PM TGU 16/1-174, left dentary teeth in lingual view; **E**, PM TGU 16/1-203, right dentary teeth in lingual view. Numbers denote tooth positions in the jaw. Scale bar = 0.5 cm. See text for abbreviations.

tuber-like outgrowth (angular tuber: Figs 10F & G). Posterior to this tuber, there is another ridge directed posteriorly. Presence of this outgrowth is the second distinctive character of the angular in *P. sibiricus*, distinguishing this species from other psittacosaurs. The ventral side of the angular bears a shallow longitudinal facet for the splenial.

The posterior portion of the lower jaw projects posteriorly beyond the articular–quadrate joint into the retroarticular process (Figs 2A & B). This retroarticular process is formed mainly by the surangular, with a thin band of the angular attaching the articular ventrally.

Dentition

The maxillary teeth are worn from the lingual side, whereas the dentary teeth are labially worn. The enamel is distributed asymmetrically; a thicker layer is present on the labial side of the maxillary crowns and on the lingual side of the dentary crowns.

There are few maxillary teeth preserved *in situ* on the known maxillae, most of which have worn crowns. The primary ridge is usually present, although it is not as bulbous as in the dentary teeth (Fig. 11A). There are 3–4 denticles on each side of the primary ridge. There is only one unworn erupting maxillary tooth (PM TGU 16/1-284, position 7: Fig. 11A), which has 11 denticles (counted from the lingual side, fore–aft–basal crown length = 5.5 mm).

There are seven unworn or little worn dentary teeth in three dentaries. Dentary tooth crowns (Figs 11B–E) are oval in lingual view, with a distinct bulbous primary ridge, broad at the base and terminating in the apical denticle, as in *P. mongoliensis* (Sereno *et al.* 1988: fig. 7) and with 3–8 denticles anterior and posterior to the apical denticle. The total denticle count varies from 6 to 17. The number of denticles generally increases with the crown fore–aft–basal length, but the correlation is low ($r = 0.54$) and not significant at $p < 0.05$, possibly due to a small sample size ($n = 13$; unworn teeth from jaws and isolated teeth).

The pattern of tooth replacement can be observed in one maxilla and four dentaries. Two stages of replacement can be recognised: (1) an earlier stage in which the predecessor is still in place and the replacement tooth appears only as the crown tip through the replacement foramen and (2) a later stage in which the predecessor is gone, the alveolar border around the replacement foramen is eroded and the replacement tooth crown is fully exposed, but not fully erupted and still placed below the tooth row. The replacement pattern can be exemplified by the following scheme (* and ** designate locus in early and late stages of tooth replacement, respectively):

PM TGU 16/1–284 (maxilla):	1234567**89
PMTGU 16/0–20 (dentary):	12345678**9
PMTGU 16/1-174 (dentary):	12*34567
PMTGU 16/1-175 (dentary):	12345678*910**
PMTGU 16/1-203 (dentary):	12**34**567*891011**

The most active replacement is observed in the largest dentary (PM TGU 16/1-203): four of 11 loci are under replacement (Figs 10B & 11E). Here two posterior to anterior waves of replacement are manifested: a first wave that reaches the anterior end of the jaw and includes loci 2 and 4 (4 is at the more derived eruption stage) and a second wave at the posterior end of the jaw, which includes loci 7 (early stage of replacement) and 11 (late stage of replacement, approximately equivalent to the tooth in locus 4). In other specimens the replacement involves one or two tooth loci only.

Hyoid apparatus

There are two rather long rod-like structures, lying parallel and between the mandibular rami on the ventral side of the skull PM TGU 16/4-21. They meet anteriorly at an acute angle. Most probably these are ceratobranchials I. In *P. sinensis* the first ceratobranchials are similarly long and rod-shaped (Young 1958: figs 52, 56; mislabelled as 'clavicle'). In *P. mongoliensis* ceratobranchials I appear to be relatively

shorter and they are widely separated anteriorly by ceratobranchials II (Colbert 1945: fig. 6A). Sereno (1990*b*) described first ceratobranchials for both *P. mongoliensis* and *P. sinensis* as gently curving and rod-shaped.

Postcranium

Vertebral column

Psittacosaurus sibiricus differs from other psittacosaurs in having a greater number of presacrals (23; 21 in *P. xinjiangensis*, *P. mongoliensis* and *P. sinensis*: Sereno & Chao 1988: 361; Sereno 1990*b*: 584; 21 or 22 in *P. neimongoliensis*: Russell & Zhao 1996: 641–642). According to Sereno (1990*b*: 590), there is individual variation in the presacral count in *P. mongoliensis*: three skeletons have 21 presacrals and one skeleton (AMNH 6254, the holotype) has 22 presacrals.

The cervicals can be distinguished from dorsals by a parapophysis (capitular facet) that is either ventral to or centred upon the neurocentral suture (Sereno 1990*b*; Russell & Zhao 1996). By this criterion, there are nine cervicals in *P. sibiricus*, as in *P. sinensis* (8 in *P. mongoliensis* and *P. neimongoliensis*: Russell & Zhao 1996: 641).

The atlas is obscured by the skull in the holotype and considerably damaged in the skeleton PM TGU 16/4-21. There is also a 50% smaller atlas intercentrum (Figs 12A–C), articulated with the basioccipital and other cervicals of a single specimen, as well as a number of isolated atlas intercentra of different size. The atlas intercentrum is a thick, dorsally concave crescent, articulating on its dorsal surface with the odontoid process of the axis. On the anterior surface there is a well-defined crescentic articulation facet for the occipital condyle. The rounded pedicels on each side of the intercentrum articulate with the neural arches.

The axis is preserved in both skeletons, in the smaller it articulates with other cervicals (Fig. 12D) and in the other it is preserved by two isolated neural arches (Figs 12E–H). The axis centrum is small, compared to the neural arch and expanded at both ends, although to a greater extent anteriorly. There is a faint ventral keel. The parapophysis is located at the anterior margin of the centrum, close to its mid-height. The intercentrum is very small, triangular in anterior view and not fused with the axis centrum in PM TGU 16/0-23, but fused in PM TGU 16/4-21, which is twice as large. The odontoid process, preserved only in PM TGU 16/4-21, is relatively large, is transversely only slightly narrower than the axis centrum, triangular in dorsal or ventral view, greatly convex ventrally and shallowly concave dorsally. The axis neural arch is relatively high. The prezygapophyses are circular in outline, placed at the anterior margin of the neural arch and their articular surfaces face dorsolaterally. The diapophysis is placed upon the neurocentral suture, approximately at the middle of the axis centrum. The axis neural spine arises dorsal to the prezygapophyses and projects slightly anteriorly beyond the level of the centrum. The dorsal margin of the neural spine arises posterodorsally at an angle of ~25°. The posterior portion of the neural spine flares laterally into a transverse plate, which is perpendicular to the more anterior part of the neural spine and almost completely overhangs the third cervical. The postzygapophyses are located on the lateral margins of this transverse plate of the neural spine, at the level of the dorsal margin of the neural canal. They are oval in shape and face ventrolaterally. The neural canal is relatively large and oval in outline.

More posterior cervicals are not completely prepared in the skeletons, but can be seen in an articulated neck fragment of another, smaller specimen (Fig. 12D) and in isolated cervicals (Figs 12I–M). The cervical centra are amphiplatyan, with rhomboid articulation surfaces. The fifth cervical centrum is the shortest, as in *P. neimongoliensis* and *P. mongoliensis* (Russell & Zhao 1996: 641, table 2): the centrum length for cervicals 2 through 6 is 14.0, 16.4, 14.8, 15.6 and 16.1 mm in PM TGU 16/0-23–27. The centrum is constricted laterally and expanded at the ends. There is no marked difference in centrum height within the cervical series. The ventral keel becomes more prominent in more posterior cervicals. The parapophyses are short and oval-shaped, dorsoventrally orientated and located approximately at the same level on cervicals 3–6, close to the neurocentral suture. The diapophyses, in contrast, move progressively higher on the neural arch in more posterior cervicals. The transverse processes are short in cervicals 3–5, become slightly longer and anteroposteriorly compressed starting with the sixth cervical. They are centrally placed in cervicals 3 and 4 and shift anteriorly in cervicals 5 and 6. The prezygapophyses are large, with oval-shaped and slightly convex articular surfaces that face dorsomedially and become more vertically orientated in the sixth cervical. The neural spines are directed posterodorsally, laterally compressed and taper distally in all cervicals except the ninth, where the distal and proximal ends are roughly equal in anteroposterior length. The neural spine is very short proximodistally and spine-like in the third cervical, but becomes progressively longer posteriorly. The postzygapophyses are large, anteroposteriorly elongate, with flat or slightly concave articulation surfaces. The neural canals are large and almost round.

The posterior cervical ribs (7–9) are preserved in the holotype and represented by some disarticulated specimens (Figs 13A & B), whereas the more anterior cervical ribs are not completely prepared in the skeletons and known only from a single isolated specimen (Figs 12N & O). The posterior cervical ribs are double headed, laterally compressed and taper distally to narrow, pointed tips. Their proximal portions are expanded noticeably dorsoventrally, with a high, longitudinal and sharp ridge, starting from the capitulum and terminating near the distal end, twisting on to the anterior face in more anterior cervical ribs. This ridge is evidently less manifest in the dorsal ribs. The posterior cervical ribs increase considerably in length along the series and the last (9th) cervical rib is about 70% of the first dorsal rib length. The tuberculum and capitulum are anteroposteriorly compressed and lie in the same plane. The capitular process is long (longer than in dorsal ribs) and set at a greater angle to the rib shaft than in the dorsal ribs. The capitular condyle is convex; the tuberculum articular surface is concave.

There are 14 dorsals in *P. sibiricus*, the largest number reported among psittacosaurs. Chao (1962: 360) reported 15 dorsals for *P. sinensis* (='*P. youngi*'), but apparently he included some posterior cervicals in this count. The dorsal centra are amphiplatyan (in fact, incipiently procoelous, with a slightly concave anterior face and a flat posterior face in the beginning of the series, and become slightly amphicoelous by the end of the series), laterally constricted, with oval intercentral articular surfaces. There is a faint ventral keel on the anterior dorsals. Centrum length increases slightly posteriorly. A subrectangular neural spine is fully developed in the third dorsal (12th presacral). The last (9th) cervical and

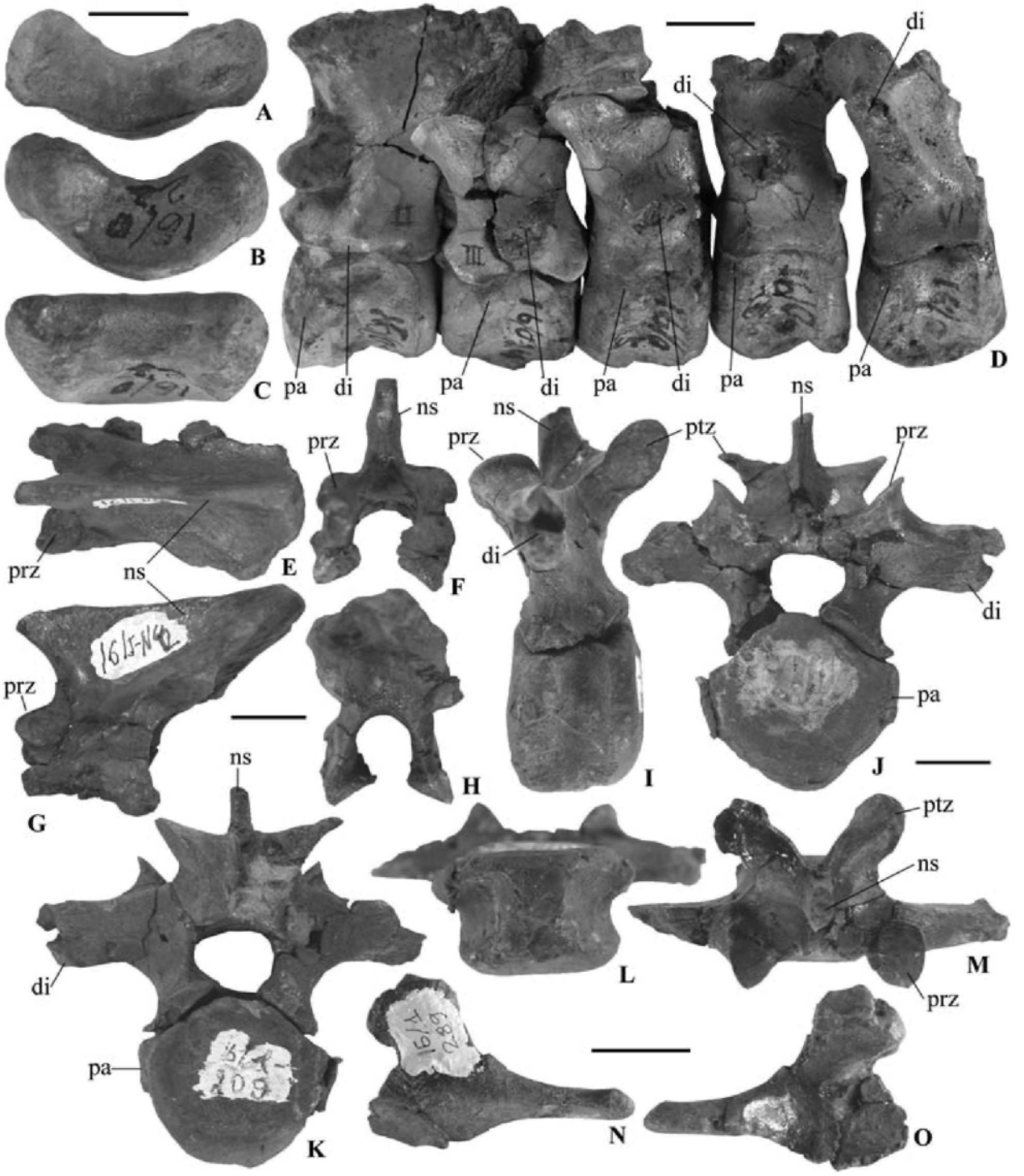

Figure 12 *Psittacosaurus sibiricus*: **A–C**, PM TGU 16/0-22, atlas intercentrum in posterior (**A**), anterior (**B**) and dorsal (**C**) views; **D**, PM TGU 16/0-23-37, cervicals 2–6 in lateral view; **E–H**, PM TGU 16/1-42, axis neural arch in dorsal (**E**), anterior (**F**), lateral (**G**) and posterior (**H**) views; **I–M**, PM TGU 16/1-209, sixth cervical in lateral (**I**), anterior (**J**), posterior (**K**), ventral (**L**) and dorsal (**M**) views; **N**, **O**, PM TGU 16/1-289, left cervical rib in lateral (**N**) and medial (**O**) views. See the text for abbreviations. Scale bars = 1 cm.

first two dorsals (Figs 14A – E) have a neural spine shape that is intermediate between that of the distally tapering cervical spines and the subrectangular dorsal spines, which are usually anteroposteriorly expanded at the distal end. The shape of the neural spines is very uniform in all dorsals after the second, only decreasing slightly in height and leaning further posteriorly along the series (Figs 14H & I). The transverse processes in the most anterior dorsals (1–3) are robust, project dorsolaterally (at ~50–60° to the neural spine) and are almost as tall as the neural spine (Figs 14B, D, F & I). Along the trunk series, the transverse processes become less robust and are directed more laterally (at an angle ~80° to the neural

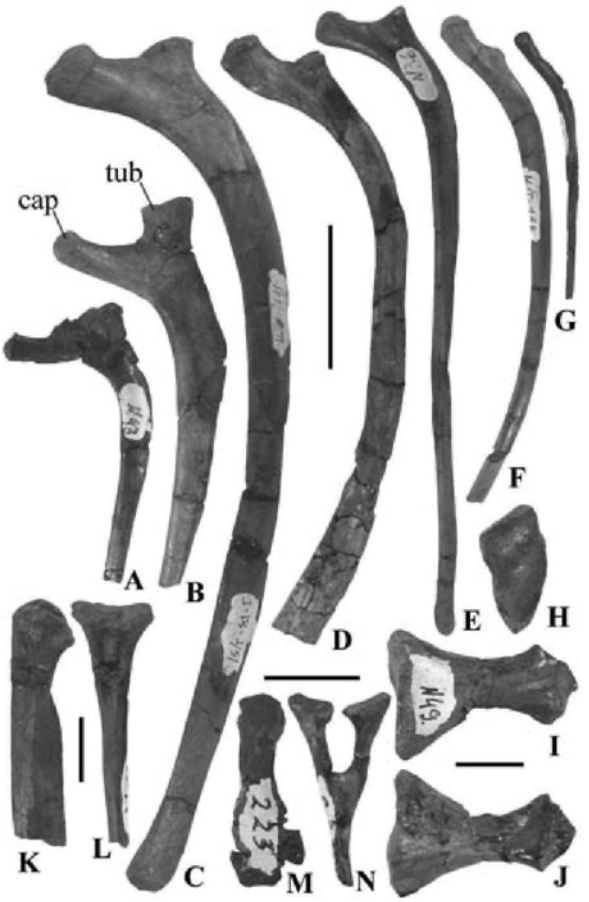

Figure 13 *Psittacosaurus sibiricus*: **A**, PM TGU 16/1-43, right cervical rib in medial view; **B**, PM TGU 16/1, 26, right cervical rib in medial view; **C**, PM TGU 16/1-111, left dorsal rib in lateral view; **D**, PM TGU 16/1-243, right dorsal rib in medial view; **E**, PM TGU 16/1-36, right dorsal rib in medial view; **F**, PM TGU 16/1-138, left dorsal rib in lateral view; **G**, PM TGU 16/1-60, left dorsal rib in lateral view; **H–J**, PM TGU 16/1-49, sacral rib in lateral (**H**), dorsal(?) (**I**) and ventral(?) (**J**) views; **K, L**, PM TGU 16/1-11, chevron in lateral (**K**) and posterior (**L**) views; **M, N**, PM TGU 16/1-223, chevron in lateral (**M**) and posterior (**N**) views. See the text for abbreviations. Scale bar = 3 cm (**A–G**) and 1 cm (**H–N**).

spine). The parapophyses are large, round to oval-shaped (in most posterior dorsals) and located above the neurocentral suture, on the ventrolateral base of the transverse processes. The diapophyses are larger than the parapophyses of the same vertebra, located ventrolateral to the tip of the transverse process in anterior dorsals and occupy the distal ends of the transverse processes in posterior dorsals. In the most posterior dorsals, the parapophyses and diapophyses coalesce. As in other psittacosaurs (Sereno & Chao 1988: 361) there is a pocket on the posterior side of the base of the transverse process in posterior dorsals. The depression is walled medially by a thin posteriorly projecting lamina, which forms the posterior margin of the neural arch. The prezygapophyses and postzygapophyses have elliptical articular surfaces, with the transverse axis being long and obliquely orientated. The articular surfaces are slightly convex in the prezygapophyses and slightly concave in the postzygapophyses. The neural canal is round and becomes relatively smaller along the series.

The almost complete series of dorsal ribs can be seen in the skeletons and there are numerous isolated dorsal ribs of all kinds from different individuals (Figs 13C–G). The anterior and middle dorsal ribs are double-headed, but the most posterior ribs (not yet prepared in the skeletons, but represented by disarticulated specimens, e.g. Fig. 13G), are single-headed. The first dorsal rib is about 1.4 times longer than the last cervical rib and similar with the latter in form, except that the dorsal ridge is less prominent and the rib shaft is more strongly bent posteriorly adjacent to the capitulum. The capitular process in all dorsal ribs is relatively long and terminates in a slightly expanded, round or laterally compressed capitular condyle. The tuberculum is short, with a very distinct articular surface that is round and slightly concave in the anterior and middle dorsal ribs, but oval-shaped in the more posterior ribs. The rib shaft is laterally compressed and tapers towards the distal end. The more anterior dorsal ribs curve ventromedially to a greater extent than the posterior ribs; the latter have straighter shafts. The dorsal ribs gradually decrease in length along the series in the posterior region, but which rib is longest amongst the anterior and middle dorsal vertebrae cannot be established confidently.

There are two sternal ribs visible on the holotype, opposite the lateral process of the sternum. They are relatively more expanded anteroposteriorly than the dorsal ribs. The second visible sternal rib is about half as long as the preceding sternal rib.

The sternum is visible on the holotype, but is unfortunately largely obscured by the vertebral column. A lateral sternal process, directed towards the two sternal ribs and tapering slightly distally, but with an abrupt distal margin, is recognisable on the left side. An almost complete disarticulated sternal plate (Fig. 15) is of similar shape, with a wider, flat anterior end and a narrower, somewhat dorsoventrally thicker, posterior end bearing a facet for the sternal rib. The lateral edge is concave and thick; medially the plate becomes very thin and the medial edge is convex. The sternal plate in *P. sibiricus* is similar to that in *P. sinensis* (Young 1958: fig. 56; labelled 'exoccipitale') and in the basal neoceratopsian *Montanoceratops cerorhynchus* (Brown & Schlaikjer, 1942) (Chinnery & Weishampel 1998: fig. 6). In *P. xinjiangensis* the sternal plate has a more developed and laterally deflected anterior end (Sereno & Chao 1988: fig. 2; the element is rotated so the anterior end is facing caudally: compare Sereno 1990*b*: fig. 28.6).

The sacral series is preserved in the skeletons, where it is obscured by the ilium and not completely prepared and in an articulated series together with four anterior caudals from another specimen (PM TGU 16/0-30-39: Figs 16A & B); the description is based largely upon the latter specimen. The sacrum is composed of six vertebrae, as in other psittacosaurs (known for *P. mongoliensis P. sinensis*, *P. xinjiangensis* and *P. neimongoliensis*). Indication of seven sacrals for *P. sinensis* [='*P. youngi*'] (Chao 1962: 360) is apparently a mistake (see Sereno & Chao 1988: 361). The sacral centra are fused and the second sacral is broadest transversely. There is a blunt and wide ventral keel. The posterior articular surface in the sixth sacral is transversely widened, dorsoventrally compressed and concave (Fig. 16B). Sacral ribs are fused to the vertebrae in PM TGU 16/0-30–35 (Fig. 16A) and in the skeletons, but remain unfused in somewhat younger individuals, as can be seen from the isolated specimens (Figs 13H–J). The sacral ribs are clearly subdivided into

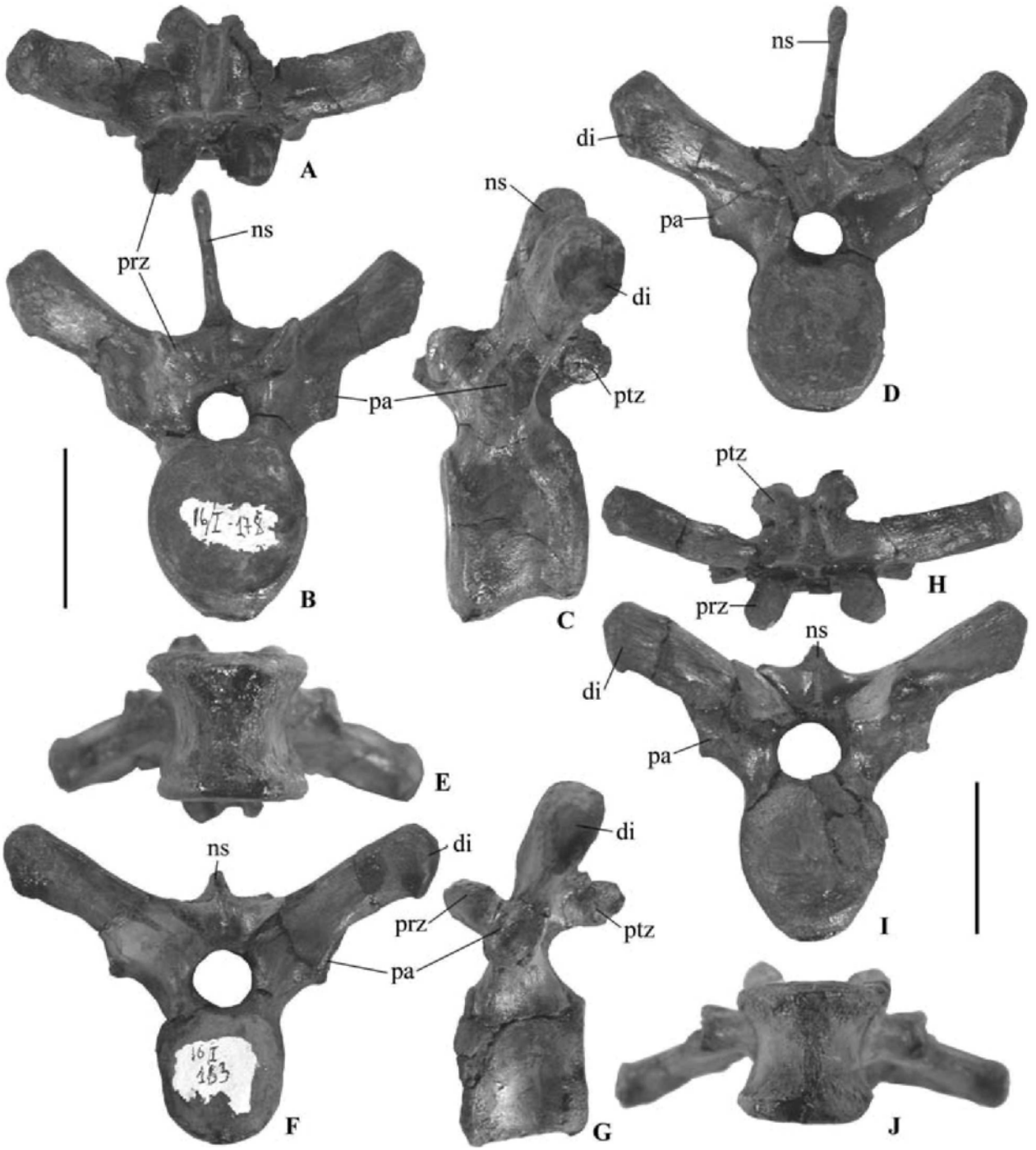

Figure 14 *Psittacosaurus sibiricus*: **A–E**, PM TGU 16/1-178, first or second dorsal in dorsal (**A**), anterior (**B**), lateral (**C**), posterior (**D**) and ventral (**E**) views; **F–J**, PM TGU 16/1-163, anterior dorsal in anterior (**F**), lateral (**G**), dorsal (**H**), posterior (**I**) and ventral (**J**) views. See the text for abbreviations. Scale bars = 3 cm.

two vertical portions by deep depressions and grooves from anterior and posterior sides. The dorsal portion is homologous with the transverse process, at least partially; the ventral part is a rib. This subdivision is less evident in the second sacral, which has the tallest sacral rib with the most expanded articulation for the ilium. This articulation is noticeably less developed in sacrals 3 and 4, but becomes larger again in sacrals 5 and 6 (Fig. 16A). Both first and second sacrals articulate with the preacetabular process of the ilium. The third sacral articulates opposite to the acetabulum. The two last sacrals articulate with the postacetabular process of the ilium. The pre- and postzygapophyses are greatly reduced and sacral neural arches are fused there. The sixth sacral has free postzygapophyses, which are almost vertically orientated. The first sacral has the neural spine (seen in PM TGU 16/4-21 and lacking in the holotype and in PM TGU 16/0-30) about half the size of that of the preceding last dorsal. In the remaining sacrals the neural spines are

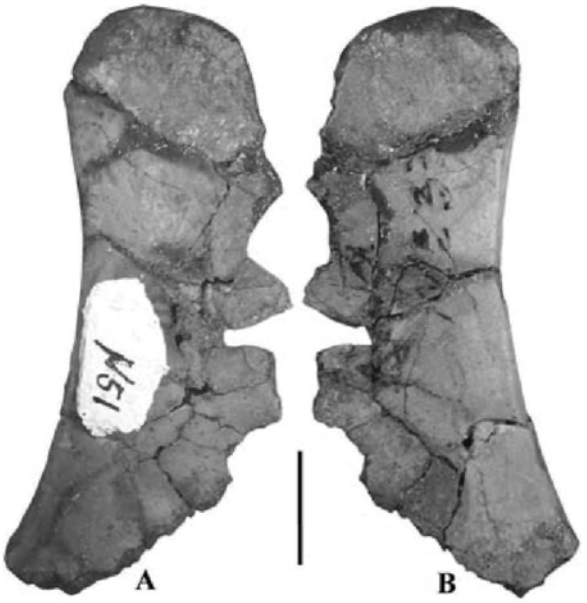

Figure 15 *Psittacosaurus sibiricus*, PM TGU 16/1-51, left(?) sternal plate in dorsal(?) (**A**) and ventral(?) (**B**) views. Anterior end is up. Scale bar = 1 cm.

rectangular, but in contrast with the dorsals, they have rounded, not straight, distal ends. They are greatly inclined posteriorly, overhanging about a half of the following vertebra.

The tail is complete in the holotype (except the last vertebra, lost in the field) and is represented by numerous isolated caudals, four articulated anteriormost caudals (PM TGU 16/0-36-39: Figs 16A & C–G), ten articulated posteriormost vertebrae (PM TGU 16/4-21) and other articulated or isolated caudals (e.g. Fig. 16H–N). The tail consists of 44 vertebrae on the holotype. The anterior caudal centra are laterally constricted, dorsoventrally compressed and with slightly concave articular surfaces and very faint ventral keels. In more posterior caudals the centra become spool-shaped with flatter, sometimes convex, articulation surfaces. The first chevron facet occurs between the second and the third caudals. The anterior caudals have relatively long and strongly posteriorly curved transverse processes (Figs 16A, C & F). In more posterior caudals the transverse processes become progressively shorter and more laterally directed and they disappear at the 22–23rd caudals. Neural spines are slightly expanded at their distal end and posterodorsally directing. The neural spines and the pre- and postzygapophyses gradually decrease in size towards the posterior end; the neural spine almost disappears posteriorly, becoming a simple rod-like projection after the 35–36th caudal, but the zygapophyses are still present in the most posterior caudals. A relatively large chevron is still present between 24th and 25th caudals in the holotype.

The majority of chevrons are obscured on the holotype, but there are some disarticulated specimens (Figs 13K–N). The anterior chevron (Figs 14K & L) has a complete bone bridge across the cleft-like haemal canal and a straight rod-like distal part with a sharp, prominent midline ridge along its posterior side. In a more posterior chevron (Figs 14M & N) the bone bridge is interrupted above the haemal canal and the distal part is more laterally compressed and anteroposteriorly expanded distally.

Numerous ossified epaxial tendons are present along the vertebral column between the transverse processes and neural spines of the first dorsal (tenth presacral) and the third caudal.

Pectoral girdle and forelimb

The scapula is preserved in both skeletons and is also represented by disarticulated fragments (Figs 17A–C). The scapular neck is constricted. The scapular blade is long, considerably expanded and thinned at the distal end and greatly curved in a frontal plane, following the contour of the rib cage. The scapular blade is distally expanded in *P. xinjiangensis*, *P. mongoliensis* and *P. meileyingensis*, but narrow in *P. sinensis* (Sereno & Chao 1988: 362–363). The anterior margin of the scapular blade is more concave than the posterior margin. The coracoid articular surface is twice as long as the glenoid. The lateral surface of the scapular shaft and acromion is concave, the medial surface is convex. The acromion projects distinctly anteriorly and articulates with the clavicle.

The coracoid is visible in one skeleton (PM TGU 16/4-21) and is represented by two disarticulated specimens (Figs 17D–G). The coracoid forms approximately half of the glenoid. An oblique crest divides the lateral surface of the coracoid into a larger anterior and a smaller posterior portion, with surfaces that meet at an angle of ~120°. The crest terminates ventrally in a prominent bump. The coracoid foramen is situated anterior to this ridge, closer to the scapular facet. There is another, smaller crest along the posterior edge of the bone. The scapular articulation surface is twice as large as the glenoid. The ventral edge of the coracoid is almost straight (broadly arched in *P. mongoliensis* and *P. meileyingensis*, sharply arched in *P. sinensis*: Sereno *et al.* 1988: 375). The medial coracoid surface is concave. There is a groove extending from the coracoid foramen dorsally towards the scapula.

The clavicle is represented by five isolated elements (Figs 17H–K). It is a rod-like vertically orientated bone with a prominent vertical ridge along the anterior side. In horizontal cross section, it is subtriangular with slightly concave anteromedial and anterolateral sides. The posterior face has a slightly convex lateral margin and a deeply convex medial margin. The dorsal larger half of the posterior side is occupied by a convex facet for the scapula. At the ventrolateral corner of this facet there is a rather big nutritient foramen. The ventral facet for the coracoid is almost flat. The opposite clavicles do not contact medially. The clavicle in *P. sibiricus* appears to be more developed than in *P. mongoliensis*, where it is thinner and contacts the scapular acromion only ventrally (Bryant & Russell 1993: fig. 3A). Clavicles have not been reported for other species of *Psittacosaurus* (supposed clavicles in *P. sinensis* (Young 1958: figs 52, 56) are displaced first ceratobranchials: Sereno 1990*b*: 585).

The humerus is not completely prepared on the skeletons but is present as isolated specimens (Figs 18A–H). The proximal and distal ends are flattened and the shaft is more round in cross section. The head is deflected medially, with a crescent-shaped articular surface (Fig. 18F). The deltopectoral crest is prominent, with a tubercle-like bump for

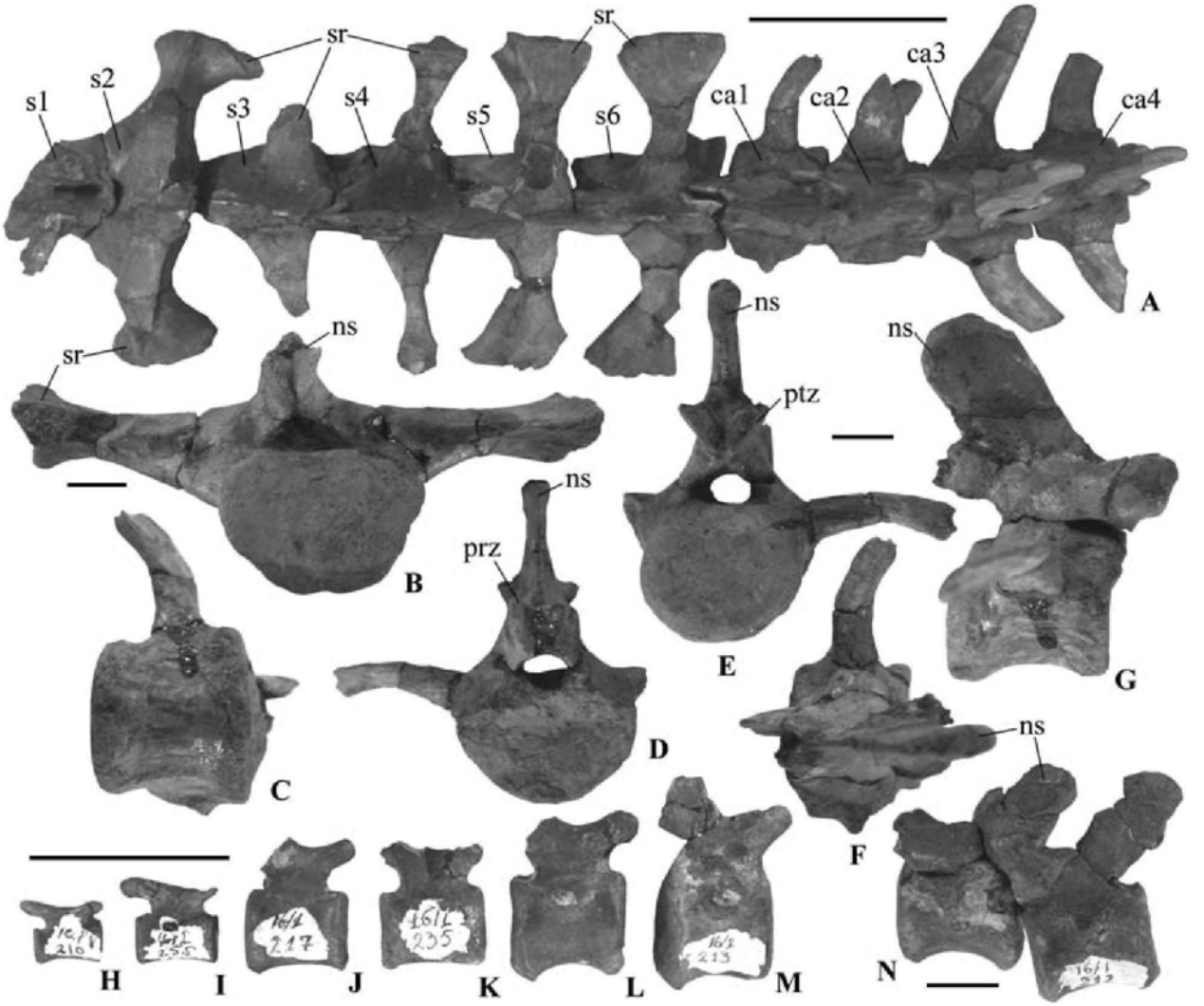

Figure 16 *Psittacosaurus sibiricus*: **A**, PM TGU 16/o-30–39, associated sacrals 1–6 and caudals 1–4 in dorsal view; **B**, PM TGU 16/o-38, sixth sacral in posterior view; **C–G**, PM TGU 16/o-39, first caudal in ventral (**C**), anterior (**D**), posterior (**E**), dorsal (**F**) and lateral (**G**) views; **H–M**, posterior caudals PM TGU 16/1-210, 16/1-255, 16/1-217, 16/1-235, 16/1-254 and 16/1-213 in lateral view; **N**, PM TGU 16/1-212, two associated posterior caudals in lateral view. See the text for abbreviations. Scale bars = 5 cm (**A**), 1 cm (**B–G**, **N**), and 3 cm (**H–M**).

insertion of *m. deltoideus*. The medial (ulnar) condyle projects further distally than the lateral (radial) condyle and is more bulbous. The lateral condyle is more expanded mediolaterally with a pointed anterolateral tip. The juvenile humerus PM TGU 16/1-84 (Figs 18G & H) is 29.7 mm long and identical in size and morphology to the juvenile psittacosaur humerus from Anda-Khuduk (Coombs 1980, 1982). From an adult humerus it differs mainly in its less developed deltopectoral crest.

The ulna (Figs 18I–N) is flattened mediolaterally, with an expanded proximal end. The olecranon process is virtually indistinct. The distal articular facet is subrectangular in outline, with its longitudinal axis rotated at ~35° to the longitudinal axis of the proximal articular surface.

The radius (Figs 18O–T) shaft is triangular in cross section and the proximal and distal ends have oval-shaped articular surfaces (more flattened proximally).

The manus is preserved in the skeletons, where it is not fully exposed, and in an isolated, incomplete specimen (Fig. 19). There are some pea-shaped bones that are evidently carpals, but their position cannot be established. Digits I–III are completely known, digit IV is represented by a partial metacarpal (Fig. 19). The metacarpals I–III are dorsoventrally flattened bones with expanded ends and ginglymoid distal articulation. Metacarpal I is 70% of the length of metacarpal II. The distal articulation of metacarpal I is obliquely set, with the medial condyle protruding more distally (Fig. 19). This results in some medial offset of the first digit. Metacarpal II is slightly shorter than metacarpal III (see Table 2). Metacarpal IV, known from its proximal end only, is more slender than metacarpals I–III. The manual phalangeal formula is 2-3-4-?-0 (2–3–4–1-0 in *P. mongoliensis*: Osborn 1923, 1924; Sereno 1990*b*). The preungular phalanges are stout and short, are markedly dorsoventrally flattened and gradually decrease in size distally. Collateral ligament pits are weakly developed and are largely exposed from the dorsal side. The unguals are elongated and claw-like. They are dorsoventrally flattened, with well developed sharp edges for supporting the horny sheaths, but with short and weak lateral grooves.

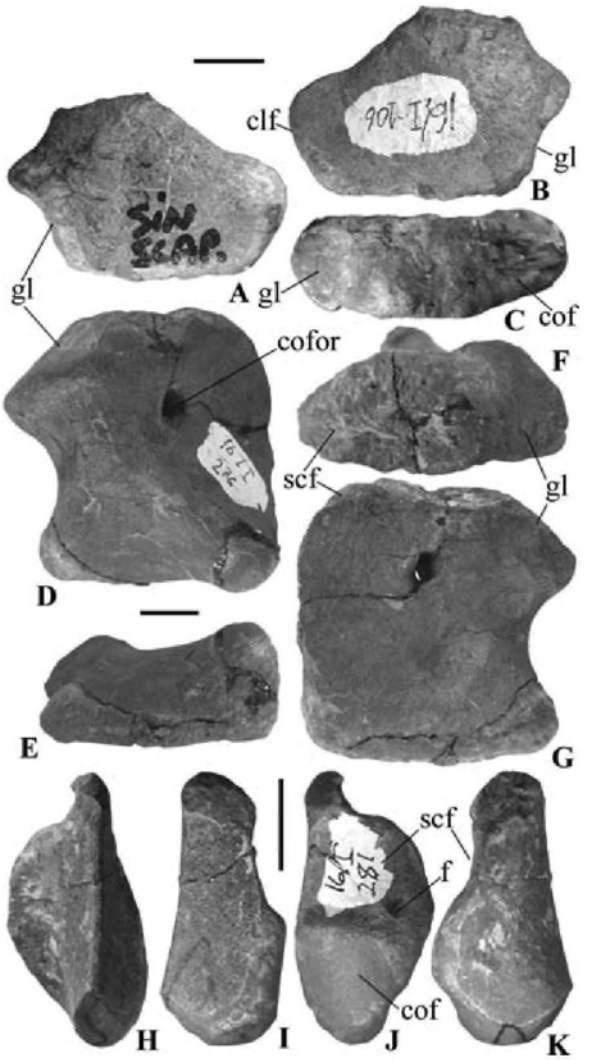

Figure 17 *Psittacosaurus sibiricus*: **A–C**, PM TGU 16/1-106, proximal end of right scapula in lateral (**A**), medial (**B**) and ventral (**C**) views; **D–G**, PM TGU 16/1-276, right coracoid in lateral (**D**), ventral (**E**), dorsal (**F**) and medial (**G**) views; **H–K**, PM TGU 16/1-281, left clavicle in anterior (**H**), lateral (**I**), posterior (**J**) and medial (**K**) views. See the text for abbreviations. Scale bars = 1 cm.

Pelvic girdle and hindlimb

The pelvic bones are known from skeletons and several isolated bones. The ilium (Figs 20A–C) is long and relatively shallow. The preacetabular and postacetabular processes are nearly equal in length, but the latter is about twice as deep as the former. The strap-like preacetabular process bears a longitudinal ridge along the medial side, giving it a triangular shape in cross section. The postacetabular process is a thin plate. The pubic peduncle is longer and more slender than the more bulbous ischiadic peduncle and is triangular in cross section.

The pubis (Figs 20D–G) has a relatively small acetabular part with concave lateral surface. There is a relatively long articular surface for the ilium anteriorly, a shorter but transversely broader and dorsolaterally facing acetabular surface at the centre and a small articular surface for the ischium posteriorly. The acetabular and articular surface for the ischium overhang a deep obturator foramen, which is not closed posteriorly (obturator notch). The prepubic process is long and dorsoventrally flattened, without the twist of the flattened plane observed in *P. xinjiangensis* (Sereno & Chao 1988: 363) and it is deflected anterolaterally. It forms an angle of ~150° with the postpubic rod. The postpubic rod is narrow and dorsoventrally flattened, with a flat or slightly concave dorsal surface and a convex ventral surface. It tapers distally quite rapidly and was apparently not very long.

The ischium (Figs 20H & I) has a long blade only slightly expanded at the end and deflected at a relatively low angle (~15°) from the shaft. The iliac peduncle has a crescent-shaped articular surface, about twice as large as that of the pubic peduncle. There is no obturator process. There is no distinct facet of the ischial symphysis. In the skeletons the ischium is not fully exposed, so its relative length compared to the femur cannot be established. However, Voronkevich (1998: 191) gave measurements of the pelvic and hind limb bones pertaining to a single, very large individual (PM TGU 16/0-1-5), which have femoral length ~210 mm and ischiadic length ~240 mm. Thus, the ischium in *P. sibiricus* is some 14% longer than the femur.

There are a number of isolated femora as well as those in the skeletons (Fig. 21). The femur is a rather stout bone with proximal and distal ends relatively less expanded compared with the robust bowed shaft. The head is confluent with the greater trochanter. The anterior (=lesser) trochanter is spine-like, but relatively large and separated from the greater trochanter by long, but shallow grooves. The fourth trochanter is large and points downward. It is situated slightly above the mid-height of the bone along its posteromedial edge. On the distal end the lateral condyle is larger than the medial condyle, with a better developed posterior ridge and bump. The flexor groove is deep. The juvenile femur PM TGU 16/1-181 is 44.5 mm long. The largest isolated femur PM TGU 16/1-271 is 167.3 mm long.

The tibia is well known from skeletons and isolated specimens (Figs 22A–E & G–K). The proximal end is anteroposteriorly expanded with a convex medial edge and a concave lateral edge. In adults the lateral condyle is almost equal to the posterior condyle in size (Fig. 22A; smaller in *P. xinjiangensis*). The proximal articular surface slants posteriorly. Ventral to the anterior condyle there is a relatively short cnemial crest, which lies adjacent to the anterior edge of the proximal end of the fibula (Figs 22C & I). The distal end is mediolaterally expanded, in a plane perpendicular to the plane of the proximal end and a twist from one plane to the other occurs on the shaft closer to the proximal end. The juvenile tibia PM TGU 16/1-115 has a 13 mm wide distal end. The largest isolated tibia, PM TGU 16/1-179, is 217.0 mm long.

The fibula (Figs 22F–I) is a thin bone with expanded and flattened proximal and distal ends twisted about 90° to each other, like the tibia. The proximal end is kidney-shaped, with a convex lateral and a concave medial surface; it is placed on the lateral side of the tibia between the cnemial crest and the lateral condyle. The distal end is attached to the anterolateral face of the distal tibia and articulates distally with the calcaneum. The distal end is expanded and rounded medially and pointed laterally.

The astragalus (Figs 22B, D, E, H, K–P) is saddle-shaped with concave dorsal and convex ventral surfaces. It is trapezoidal in dorsal/ventral view and has an incised lateral edge articulating with the calcaneum. There is not even an incipient ascending process.

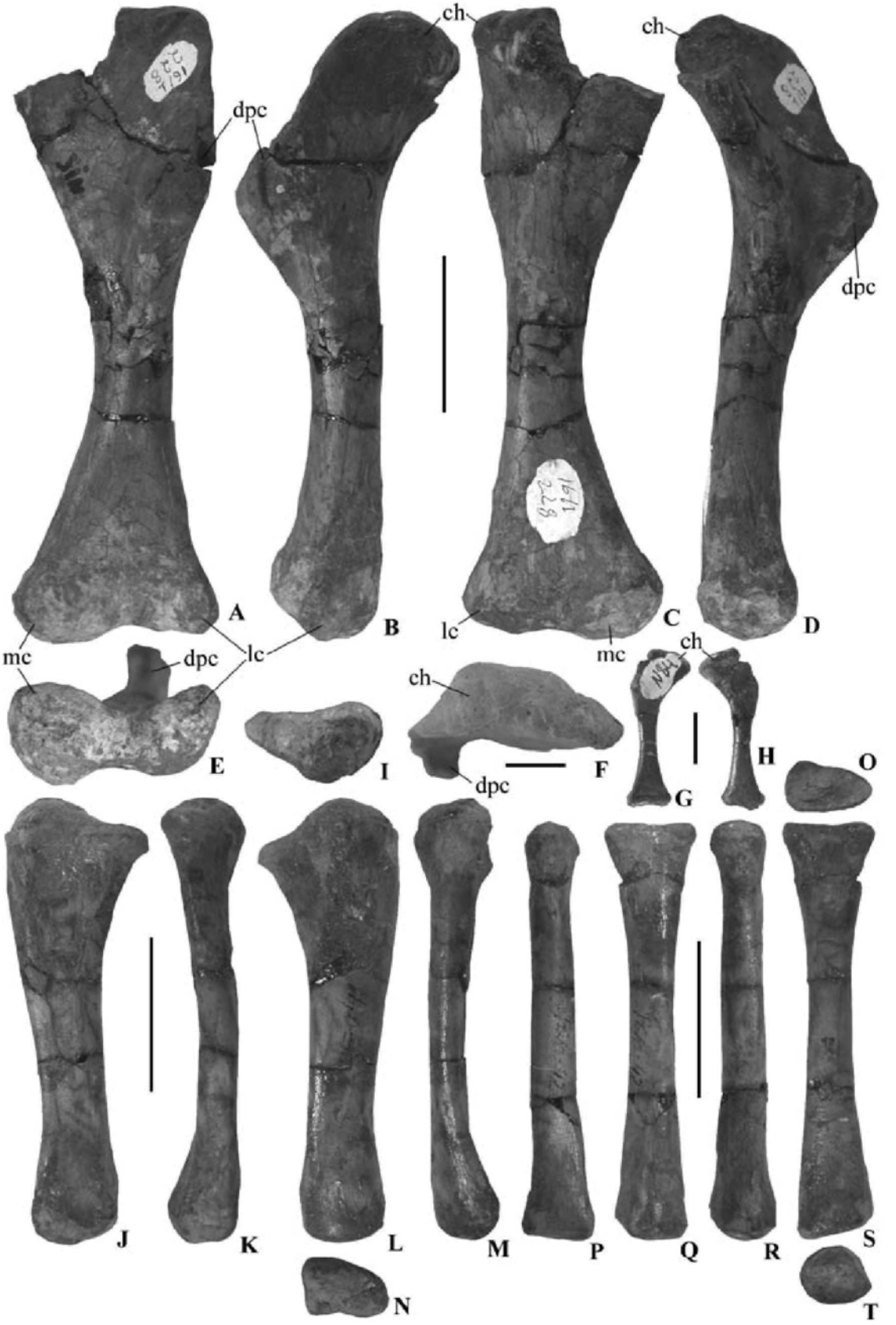

Figure 18 *Psittacosaurus sibiricus*: **A–E**, PM TGU 16/1-228, left humerus with incomplete proximal end in anterior (**A**), lateral (**B**), posterior (**C**), medial (**D**) and distal views (**E**); **F**, PM TGU 16/1-290, proximal end of right humerus in proximal view; **G**, **H**, PM TGU 16/1-84, juvenile right humerus in anterior (**G**) and posterior (**H**) views; **I–N**, PM TGU 16/0-41, left ulna in proximal (**I**), medial (**J**), anterior (**K**), lateral (**L**), posterior (**M**) and distal (**N**) views; **O–T**, PM TGU 16/0-42, left radius in proximal (**O**), anterior (**P**), lateral (**Q**), posterior (**R**), medial (**S**) and distal (**T**) views. See the text for abbreviations. Scale bars = 3 cm (**A–E**, **I–T**) and 1 cm (**F–H**).

Figure 19 *Psittacosaurus sibiricus*, PM TGU 16/1-201, incomplete left manus in anterior view. Distal carpals unidentified. See the text for abbreviations. Scale bar = 1 cm.

The calcaneum (Figs 22K & Q–U) is about the size of the astragalus and has a complex shape. The proximal surface, which articulates with the tibia, and the medial surface, which articulates with the astragalus, are flattened. The oblique lateral surface is concave and the anterior surface is convex. The ventral surface is gently convex and articulates with the lateral distal tarsal. Dorsally there is an oval-shaped concave facet for the fibula.

The pes is preserved in the skeletons and as one almost complete specimen (Fig. 23). In PM TGU 16/1-200 there is a plate-like medial distal tarsal preserved in articulation with the metatarsal III and lapping medially onto the lateral edge of metatarsal II. Its dorsal surface, articulating with the convex ventral surface of the astragalus, is also convex, which facilitates significant flexibility in the intertarsal ankle joint.

As in other psittacosaurs, metatarsal III is the longest among the metatarsals in PM TGU 16/1-200, metatarsals II and IV are of subequal length, while metatarsal I is shorter, 69% of the length of metatarsal III. However, in the holotype, which represents a larger individual, the metatarsal II is almost equal to the metatarsal III in length (see Table 2). Metatarsal IV is considerably curved laterally in contrast with the straighter metatarsals I–III. Metatarsal V is much shorter and more slender and attaches to the posterior side of the metatarsal IV (Fig. 23C). It has a pointed distal end lacking an articular surface, which indicates absence of phalanges in the fifth digit. The juvenile metatarsal I (PM TGU 16/1-116) is 22.6 mm long. The largest metatarsal I (PM TGU 16/0-47) is 89.3 mm long. The largest metatarsal III (PM TGU 16/0-50) is 93.2 mm long. The distal articulation is ginglymoid in metatarsal III and is flatter in the other metatarsals.

The pedal phalangeal formula is 2-3-4-5-0. The preungual phalanges are dorsoventrally flattened and gradually decrease in size distally. The ligament pits are weak and dorsally exposed. The unguals are claw-like, long, narrow and slightly dorsoventrally flattened. The claw grooves are well developed, in unguals of the second and fourth digits they are asymmetrical: the groove is distinctly longer on the side adjacent to the third digit.

DISCUSSION

Psittacosaurus anatomy

Antorbital fossa

In *Psittacosaurus* the antorbital fenestra is closed and the antorbital fossa is lacking (Sereno 1990*b*, 2000). Some psittacosaur species may have a secondary maxillary depression of triangular shape on the maxilla dorsal to the external maxillary rim, which is not homologous with the antorbital fossa (Sereno 1990*b*; Witmer 1997). In *P. sibiricus* there is a deep maxillary recess on the posterior portion of the maxilla between the maxillary posterior process and palatine (Fig. 4A). This recess opens externally by at least some of the row of foramina ventral to the external maxillary rim. The position of this recess on the posterior part of the maxilla above the tooth row largely corresponds to the 'intermaxillary sinus' in the basal neoceratopsians (Osmólska 1986). This recess might be a rudiment of the antorbital fossa.

Braincase

There are a number of uncertainties concerning interpretation of braincase morphology in early ceratopsians and some other ornithischians, notably the interpretations of exits for the posterior cranial nerves.

According to Brown & Schlaikjer (1940: 178) in *Protoceratops andrewsi* Granger & Gregory, 1923 there are three closely spaced lateral foramina on the exoccipital at the base of the paroccipital process (Fig. 24C): *A*, the posteriormost foramen, which enters the brain cavity 'just inside the foramen magnum', *B*, the anteriormost foramen, which enters the brain cavity in front of the exit of foramen *A*, and *C*, a foramen just ventral to *A*, which 'passes forward through the ventral portion of the exoccipital and enters the fenestra ovalis'. *A* is probably the exit for the nerve XII, *B* 'gave passage to the XI nerve' and *C* is 'undoubtedly the foramen lacerum posterius and probably transmitted the IX and X nerves' (Table 3). Later in that paper, Brown & Schlaikjer (1940: 193), however, challenged this interpretation. Because in ceratopsids, opening *B* is absent and the exits of cranial nerves X and XI are confluent, they proposed that 'since the XI is really nothing more than a branch of the X, it does not seem probable that it would first become separated [in *Protoceratops*], and later become confluent again with that nerve [in ceratopsids].' In conclusion, opening *B* might be the exit for 'a separate branch of the hypoglossal [XII] nerve.' This explanation was considered as 'more reasonable' (Brown & Schlaikjer 1940: 193). On the endocranial cast of *P. andrewsi*

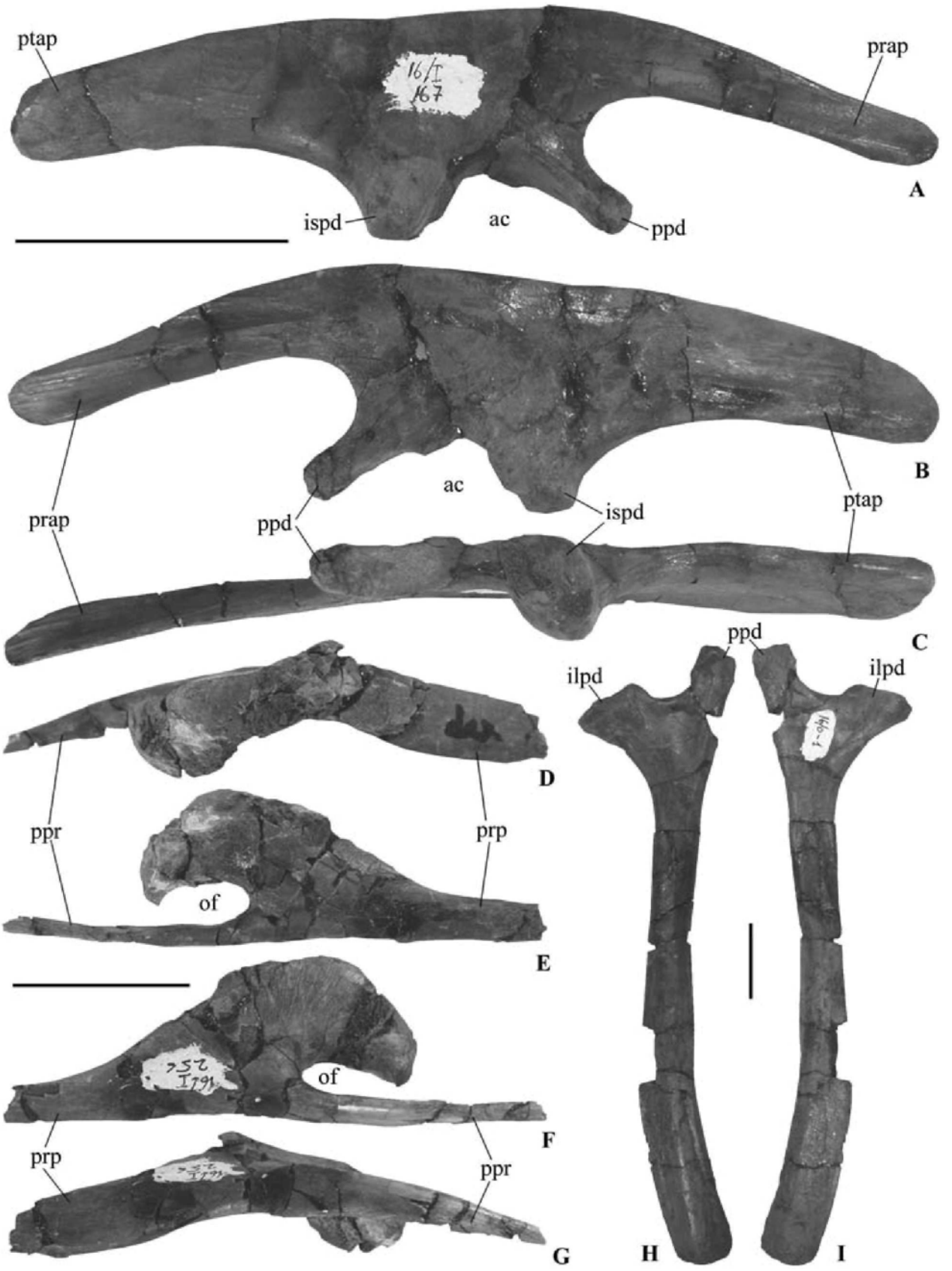

Figure 20 *Psittacosaurus sibiricus*: **A–C**, PM TGU 16/1-167, right ilium in lateral (**A**), medial (**B**) and ventral (**C**) views; **D–G**, PM TGU 16/1-256, right pubis in dorsal (**D**), lateral (**E**), medial (**F**) and ventral (**G**) views; **H, I**, PM TGU 16/0-1, left ischium in medial (**H**) and lateral (**I**) views. See the text for abbreviations. Scale bars = 5 cm (**A–C**) and 3 cm (**D–I**).

Figure 21 *Psittacosaurus sibiricus*, PM TGU 16/1-271, left femur in proximal (**A**), posterior (**B**), medial (**C**), anterior (**D**), lateral (**E**) and distal (**F**) views. See the text for abbreviations. Scale bar = 5 cm.

(Brown & Schlaikjer 1940: pl. 7) two separate branches of nerve XII were marked, albeit one with the question mark.

Maryańska & Osmólska (1975: 149–150) described three openings in the exoccipital (=exoccipital/opisthotic) of *Bagaceratops rozhdestvenskyi* Maryańska & Osmólska: *A*, a large posterior elongated foramen, *B*, a smaller foramen ventral to the former and *C*, a third foramen anterior to the *A*. Foramina *A* and *B* enter the endocranial cavity in the medulla oblongata region. Foramen *C* pierces the exoccipital laterally through the metotic strut, but opens on the posterior wall of the middle ear cavity. This pattern is very close to that in *P. sibiricus*, except in *P. sibiricus* the foramen *B* is in a more anterior position (Figs 9C & 24D). Foramen *A* was interpreted as the exit for cranial nerve XII, *B* 'probably represents the exit for cranial nerve XI' and *C* 'most probably . . . transmitted nerves IX and X [and possibly the jugular vein] from the foramen rotundum [=metotic fissure] through the middle ear cavity'. However, on their reconstruction (Maryanska & Osmólska 1975: fig. 8B) they showed the 'foramen rotundum' as confluent with the fenestra ovalis and separated from the latter by a thin bone bridge only, with a separate exit for IX ventral and posterior to it.

As can be assumed from the description by Chinnery & Weishampel (1998: 570, fig. 1) in *Montanoceratops cerorhynchus* there are three separate foramina on the exoccipital, interpreted as exits for the nerves X, XI and XII (designated by single arrow on their figure). According to the study of Makovicky (2001: 251) based on another braincase of *Montanoceratops* in this taxon there are three exoccipital lateral foramina and the nerves IX and X exited the braincase through the metotic fissure, 'but the vagus (X) nerve turned posteriorly and passed through the metotic strut to emerge through the most lateral of the three exoccipital foramina'. The two other exoccipital foramina are for the XI and XII nerves.

According to Forster (1996: 254) 'in *Psittacosaurus* and *Protoceratops*, cranial nerves X, XI, and XII each exit through a separate foramen in the exoccipital at the base of the paroccipital process' (foramina *C*, *B* and *A*, respectively). In ceratopsids 'the exit for the anteriormost branches of XII is confluent with the exit for X and XI, reducing the number of exits from three to two' (foramina *A* and *B*+*C*). This reduction of exoccipital cranial nerve foramina from three to two is often cited as a synapomorphy for Ceratopsidae (e.g. Dodson & Currie 1990; Chinnery & Weishampel 1998). Makovicky (2001: 252), refers to this synapomorphy as a 'reduction of number of hypoglossal [XII] exits from three to two' in spite of the fact that he himself interpreted in the same paper these openings in *Montanoceratops* as for X, XI and XII. Forster (1996: fig. 8) figured three roots of the hypoglossal (XII) nerve on the endocast of the *Triceratops* brain cavity. According to her interpretation (Forster 1996: 256) in *Triceratops*, cranial nerves IX, X and XI exited the brain cavity through the metotic fissure, which opens laterally into the recessus scalae tympani and the jugular foramen. The *IX*th nerve passed laterally through the recessus scalae tympani and exited behind through the foramen pseudorotunda. The nerves X and XI exited through the jugular

Table 3 Interpretation of three lateral foramina (*A–C*, see Fig. 24) for the posterior cranial nerves on the exoccipital/opisthotic in some ornithischians.

	Foramina/nerves		
References	*A*	*B*	*C*
Brown & Schlaikjer 1940	XII, or XII_2[†]	XI, or XII_1[†]	IX and X, or IX, X, and XI*
Galton 1974	XII		IX
Maryańska & Osmólska 1974	XII	X and XI	IX
Maryańska & Osmólska 1975; Dodson & Currie 1990	XII	XI	IX and X
Forster 1996; Chinnery & Weishampel 1998; Makovicky 2001	XII	XI	X
Interpretation accepted in this work	XII_3	XII_{1+2}	X and XI

[†]'more reasonable explanation' (Brown & Schlaikjer 1940: 193).

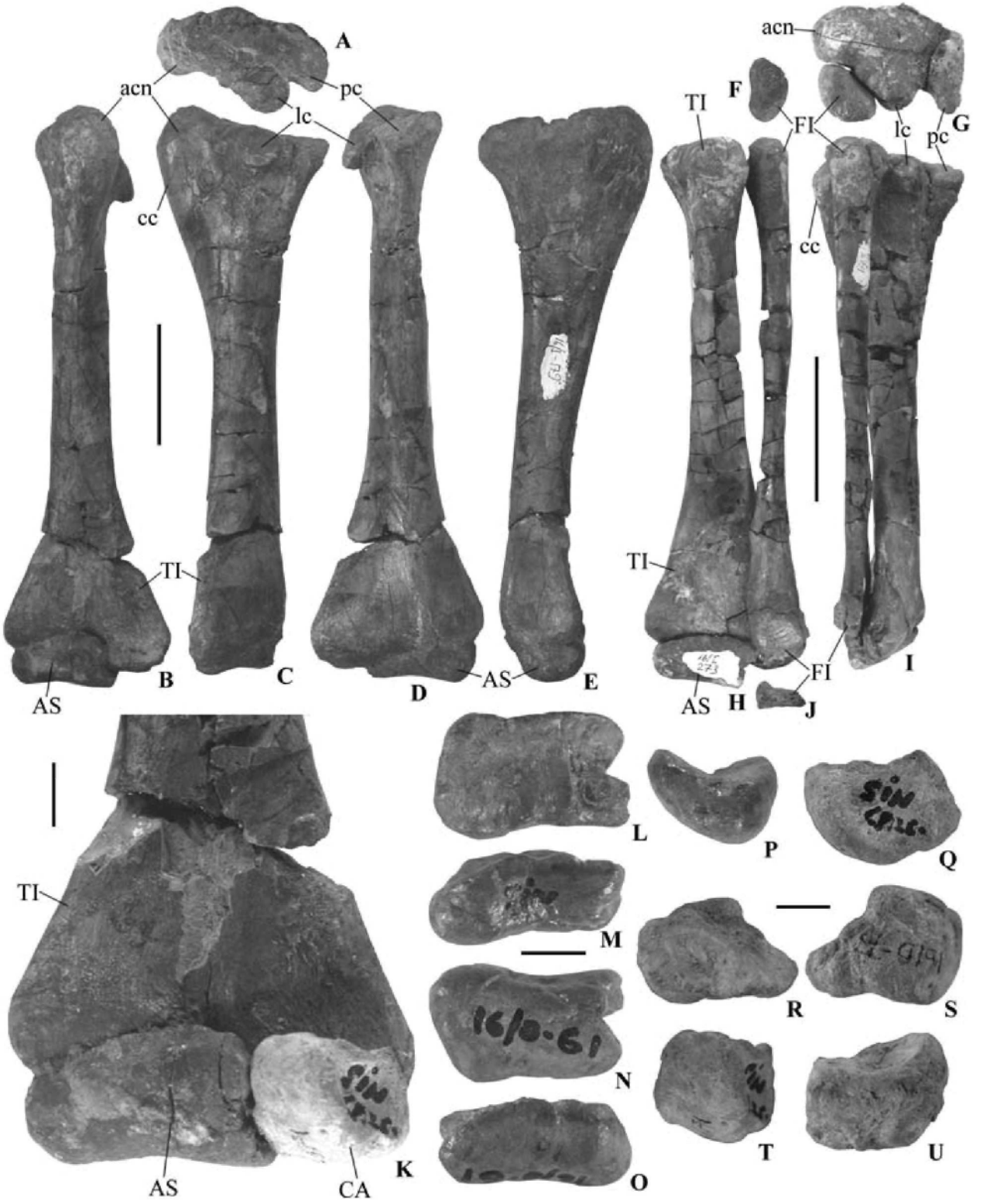

Figure 22 *Psittacosaurus sibiricus*: **A–E**, PM TGU 16/1-179, associated left tibia and astragalus in proximal (**A**), anterior (**B**), lateral (**C**), posterior (**D**) and medial (**E**) views; **F–J**, PM TGU 16/1-272–274, associated left tibia, fibula and astragalus in proximal (**F**, **G**), anterior (**H**), lateral (**I**) and distal (**J**) views; **K**, PM TGU 16/1-179, distal end of associated left tibia and astragalus and PM TGU 16/0-177, left calcaneum of similar size placed in anatomical position, in anterior view; **L–P**, PM TGU 16/0-61, left astragalus in proximal (**L**), anterior (**M**), distal (**N**), posterior (**O**) and medial (**P**) views; **Q–U**, PM TGU 16/0-77, left calcaneum in lateral (**Q**), proximal (**R**), distal (**S**), anterior (**T**) and posteromedial (**U**) views. See the text for abbreviations. Scale bars = 5 cm (**A–J**) and 1 cm (**K–U**).

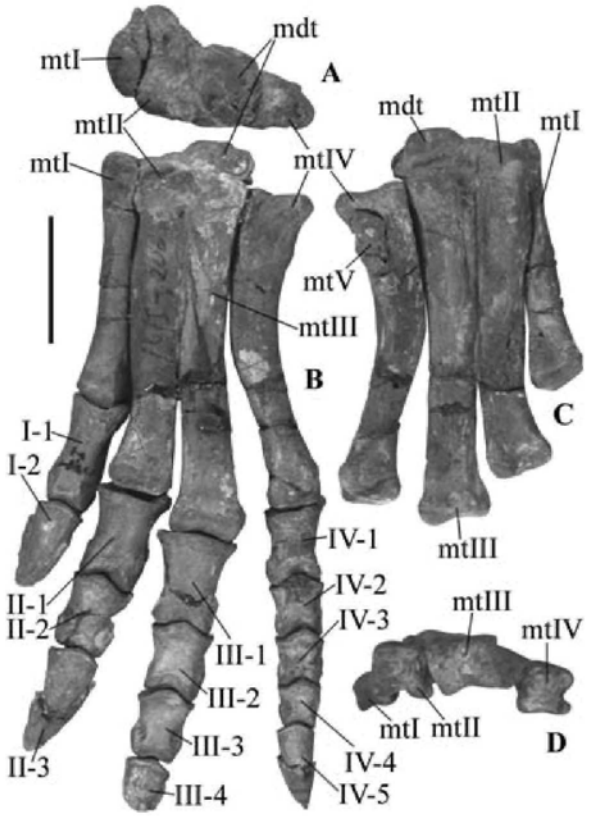

Figure 23 *Psittacosaurus sibiricus*, PM TGU 16/1-200, articulated left pes. **A**, metatarsus in proximal view; **B**, pes in anterior view; **C**, metatarsus in posterior view; **D**, metatarsus in distal view. See the text for abbreviations. Scale bar = 3 cm.

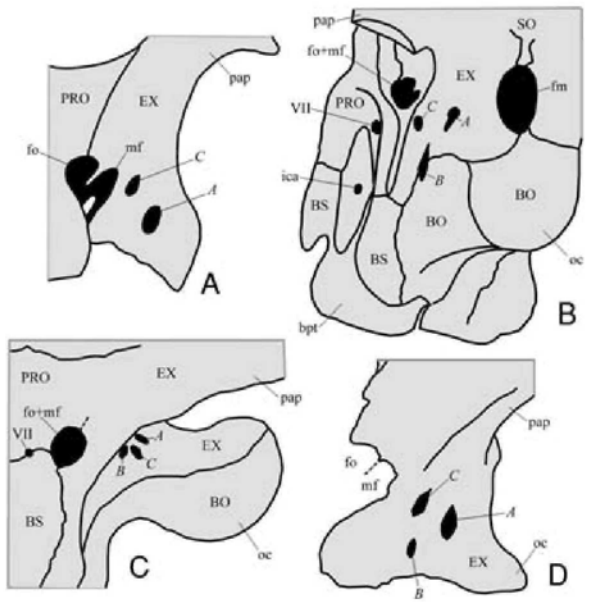

Figure 24 Braincase lateral wall (left side) in *Hypsilophodon foxii* (**A**, modified from Galton 1974), *Prenocephale prenes* (**B**, modified from Maryańska & Osmólska 1974), *Protoceratops andrewsi* (**C**, modified from Brown & Schlaikjer 1940) and *Psittacosaurus sibiricus* (**D**, PM TGU 16/1-136). Anterior is to the left. *A*, *B*, *C*, openings for posterior cranial nerves, see Table 3 and discussion in the text. See the text for abbreviations. Without scale.

(=vagus) foramen (=foramen *C*). The nerve XII exited the brain cavity through three separate openings on the medial wall of the exoccipital. The two anterior roots of this nerve join the jugular channel and exit through the jugular foramen together with the nerves X and XI (foramen *C*). The large third root of the hypoglossal nerve exited the brain cavity through the separate opening (foramen *A*).

We assume that Forster's (1996) interpretation of *Triceratops* braincase morphology, based on a rather well preserved endocast, is correct. This interpretation agrees with the pattern observed, for example, in Ankylosauria (Averianov 2002), where the nerves IX, X and XI exited through the common jugular foramen (=metotic fissure) adjacent to the fenestra ovalis and there is a trend to reduce the external exits for cranial nerve XII from three to one. The previous interpretations for the cranial nerve exits through the exoccipital in early ceratopsians, summarised in Table 3, do not agree with this pattern and appear incorrect. There are no reasons to suppose that there was a separate opening for cranial nerve XI and that all three roots of cranial nerve XII exited through the single opening (see also 'more reasonable' interpretation of this pattern in *Protoceratops* by Brown & Schlaikjer 1940 above). In the majority of vertebrates cranial nerves X and XI have a common exit through the jugular foramen (=metotic fissure) on the border between the opisthotic and the exoccipital (Romer 1997). There is, however, some confusion with the application of terms 'metotic fissure', 'jugular foramen' and 'vagus foramen'. They are all synonyms, if the IX, X and XI nerves and jugular vein exit from a single foramen just posterior to (sometimes confluent with) the fenestra ovalis (as in ankylosaurs). If X and XI exit through a separate opening posterior to the metotic strut, this opening is better called the vagus foramen and 'metotic fissure' would be synonymous with 'jugular foramen', or 'foramen pseudorotunda'. In *Psittacosaurus* an external foramen (foramen *C*) just posterior to the metotic strut would thus fit the position for the vagus foramen. Moreover, this foramen leads to the channel that opens medially on the posterior wall of the metotic fissure, as described for the 'jugular' foramen in *Triceratops* and *Montanoceratops* (Forster 1996; Makovicky 2001); 'posterior wall of the middle ear cavity' of Maryańska & Osmólska (1975) in *Bagaceratops*. The similar jugular channel, opening medially into the metotic fissure ('internal auditory meatus') and laterally at the metotic strut, was observed in the basal ornithopod *Hypsilophodon foxii* Huxley (Galton 1974: fig. 9A; Fig. 24A) and was interpreted as a passage for cranial nerve XI. More probably, it was the common passage for cranial nerves X and XI. Thus, foramen *C* is interpreted here as the vagus foramen for the exit of cranial nerves X and XI. The posteriormost of the three exoccipital foramina (foramen *A*) is undoubtedly for the largest posterior root of the hypoglossal nerve (XII_3). A small intermediate foramen *B* was most probably for the exit of two more anterior roots of the hypoglossal nerve (XII_{1+2}). If this interpretation is accepted, the condition of early ceratopsians would differ from that in derived ceratopsids only in the reduction of foramen *B* and in the passage of branches XII_{1+2} through the common foramen *C* (vagus foramen). The previous interpretations (e.g. Forster 1996) suggest more complex transformations: (1) a shift of cranial nerve XI from a separate opening (foramen *B*) to the common opening with cranial nerve X (foramen *C*) and reduction of foramen *B*; (2) shift of two anterior branches of cranial nerve XII from the common

opening with the branch XII_3 (foramen *A*) to the common opening with cranial nerves X and XI (foramen *C*).

Somewhat more problematic is the course of the IX nerve. In some vertebrates, it closely associates with cranial nerve X and exits through the common opening (Romer 1997). However, we think more likely that in *Psittacosaurus* cranial nerve IX might exit directly through the metotic fissure, as in lizards, dromaeosaurids, oviraptorosaurs, *Montanoceratops* and *Triceratops* (Oelrich 1956; Currie 1995; Forster 1996; Sues 1997; Makovicky 2001). This conclusion is based on the interpretation of a groove along the posterior wall of metotic fissure (Figs 9A & C) as an impression of the cranial nerve IX and possibly the jugular vein.

Xu (1997: 51, fig. 2) published the first description and reconstruction of a psittacosaur basicranium, based on *P. mazongshanensis*. However, his interpretation requires some comment. Xu described the basal tubera, two-thirds of which are formed by the basioccipital and one third by the basisphenoid (almost equally by these two bones in *P. sibiricus*). But on his reconstruction, the basal tubera are incorrectly labelled as 'basipterygoid'. It is evident that on that specimen, most of the anterior part of the basisphenoid and the parasphenoid are missing and a bone described and labelled by him as 'parasphenoid' is the prootic. The orientation of the occipital condyle as being almost parallel to the basal tubera seems unlikely and was possibly caused by post-mortem deformation. Xu described three separate foramina for the exits of cranial nerves X, XI and XII but figured only two foramina with a common exit for cranial nerves X and XI situated ventral to the exit for cranial nerve XII. If the ventral orientation of the occipital condyle on the figured specimen is taken into account, his foramen for cranial nerve XII would be posterior to the common foramen for cranial nerves X and XI. This interpretation of the exoccipital cranial nerve openings, presented on the Xu's figure (but not in his text), is close to our interpretation (see above).

Brinkman *et al.* (2001: 1782, fig. 2C, D) described a basicranium fragment of *P. xinjiangensis* interpreted as a "basioccipital-basisphenoid fragment" with two cranial nerve foramina lateral to the occipital condyle. Evidently this fragment also includes fused basal parts of the exoccipital through which the posterior cranial nerves make their exit in *P. sibiricus* and other reptiles (Romer 1997; see above). The foramina were interpreted as exits for cranial nerves IX–X and XI with reference to Xu's (1997) reconstruction. However, Xu (1997: fig. 2) showed two foramina in this region of the exoccipital/opisthotic for the exits of cranial nerves X–XI and XII, which agrees with our interpretation (see above). It should be noted here that a third foramen on exoccipital/opisthotic in *Psittacosaurus* (foramen *B* on Fig. 24D) is rather small and can easily be overlooked if filled by matrix or in case of inadequate preservation. This may be the reason for interpretation of only two cranial nerve foramina in the exoccipital of some *Psittacosaurus* specimens.

Occipital condyle

According to Xu (1997: 51) in *P. mazongshanensis* the occipital condyle is formed exclusively by the basioccipital. However, it is more likely that in the adult specimen the basioccipital/exoccipital suture is obliterated and the condyle is formed by the basioccipital and the exoccipitals, as in other psittacosaurs and the majority of dinosaurs. In *P. xinjiangensis* (Sereno & Chao 1988: 357) the basioccipital contribution to the border of the foramen magnum is equal to that of exoccipitals and the supraoccipital. Similarly, a large basioccipital contribution to the foramen magnum may also be present in *P. mongoliensis* and *P. meileyingensis* (Osborn 1923: fig. 2D; Sereno *et al.* 1988: fig. 2B). In *P. sibiricus* the basioccipital forms only a very narrow portion of the ventral floor of the foramen magnum and the neurocranial cavity. This is possibly a derived condition, as in the neoceratopsians in which the basioccipital is completely excluded from the foramen magnum by the exoccipitals, which may form up to two-thirds of the occipital condyle (Brown & Schlaikjer 1940; Currie 1997*a*).

Cervicals

In neoceratopsians the first three cervicals coalesce to form a syncervical (Dodson & Currie 1990; Penkalski & Dodson 1999; anon. reviewer, pers. comm.). In *Psittacosaurus* the anterior cervicals do not coalesce, but cervicals 2 (axis) and 3 are consolidated by the hypertrophied axis neural arch, which completely covers the third cervical neural arch. This might be a preadaptation toward the neoceratopsian derived condition.

Clavicles

Ossified clavicles are present in *Psittacosaurus* and a few basal neoceratopsians. In *Psittacosaurus* the clavicle is a short, rod-like, structure lying along the anterior margin of the scapula and coracoid at their junction and not contacting the opposite clavicle medially. Such a clavicle is characteristic also for *Protoceratops* (Brown & Schlaikjer 1940), but not for *Montanoceratops*, where the clavicles are slim, flat, S-shaped bones contacting the end of the scapula and coracoid laterally and, by the medial end, each other (Chinnery & Weishampel 1998). In *Leptoceratops gracilis* Brown the clavicles also contact each other medially, but have a unique boot-like shape and contact only the coracoid (Sternberg 1951). The function of clavicles in *Psittacosaurus* is not clear.

Phylogenetic relationships within *Psittacosaurus*

The first phylogenetic analysis of *Psittacosaurus* species was presented by Russell & Zhao (1996). This analysis was followed by Xu (1997), who added some new characters. However, the coding of psittacosaur species by Xu differs from that of Russell & Zhao and his tables 1 (character descriptions) and 2 (character distribution) do not correspond completely to each other. For example, there are two derived states (1 and 2) for character 17 in his table 2 and only one derived state for this character in his table 1. In our analysis we used some characters that were modified from Russell & Zhao (1996; designated 'RZ') and Xu (1997; designated 'X'), but coded all taxa ourselves according to the original descriptions. Basal ornithopods *Heterodontosaurus tucki* Crompton & Charig from the Early Jurassic of South Africa and *Hypsilophodon foxii* Huxley from the Early Cretaceous of Europe, as well as a basal neoceratopsian *Protoceratops andrewsi* Granger & Gregory from the Late Cretaceous of Mongolia, are used in the analysis as outgroup taxa. Morphological characters for these taxa were scored from Galton (1974), Brown & Schlaikjer (1940), Dodson & Currie (1990), Weishampel & Witmer (1990) and Norman *et al.* (2004). Appendix 2 lists the characters scored for this phylogenetic analysis.

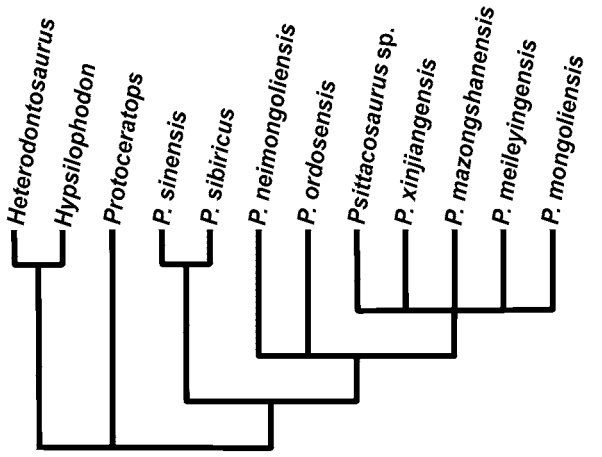

Figure 25 A strict consensus cladogram from seven trees produced by exhaustive search of data matrix present in Appendix 3. *Psittacosaurus* sp. is from the Yixian Formation, China (Xu & Wang 1998; Mayr *et al.* 2002).

The data matrix (Appendix 3) was analysed using the exhaustive search algorithm of PAUP 4.0b10 (Swofford 1993). Seven most parsimonious trees were found with tree length (TL) = 58, Consistency Index (CI) = 0.54, Retention Index (RI) = 0.58, Rescaled Consistency Index (RC) = 0.31. A strict consensus tree is shown in Fig. 25. The analysis recognises within *Psittacosaurus* a divergence between clade *P. sinensis* + remaining species and polytomy of *P. neimongoliensis*, *P. ordosensis* and a clade consisting of *Psittacosaurus* sp., *P. xinjiangensis*, *P. mazongshanensis*, *P. meileyingensis* and *P. mongoliensis*.

The first discussion of psittacosaurid interrelationships can be found in Sereno (1990*a*, *b*) and Sereno & Chao (1988). At that time few derived characters were known that were distributed in more than one, but not in all, psittacosaurid species. Sereno (1990*b*: 591) cited only one potential synapomorphy favouring a subgroup of psittacosaurid species: the prominent, laterally projecting jugal horn (*P. sinensis* + *P. xinjiangensis*). In our analysis this is one of the most homoplastic characters with a CI = 0.36 and grouping of *P. sinensis* and *P. xinjiangensis* is not supported. This is not surprising, because this character is ontogenetically controlled and possibly sexually correlated (Xu 1997).

The analyses of Russell & Zhao (1996) and Xu (1997) differ in a number of details from each other and from our analysis; in part due to different species sampling and rooting (they used *Lesothosaurus* or *Chaoyangsaurus* as the outgroup, respectively). Areas of congruence include grouping of *P. ordosensis* and *P. neimongoliensis* by Russell & Zhao (1996) and in six of seven trees in our analysis, and of *P. mongoliensis*, *P. xinjiangensis* and *P. mazongshanensis* by Xu (1997) and in our analysis.

PSITTACOSAURUS PALAEOECOLOGY AND BIOLOGY

The slicing psittacosaur dentition with self-sharpening, cutting edges is clearly suitable for processing of plant material (Sereno 1990*b*, 1997). Abundant gastroliths, often associated with *Psittacosaurus* skeletons (Sereno 1990*b*, 1997; Xu 1997; Mayr *et al.* 2002; PM TGU 16/4-21) are also indicative of a herbivorous diet.

In the proportions of the fore- and hindlimbs *Psittacosaurus* is similar to presumed cursorial ornithopods and probably was facultatively bipedal (Rozhdestvensky 1955*b*; Sereno 1990*b*, 1997).

Almost universally psittacosaurs were considered as terrestrial animals (Osborn 1923, 1924; Young 1958; Sereno 1990*b*, 1997). Only Rozhdestvensky (1955*a*, *b*), Suslov (1983) and Currie (1997*b*) considered *Psittacosaurus* as an aquatic, or amphibiotic animal. Most *Psittacosaurus* localities are lacustrine deposits, which leave little doubt that these animals lived close to water. *Psittacosaurus* localities are especially abundant around two great Early Cretaceous lakes in northern China: Qingyang Lake on the modern Ordos Plateau and a lake in Junggar Basin (Chen 1987: fig. 1). Around these lakes a peculiar ecosystem was formed, whose main elements were psittacosaurs and dsungaripterid pterosaurs (Dong 1992, 1994). Suslov (1983) studied the taphonomy of *Psittacosaurus* in the lacustrine deposits of the Khamryn-Us locality in Mongolia and suggested that their much better preservation, compared with that of theropods, sauropods and ankylosaurs, could be explained by the fact that they lived very close to or in the lake.

The skin of *Psittacosaurus* was covered by large, round cone-like scales separated by numerous small polygonal and tubercle-like scales (Mayr *et al.* 2002). Osborn (1923: fig. 2B, E) described 'epidermal ossifications' in the holotype skull of *P. mongoliensis*. Sereno (1990*b*: 589) interpreted these knob-like structures as sedimentary artefacts. However, they may be impressions of the large cone-like scales.

Psittacosaurus had precocial, self-feeding juveniles as evident from tooth wear and well-ossified limb bones in very small post-hatching individuals (Coombs 1980, 1982).

GEOLOGICAL AGE OF *PSITTACOSAURUS* FAUNAS

Psittacosaurus is the most characteristic member of a distinctive Early Cretaceous Asiatic vertebrate fauna, sometimes called the *Psittacosaurus* fauna (biochron). Although the Early Cretaceous age for this fauna has long been appreciated, its temporal range has been interpreted differently: as first half of 'Neocomian' (Rozhdestvensky 1971, 1974, 1977), Aptian–Albian (Sereno 1990*b*, 1997), Valanginian–Albian (Russell & Zhao 1996), Barremian–early Albian (Lucas & Estep 1998), Barremian–early Aptian (Sereno 2000).

There are two factors that hampered the study of the stratigraphic distribution of *Psittacosaurus*: the well known problem of age determination for continental Mesozoic deposits in Central Asia and inadequate documentation of this taxon in some local faunas. For the majority of localities it was only cited in faunal lists without description of material, or indication upon which material this determination was made. The latter is crucially important, because the reliable determination of *Psittacosaurus* can be based on cranial material only. The *Psittacosaurus* postcranium is 'remarkably

primitive compared to most other Cretaceous ornithischians' (Sereno 2000: 486–487) and most of the postcranial elements can easily be confused with those of contemporary hypsilophodontids or basal neoceratopsians. Isolated psittacosaur teeth, however, are quite distinctive and may safely indicate the presence of this taxon in the fauna, but they are not diagnostic at the species level.

There are very few *Psittacosaurus* localities for which any meaningful biostratigraphic or radiometric data are known.

At Sihetun and other localities around Beipiao city in Liaoning Province, China, the Yixian Formation, producing remains of *Psittacosaurus* sp., is Hauterivian–Barremian according to radiometric dating (Swisher *et al.* 1999, 2002; Zhou *et al.* 2003).

The Tebch basalt in Inner Mongolia Autonomous Region, China, overlying deposits with *P. mongoliensis* [=*P. osborni*, =*P. tingi*], was dated by radiometric analysis as 110 Ma, which is early Albian (Eberth *et al.* 1994). Combined palynological and invertebrate evidence points to a Barremian–early Aptian age for the fossil bed at Tebch (Eberth *et al.* 1994).

The Doushan Formation in the upper part of Qingshan Group in Shandong Province, China, with type localities of *P. sinensis* and *P. 'youngi'*, was radiometrically dated as 119–121 Ma. This time interval is within the Aptian, according to Harland *et al.* (1989), not Barremian, as was thought by Gao & Cheng (1999) with reference to the same stratigraphic charts.

There is some palynological evidence for an Albian age for the Lower Xinminbao Formation of Xinminbao Group at Mazongshan area in Gansu Province, China, producing remains of *P. mazongshanensis* (Tang *et al.* 2001).

The Tujingzi Formation in Hebei Province, China, with several skeletons of *Psittacosaurus* sp., is dated as early Albian by pollen (Gan & Zhang 1985).

For the Khuren Dukh locality of *P. mongoliensis* in Mongolia there are some palaeomagnetic and palynological data suggesting middle–late Albian age (Hicks *et al.* 1999).

In conclusion, the age of the *Psittacosaurus* biochron may be currently roughly estimated as Hauterivian–Albian.

ACKNOWLEDGEMENTS

We express our sincere thanks to Professor V. M. Podobina, the director of the Siberian Paleontological Scientific Centre and to Professor G. M. Tatyanin, the dean of the Geologic and Geographic Faculty of the Tomsk State University, for their invaluable help in the organisation of the field work and permanent support of our investigations. We are grateful to two anonymous reviewers for reading the manuscript, their useful comments and linguistic corrections. We thank A. S. Rezvyi for help with studying the material and preparing some of the specimens, Professor H. Osmólska for help with the literature and Professor J. D. Archibald for help with the PAUP program. The work of A.A., including three visits to Tomsk, was financially supported by the Russian Fund of Basic Research (RFBR) grant 00-15-99355, the Tomsk State University, the PalSIRP (Paleontological Society International Research Program) – Sepkoski grants project RXO-1337(1) and by the Russian Science Support Foundation.

REFERENCES

Alifanov, V. R., Efimov, M. B., Novikov, I. V. & Morales, M. 1999. A new psittacosaur complex of tetrapods from the Lower Cretaceous Shestakovo locality (southern Siberia). *Doklady Akademii Nauk* **369**: 491–493. [In Russian]

Averianov, A. O. 2002. An ankylosaurid (Ornithischia: Ankylosauria) braincase from the Upper Cretaceous Bissekty Formation of Uzbekistan. *Bulletin de l'Institut Royal des Sciences Naturelles de Belgique, Sciences de la Terre* **72**: 97–110.

— **& Skutschas, P. P.** 2000. A vertebrate assemblage from the Early Cretaceous of Transbaikalia (locality Mogoito). Pp. 357–358 *in* A. V. Komarov (ed.) *Materials of the regional conference of the geologists of Siberia, Far East and North East of Russia*. GalaPress: Tomsk. [In Russian]

—, **Voronkevich, A. V., Maschenko, E. N., Leshchinskiy, S. V. & Fayngertz, A. V.** 2002. A sauropod foot from the Early Cretaceous of Western Siberia, Russia. *Acta Palaeontologica Polonica* **47**: 117–124.

—, **Leshchinskiy, S. V., Fayngertz, A. V., Skutschas, P. P. & Rezvyi, A. S.** 2003*a*. A new complex of Early Cretaceous vertebrates of Western Siberia (Krasnoyarsk Territory). Pp. 106–108 *in State and problems of the geological investigation of the entrails of the earth and development of the mineral resources base of Krasnoyarsk Territory. Materials of reports of the scientific practical conference devoted to the 60th anniversary of the Krasnoyarsk geology (1943–2003), October 7–10, 2003*. Izdatel'stvo KNIIGiMS: Krasnoyarsk. [In Russian]

—, **Starkov, A. I. & Skutschas, P. P.** 2003*b*. Dinosaurs from the Early Cretaceous Murtoi Formation in Buryatia, Eastern Russia. *Journal of Vertebrate Paleontology* **23**: 586–594.

Brinkman, D. B., Eberth, D. A., Ryan, M. J. & Chen, P.-J. 2001. The occurrence of *Psittacosaurus xinjiangensis* Sereno and Chow, 1988 in the Urho area, Junggar Basin, Xinjiang, People's Republic of China. *Canadian Journal of Earth Sciences* **38**: 1781–1786.

Brown, B. & Schlaikjer, E. M. 1940. The structure and relationships of *Protoceratops*. *Annals of the New York Academy of Sciences* **40**: 133–266.

Bryant, H. N. & Russell, A. P. 1993. The occurrence of clavicles within Dinosauria: implications for the homology of the avian furcula and the utility of negative evidence. *Journal of Vertebrate Paleontology* **13**: 171–184.

Buffetaut, E. 2001. Tantalizing glimpse of a vanishing dinosaur. *Nature* **414**: 147.

— **& Suteethorn, V.** 1992. A new species of the ornithischian dinosaur *Psittacosaurus* from the Early Cretaceous of Thailand. *Palaeontology* **35**: 801–812.

— **&** — 2002. Remarks on *Psittacosaurus sattayaraki* Buffetaut & Suteethorn, 1992, a ceratopsian dinosaur from the Lower Cretaceous of Thailand. *Oryctos* **4**: 71–73.

—, **Sattayarak, N. & Suteethorn, V.** 1989. A psittacosaurid dinosaur from the Cretaceous of Thailand and its implications for the palaeogeographical history of Asia. *Terra Nova* **1**: 370–373.

Bulynnikova, A. A. & Trushkova, L. Y. 1967. Continental Cretaceous deposits of eastern and central parts of the Western Siberian lowland. Pp. 40–46 *in* G. G. Martinson (ed.) *Stratigraphy and palaeontology of Mesozoic and Palaeogene–Neogene continental deposits of the Asiatic part of the USSR*. Nauka: Leningrad. [In Russian]

Chao, S. 1962. New species of *Psittacosaurus* from Laiyang, Shantung. *Vertebrata PalAsiatica* **6**: 349–360.

Chen, P.-J. 1987. Cretaceous paleogeography in China. *Palaeogeography, Palaeoclimatology, Palaeoecology* **59**: 49–56.

Cheng, Z.-W. 1983. Reptilia. Part 7. Pp. 123–136 *in The Mesozoic stratigraphy and paleontology of Guyang coal-bearing basin, Nei Mongol Autonomous Region, China*. Geology Press: Beijing.

Chinnery, B. J. & Weishampel, D. B. 1998. *Montanoceratops cerorhynchus* (Dinosauria: Ceratopsia) and relationships among basal neoceratopsians. *Journal of Vertebrate Paleontology* **18**: 569–585.

—, Lipka, T. R., Kirkland, J. I., Parrish, J. M. & Brett-Surman, M. K. 1998. Neoceratopsian teeth from the Lower to middle Cretaceous of North America. *Bulletin of the New Mexico Museum of Natural History and Science* **14**: 297–302.

Colbert, E. H. 1945. The hyoid bones in *Protoceratops* and in *Psittacosaurus*. *American Museum Novitates* **1301**: 1–10.

Coombs, W. P., Jr. 1980. Juvenile ceratopsians from Mongolia – the smallest known dinosaur specimens. *Nature* **283**: 380–381.

— 1982. Juvenile specimens of the ornithischian dinosaur *Psittacosaurus*. *Palaeontology* **25**: 89–107.

Currie, P. J. 1995. New information on the anatomy and relationships of *Dromaeosaurus albertensis* (Dinosauria: Theropoda). *Journal of Vertebrate Paleontology* **15**: 576–591.

— 1997*a*. Braincase anatomy. Pp. 81–85 in P. J. Currie & K. Padian (eds) *Encyclopedia of dinosaurs*. Academic Press: San-Diego, London.

— 1997*b*. Gastroliths. Pp. 270 in P. J. Currie & K. Padian (eds) *Encyclopedia of dinosaurs*. Academic Press: San-Diego, London.

Dodson, P. & Currie, P. J. 1990. Neoceratopsia. Pp. 593–618 in D. B. Weishampel, P. Dodson & H. Osmólska (eds) *The Dinosauria*. University of California Press: Berkeley.

Dong, Z.-M. 1992. *Dinosaurian faunas of China*. China Ocean Press & Springer-Verlag: Beijing & Berlin; 188 pp.

— 1994. Early Cretaceous dinosaur faunas in China: an introduction. *Canadian Journal of Earth Sciences* **30**: 2096–2100.

Eberth, D. A., Russell, D. A., Braman, D. R. & Deino, A. L. 1994. The age of the dinosaur bearing sediments at Tebch, Inner Mongolia, People's Republic of China. *Canadian Journal of Earth Sciences* **30**: 2101–2106.

Erickson, G. M. & Tumanova, T. A. 2000. Growth curve of *Psittacosaurus mongoliensis* (Ceratopsia: Psittacosauridae) inferred from long bone histology. *Zoological Journal of the Linnean Society* **130**: 551–566.

Forster, C. A. 1996. New information on the skull of *Triceratops*. *Journal of Vertebrate Paleontology* **16**: 246–258.

Galton, P. M. 1974. The ornithischian dinosaur *Hypsilophodon* from the Wealden of the Isle of Wight. *Bulletin of the British Museum of Natural History (Geology)* **25**: 1–152.

Gan, Z.-B. & Zhang, C.-Y. 1985. Early Cretaceous palynology in northern Hebei. *Acta Palaeontologica Sinica* **24**: 558–567.

Gao, K. & Cheng, Z.-W. 1999. A new lizard from the Lower Cretaceous of Shandong, China. *Journal of Vertebrate Paleontology* **19**: 456–465.

Harland, W. B., Armstrong, R. L., Cox, A. V., Craig, L. E., Smith, A. G. & Smith, D. G. 1989. *A geologic time scale*. Cambridge University Press: Cambridge; 263 pp.

Hicks, J. F., Brinkman, D. L., Nichols, D. L. & Watabe, M. 1999. Palaeomagnetic and palynologic analyses of Albian to Santonian strata at Bayn Shireh, Burkhant, and Khuren Dukh, eastern Gobi Desert, Mongolia. *Cretaceous Research* **20**: 829–850.

Hopson, J. A. 1979. Paleoneurology. Pp. 39–146 in C. A. Gans, R. G. Northcutt & P. Ulinsky (eds) *Biology of the Reptilia, Volume 9: Neurology A*. Academic Press: London.

Ji, S.-A. & Bo, H.-C. 1998. Discovery of the psittacosaurid skin impressions and its significance. *Geological Review* **44**: 603–606.

Kielan-Jaworowska, Z., Novacek, M. J., Trofimov, B. A. & Dashzeveg, D. 2000. Mammals from the Mesozoic of Mongolia. Pp. 573–626 *in* M. J. Benton, M. A. Shishkin, D. M. Unwin & E. N. Kurochkin (eds) *The age of dinosaurs in Russia and Mongolia*. Cambridge University Press: Cambridge.

Kurzanov, S. M. 1976. Structure of the braincase of carnosaur *Itemirus* gen. nov. and some questions of dinosaur cranial anatomy. *Paleontologicheskii Zhurnal* **3**: 127–137. [In Russian]

Leshchinskiy, S. V., Voronkevich, A. V., Fayngertz, A. V. & Schikhovtzeva, L. G. 1997. Some aspects of taphonomy and stratigraphic position of the localities of the Shestakovo complex of Early Cretaceous vertebrates. Pp. 83–90 *in* V. M. Podobina (ed.) *Questions of geology and palaeontology of Siberia*. Tomskii Gosudarstvennyi Universitet: Tomsk. [In Russian]

—, Fayngertz, A. V., Voronkevich, A. V., Maschenko, E. N. & Averianov, A. O. 2000. Preliminary results of the investigation of the Shestakovo localities of Early Cretaceous vertebrates. Pp. 363–366 *in* A. V. Komarov (ed.) *Materials of the regional conference of the geologists of Siberia, Far East and North East of Russia*. GalaPress: Tomsk. [In Russian]

—, Voronkevich, A. V., Fayngertz, A. V., Maschenko, E. N., Lopatin, A. V. & Averianov, A. O. 2001. Early Cretaceous vertebrate locality Shestakovo, Western Siberia, Russia: a refugium for Jurassic relicts? *Journal of Vertebrate Paleontology* **21**: 73A.

—, Averianov, A. O., Fayngertz, A. V., Skutschas, P. P. & Rezvyi, A. S. 2003. New locality of Early Cretaceous mammals in Western Siberia. *Doklady Akademii Nauk* **391**: 426–429. [In Russian]

Lucas, S. G. & Estep, J. W. 1998. Vertebrate biostratigraphy and biochronology of the Cretaceous of China. *Bulletin of the New Mexico Museum of Natural History and Science* **14**:1–20.

Makovicky, P. J. 2001. A *Montanoceratops cerorhynchus* (Dinosauria: Ceratopsia) braincase from the Horseshoe Canyon Formation of Alberta. Pp. 243–262 *in* D. H. Tanke & K. Carpenter (eds) *Mesozoic vertebrate life*. Indiana University Press: Bloomington and Indianapolis.

Manabe, M. & Hasegawa, Y. 1991. The Cretaceous dinosaur fauna of Japan. Pp. 41–42 *in* Z. Kielan-Jaworowska, N. Heintz & H.-A. Nakrem (eds) *Fifth symposium on Mesozoic terrestrial ecosystems and biota. Extended abstracts*. Contributions from the Paleontological Museum, University of Oslo volume 364.

Marsh, O. C. 1890. Additional characters of the Ceratopsidae with notice of new Cretaceous dinosaurs. *American Journal of Science, Series 3* **39**: 418–426.

Maryańska, T. & Osmólska, H. 1974. Pachycephalosauria, a new suborder of ornitischian dinosaurs. *Palaeontologia Polonica* **30**: 45–102.

— **&** — 1975. Protoceratopsidae (Dinosauria) of Asia. *Palaeontologia Polonica* **33**: 133–182.

Maschenko, E. N. & Lopatin, A. V. 1998. First record of an Early Cretaceous triconodont mammal in Siberia. *Bulletin de l'Institut Royal des Sciences Naturelles de Belgique, Sciences de la Terre* **68**: 233–236.

Mayr, G., Peters, D. S., Plodowski, G. & Vogel, O. 2002. Bristle-like integumentary structures at the tail of the horned dinosaur *Psittacosaurus*. *Naturwissenschaften* **89**: 361–365.

Nessov, L. A. 1995. *Dinosaurs of Northern Eurasia: New data about assemblages, ecology and paleobiogeography*. Izdatel'stvo Sankt-Peterburgskogo Universiteta: St. Petersburg; 156 pp. [In Russian]

Norman, D. B., Sues, H.-D., Witmer, L. M. & Coria, R. A. 2004. Basal Ornithopoda. Pp. 393–437 *in* D. B. Weishampel, P. Dodson & H. Osmólska (eds) *The Dinosauria. Second Edition*. University of California Press: Berkeley.

Oelrich, T. M. 1956. The anatomy of the head of *Ctenosaura pectinata* (Iguanidae). *Miscellaneous Publications, Museum of Zoology, University of Michigan* **94**: 1–122.

Osborn, H. F. 1923. Two Lower Cretaceous dinosaurs from Mongolia. *American Museum Novitates* **95**: 1–10.

— 1924. *Psittacosaurus* and *Protiguandon*: Two Lower Cretaceous iguanodonts from Mongolia. *American Museum Novitates* **127**: 1–16.

Osmólska, H. 1986. Structure of nasal and oral cavities in the protoceratopsid dinosaurs (Ceratopsia, Ornithischia). *Acta Palaeontologica Polonica* **31**: 145–157.

Penkalski, P. & Dodson, P. 1999. The morphology and systematics of *Avaceratops*, a primitive horned dinosaur from the Judith River Formation (Late Campanian) of Montana, with the description of a second skull. *Journal of Vertebrate Paleontology* **19**: 692–711.

Romer, A. S. 1997. *Osteology of the reptiles*. Krieger Publishing Company: Malabar, FL; xxvii+772 pp.

Rozhdestvensky, A. K. 1955*a*. The first discovery of a dinosaur in the USSR in the indigenous locality. *Byuleten' Moskovskogo Obschestva Ispytatelei Prirody, Otdel Geologicheskii* **30**: 118. [In Russian]

— 1955*b*. New data on psittacosaurs – Cretaceous ornithopods. Pp. 783–788 *in Questions on the geology of Asia, Volume 2*. Izdatel'stvo Akademii Nauk SSSR: Moscow. [In Russian]
— 1960. Locality of Lower Cretaceous dinosaurs in Kuzbass. *Paleontologicheskii Zhurnal* **2**: 165. [In Russian]
— 1971. Study of dinosaurs of Mongolia and their role in biostratigraphy of the continental Mesozoic. *Trudy Sovmestnoi Sovetsko-Mongol'skoi Nauchno-Issledovatel'skoi Geologicheskoi Ekspeditsii* **3**: 21–32. [In Russian]
— 1973. Study of Cretaceous reptiles in Russia. *Paleontologicheskii Zhurnal* **2**: 90–99. [In Russian]
— 1974. History of dinosaur faunas in Asia and other continents and questions of paleogeography. *Trudy Sovmestnoi Sovetsko-Mongol'skoi Paleontologicheskoi Ekspeditsii* **1**: 107–131. [In Russian]
— 1977. The study of dinosaurs in Asia. *Journal of the Palaeontological Society of India* **20**: 102–119.
Rozhdestvensky, A. K. & Khozatsky, L. I. 1967. Late Mesozoic terrestrial vertebrates of Asiatic part of the USSR. Pp. 82–92 *in* G. G. Martinson (ed) *Stratigraphy and paleontology of Mesozoic and Palaeogene-Neogene continental deposits of Asiatic part of the USSR*. Nauka: Leningrad. [In Russian]
Russell, D. A. & Zhao, X.-J. 1996. New psittacosaur occurrences in Inner Mongolia. *Canadian Journal of Earth Sciences* **33**: 637–648.
Ryan, M. J. & Currie, P. J. 1998. First report of protoceratopsians (Neoceratopsia) from the Late Cretaceous Judith River Group, Alberta, Canada. *Canadian Journal of Earth Sciences* **35**: 820–826.
Seeley, H. G. 1888. The classification of the Dinosauria. *Report of the British Association for Advancement of Science* **1887**: 689–699.
Sereno, P. C. 1990*a*. New data on parrot-beaked dinosaurs (*Psittacosaurus*). Pp. 203–210 *in* K. Carpenter & P. J. Currie (eds) *Dinosaur systematics. Approaches and perspectives*. Cambridge University Press: Cambridge.
— 1990*b*. Psittacosauridae. Pp. 579–592 *in* D. B. Weishampel, P. Dodson & H. Osmólska (eds) *The Dinosauria*. University of California Press: Berkeley.
— 1997. Psittacosauridae. Pp. 611–613 *in* P. J. Currie & K. Padian (eds) *Encyclopedia of dinosaurs*. Academic Press: San-Diego.
— 2000. The fossil record, systematics and evolution of pachycephalosaurs and ceratopsians from Asia. Pp. 480–516 *in* M. J. Benton, M. A. Shishkin, D. M. Unwin & E. N. Kurochkin (eds) *The age of dinosaurs in Russia and Mongolia*. Cambridge University Press: Cambridge.
— **& Chao, S.** 1988. *Psittacosaurus xinjiangensis* (Ornithischia: Ceratopsia), a new psittacosaur from the Lower Cretaceous of northwestern China. *Journal of Vertebrate Paleontology* **8**: 353–365.
—, —, **Cheng, Z.-W. & Rao, C.** 1988. *Psittacosaurus meileyingensis* (Ornithischia: Ceratopsia), a new psittacosaur from the Lower Cretaceous of northeastern China. *Journal of Vertebrate Paleontology* **8**: 366–377.
Sternberg, C. M. 1951. Complete skeleton of *Leptoceratops gracilis* Brown from the Upper Edmonton member on the Red Deer River, Alberta. *Bulletin of the National Museum of Canada* **123**: 225–255.
Sues, H.-D. 1997. On *Chirostenotes*, a Late Cretaceous oviraptorosaur (Dinosauria: Theropoda) from western North America. *Journal of Vertebrate Paleontology* **17**: 698–716.
Suslov, Y. V. 1983. The burial of psittacosaurs at Khamryn-Us (Eastern Gobi, MPR). *Trudy Sovmestnoi Sovetsko-Mongol'skoi Paleontologicheskoi Ekspeditsii* **24**: 118–120. [In Russian]
Swisher, C. C., III, Wang, Y.-Q., Wang, X., Xu, X. & Wang, Y. 1999. Cretaceous age for the feathered dinosaurs of Liaoning, China. *Nature* **398**: 58–61.
—, **Wang, X., Zhou, Z., Wang, Y., Jin, F., Zhang, J., Xu, X., Zhang, F. & Wang, Y.** 2002. Further support for a Cretaceous age for the feathered-dinosaur beds of Liaoning, China: New 40Ar/39Ar dating of the Yixian and Tuchengzi Formations. *Chinese Science Bulletin* **47**: 135–138.
Swofford, D. L. 1993. *PAUP: Phylogenetic analysis using parsimony, version 3.1.1*. Natural History Society: Champaign, IL.
Tang, F., Luo, Z.-X., Zhou, Z., You, H., Georgi, J. A., Tang, Z.-L. & Wang, X.-Z. 2001. Biostratigraphy and palaeoenvironment of the dinosaur-bearing sediments in Lower Cretaceous of Mazongshan area, Gansu Province, China. *Cretaceous Research* **22**: 115–129.
Tatarinov, L. P. & Maschenko, E. N. 1999. A find of an aberrant tritylodont (Reptilia, Cynodontia) in the Lower Cretaceous of Kemerovo Region. *Paleontologicheskii Zhurnal* **4**: 85–92. [In Russian]
Voronkevich, A. V. 1998. A large representative of the genus *Psittacosaurus* from the locality Shestakovo – 3. Pp. 190–193 *in* I. A. Vyltsan (ed.) *Actual Questions of the Geology and Geography of Siberia. Materials of the Scientific Conference*. Tomskii Gosudarstvennyi Universitet: Tomsk. [In Russian]
Weishampel, D. B. 1990. Dinosaurian distribution. Pp. 63–140 *in* D. B. Weishampel, P. Dodson & H. Osmólska (eds) *The Dinosauria*. University of California Press: Berkeley.
— **& Witmer, L. M.** 1990. Heterodontosauridae. Pp. 486–497 *in* D. B. Weishampel, P. Dodson & H. Osmólska (eds) *The Dinosauria*. University of California Press: Berkeley.
Witmer, L. M. 1997. The evolution of the antorbital cavity of archosaurs: a study in soft-tissue reconstruction in the fossil record with an analysis of the function of pneumaticity. *Journal of Vertebrate Paleontology* **17** (Supplement 1): 1–73.
Xu, X. 1997. A new psittacosaur (*Psittacosaurus mazongshanensis* sp. nov.) from Mazongshan Area, Gansu Province, China. Pp. 68–89 *in* Z.-M. Dong (ed.) *Sino-Japanese silk road dinosaur expedition*. China Ocean Press: Beijing.
— **& Wang, X.** 1998. New psittacosaur (Ornithischia, Ceratopsia) occurrence from the Yixian Formation of Liaoning, China and its stratigraphical significance. *Vertebrata PalAsiatica* **36**: 147–158.
—, **Makovicky, P. J., Wang, X., Norell, M. A. & You, H.** 2002. A ceratopsian dinosaur from China and the early evolution of Ceratopsia. *Nature* **416**: 314–317.
Young, C. C. 1931. On some new dinosaurs from western Suiyan, Inner Mongolia. *Bulletin of the Geological Survey of China* **11**: 159–226.
— 1958. The dinosaurian remains of Laiyang, Shantung. *Palaeontologia Sinica, New Series C* **16** (142): 1–138.
Zhou, Z., Barrett, P. M. & Hilton, J. 2003. An exceptionally preserved Lower Cretaceous ecosystem. *Nature* **421**: 807–814.

APPENDIX 1: LIST OF REFERRED SPECIMENS

All specimens from Shestakovo 3, PM TGU collection: **16/4-21**, nearly complete articulated adult skeleton with the skull, buried together with the holotype, possibly female; **16/1-216**, fragmentary rostral; **16/1-294**, right nasal; **16/1-245**, fragmentary left nasal; **16/1-207**, left premaxilla; **16/1-133**, juvenile right premaxilla; **16/1-204**, right premaxilla and **16/1-206**, right maxilla from a single individual; **16/1-46**, fragmentary right premaxilla and **16/1-73**, right maxilla from a single individual; **16/1-284**, left maxilla; **16/1-283**, fused parietals; **16/1-166** and **16/1-285**, left postorbitals; **16/0-10** and **16/1-58**, right postorbitals; **16/0-12** and **16/0-13**, left jugal horns; **16/1-292** and **16/1-293**, fragmentary juvenile left and right jugals; **16/1-17**, left palpebral; **16/0-14**, **16/1-13**, **16/1-48** and **16/1-211**, right palpebrals; **16/1-202**, left quadrate; **16/1-258**, right quadrate; **16/0-19**, left quadrate condyle; **16/1-135**, fragmentary left juvenile quadrate; **16/1-92** and **16/1-107**, left pterygoids; **16/1-173**, right pterygoid; **16/0-16**, fragmentary right pterygoid; **16/1-44**, left palatine fragment; **16/1-297**, right palatine fragment; **16/1-79**, left ectopterygoid **16/0-17**, fragmentary left pterygoid articulated with the quadrate pterygoid ramus, **16/0-18**, left ectopterygoid and **16/0-15**, fused basioccipital and basisphenoid from a single individual; **16/0-21**, basioccipital; **16/1-136**, left exoccipital/opisthotic; **16/1-264**, right exoccipital/opisthotic; **16/1-286** and **16/1-287**, fragmentary

left exoccipital/opisthotic; **16/1-104** and **16/1-288**, fragmentary right exoccipital/opisthotic; **16/1-56**, **16/1-85** and **16/1-174**, left dentaries; **16/0-20**, **16/1-175** and **16/1-203**, right dentaries; **16/1-291**, fragmentary right dentary; **16/1-176** and **16/1-246**, fragmentary left angulars; **16/1-137**, fragmentary right angular; **16/1-177** and **16/3–30–34**, isolated teeth; **16/0-22**, atlas intercentrum, **16/0-23**, axis and **16/0-24–27**, cervicals 3–6 from a single individual; **16/1-230**, atlas intercentrum; **16/1-42** and **16/1-153**, axis neural arches; **16/1-209**, 16/1-232 and **16/1-233**, cervicals; **16/1-22**, **16/1-26**, **16/1-43**, **16/1-89**, **16/1-151** and **16/1-227**, **16/1-289**, cervical ribs; **16/1-163**, **16/1-178** and **16/1-183**, anterior dorsals; **16/0-28** and **16/0-29**, articulated posterior dorsals; **16/1-45**, **16/1-72**, **16/1-74**, **16/1-76**, **16/1-94**, **16/1-215**, **16/1-231** and **16/1-234**, neural arches of posterior dorsals; **16/1-19**, **16/1-22**, **16/1-25**, **16/1-27**, **16/1-33**, **16/1-36**, **16/1-41**, **16/1-109**, **16/1-111**, **16/1-138**, **16/1-243**, **16/1-260** and **16/1-278**, dorsal ribs (double-headed); **16/1-23** and **16/1-60**, dorsal ribs (single-headed); **16/1-51**, sternal plate; **16/0-30–39**, articulated series from the first sacral (fragmentary) towards fourth caudal; **16/1-49**, **16/1-63** and **16/1-154**, sacral ribs; **16/1-28**, **16/1-30**, **16/1-31**, **16/1-50**, **16/1-77**, **16/1-95**, **16/1-143**, **16/1-145**, **16/1-210**, **16/1-213**, **16/1-214**, **16/1-217**, **16/1-235**, **16/1-254** and **16/1-255**, caudals; **16/1-212**, two associated caudals; **16/1-208**, three associated caudals; **16/1-18**, **16/1-20**, **16/1-21**, **16/1-112**, **16/1-117**, **16/1-164**, **16/1-168**, **16/1-169**, **16/1-170**, **16/1-182**, **16/1-248**, **16/1-249**, **16/1-250**, **16/1-251**, **16/1-252** and **16/1-253**, caudal centra; **16/1-29**, **16/1-102**, **16/1-103**, **16/1-105**, **16/1-152**, **16/1-259**, caudal neural arches; **16/1-11**, **16/1-220**, **16/1-223** and **16/1-225**, chevrons; **16/1-106**, right scapula proximal fragment; **16/1-129**, fragmentary right scapula; **16/0-14** and **16/0-75**, fragmentary scapular blades; **16/1-158** and **16/1-276**, right coracoids; **16/1-281**, **16/1-295** and **16/1-127**, left clavicles; **16/1-296**, right clavicle; **16/1-282**, fragmentary right clavicle; **16/0-64**, left humerus, **16/0-41**, left ulna and **16/0-42**, left radius from a single individual; **16/1-228**, left humerus; **16/1-247**, right humerus; **16/0-76**, left humerus distal end; **16/1-290**, right humerus proximal end; **16/0-71**, right humerus distal end; **16/1-84**, juvenile right humerus; **16/-82**, juvenile right humerus distal end; **16/1-47**, **16/1-52** and **16/0-40**, right ulnae; **16/0-7** and **16/1-277**, right radius; **16/1-201**, almost complete left manus lacking; **16/1-279**, incomplete right manus; **16/0-2**, fragmentary left ilium, **16/0-3**, fragmentary right ilium and **16/0-1**, left ischium from a single large individual described by Voronkevich (1998); **16/1-167**, right ilium; **16/1-34** and **16/1-256**, right pubes; **16/1-257**, left pubis; **16/1-270**, left ischium; **16/0-79**, fragmentary right ischium; **16/0-62**, **16/0-65** and **16/1-271**, left femora; **16/0-55** and **16/0-66**, right femur proximal ends; **16/0-56**, left femur distal end; **16/0-54**, right femur distal end; **16/1-181**, juvenile left femur; **16/1-272**, **16/1-273** and **16/1-274**, associated left tibia, astragalus and fibula; **16/1-179**, articulated left tibia and astragalus; **16/0-68**, articulated right tibia and fibula distal ends and right astragalus; **16/0-69** and **16/0-70** left tibia proximal ends; **16/0-67** and **16/0-73**, left tibia distal ends; **16/0-63** and **16/0-72**, right tibia distal ends; **16/1-83**, **16/1-115** and **16/1-126**, juvenile left tibia distal ends; **16/1-287**, left fibula lacking distal end; **16/0-61**, left astragalus; **16/1-171**, fragmentary left astragalus; **16/0-77** and **16/1-275**, left calcanei; **16/0-78**, right calcaneum; **16/1-200**, articulated left pes; **16/0-47** and **16/0-57**, right metatarsals I; **16/0-52**, left metatarsal I distal end; **16/0-49**, right metatarsal I distal end; **16/1-116**, juvenile left metatarsal I; **16/0-46**, right metatarsal II; **16/0-48**, **16/0-50**, **16/1-5** and **16/1-146**, left metatarsals III; **16/1-261**, right metatarsal III lacking proximal end; **16/1-37**, left metatarsal IV; **16/1-40**, right metatarsal IV; **16/0-43** and **16/0-51**, left metatarsal IV proximal ends; **16/0-44**, right metatarsal IV proximal end; **16/0-45**, right metatarsal IV distal end; and numerous less important isolated vertebrae, ribs, chevrons, teeth, phalanges, metapodials and bone fragments.

APPENDIX 2: CHARACTER DESCRIPTIONS

Characters modified from Russell & Zhao (1996) are designated 'RZ'. Characters modified from Xu (1997) are designated 'X'. Consistency Index (CI) is given for the seven most parsimonious trees.

1. Preorbital segment more than 40% of skull length (0), less than 40% (1). CI = 1.00.
2. Skull profile rectangular (0), rounded (1) [RZ 1; X 1; modified]. CI = 0.33.
3. Skull width less than skull length (0), exceeds skull length (1) [X 9, modified]. CI = 1.00.
4. Rostral absent (0), present (1). CI = 1.00.
5. Nasal does not extend ventrally beyond the external naris (0), extends ventrally (1). CI = 1.00.
6. Ventral border of external naris is ventral to the dorsal end of maxilla (0), dorsal to the maxillary dorsal end (1). CI = 1.00.
7. Posterolateral process of premaxilla narrow (0), expanded (1). CI = 1.00.
8. Premaxillary teeth absent (0), present (1). CI = 1.00.
9. Premaxilla–lacrimal contact absent (0), present (1). CI = 1.00.
10. Premaxilla does not contact jugal posteriorly (0), contacts jugal (1). CI = 1.00.
11. Ventral margin of premaxilla–maxilla contact incised (0), straight (1). CI = 0.33.
12. Antorbital fenestra present (0), absent (1). CI = 1.00.
13. Secondary maxillary depression (='antorbital fossa' in Russell & Zhao (1996) and Xu (1997)) absent (0), present (1) [RZ 2; X 2; modified]. A shallow 'antorbital fossa' has been described for some *Psittacosaurus* species, such as *P. xinjiangensis* and *P. meileyingensis* (Sereno & Chao 1988; Sereno *et al.* 1988). Here only *P. mongoliensis* and *P. mazongshanensis*, who have distinctly delimited and deep triangular fossae, are coded as having the derived state of this character. CI = 0.36.
14. 'Maxillary process' of maxilla lacking (0), present (1) [X 11, modified]. CI = 1.00.
15. Ventral postorbital horn absent (0), present (1). CI = 1.00.
16. Pyramidal, laterally projecting jugal horn absent (0), present (1) [RZ 8; X 4]. *Psittacosaurus* sp. from the Yixian Formation is scored here with the derived state for this character. The specimen described by Xu & Wang (1998) has a weakly developed jugal horn and may be immature (this is evident also from the lack of fusion between the cranial bones, which are dissociated in a slightly macerated skeleton). In the specimen described by Mayr *et al.* (2002) the jugal horn is strongly developed. CI = 0.36.

17. Anterior ramus of squamosal does not extend as far as the anterior wall of the supratemporal fenestra (0), extends to anterior wall (1) [RZ 7]. CI = 0.50.
18. Parietal–squamosal frill absent (0), present (1). CI = 1.00.
19. Quadrate shaft moderately arched in lateral view and its posterior margin gently excavated (0), strongly arched with posterior margin deeply excavated (1) [RZ 9; X 5; modified]. CI = 0.50.
20. External mandibular fenestra present (0), absent (1) [RZ 10; X 6]. CI = 0.36.
21. Lateral surface of the mandible laterally bowed (0), straight (1) [X 16]. CI = 1.00.
22. Ventral flange on dentary absent (0), present (1) [RZ 11; X 7]. CI = 0.25.
23. Maxillary and dentary tooth rows laterally concave (0), straight (1) [X 14, modified]. CI = 0.50.
24. Primary ridge on maxillary teeth weakly developed or absent (0), well developed (1). CI = 0.25.
25. Primary ridge on maxillary teeth vertical (0), posteroventrally angled (1) [RZ 12; X 8]. CI = 0.40.
26. Denticle number on maxillary teeth less than 14 (0), equal to or more than 14 (1) [X 12]. The number of denticles in *Psittacosaurus* species may vary considerably with tooth size, position in the jaw and, possibly, with ontogenetic age. The largest count for maxillary teeth has been reported for *P. xinjiangensis* and *P. mazongshanensis* (Sereno & Chao 1988; Xu 1997). However, according to Brinkman *et al.* (2001) the range of variation in denticle number in *P. xinjiangensis* is wider than was thought before. CI = 0.71.
27. Nine or more cervicals (0), eight cervicals (1). CI = 1.00.
28. Ossified epaxial tendons do not span the sacral region (0), extend posteriorly to the anterior caudals at least (1). CI = 0.25.
29. Acromion process on scapula well developed (0), small (1). CI = 1.00.
30. Ischium distinctly longer than femur (0), shorter than or approximately equal to femur (1). CI = 0.50.
31. Length of metatarsal I less than 70% that of metatarsal III (0), equal to or more than 70% (1) [RZ 13, modified]. CI = 0.33.

Appendix 3: Data matrix

Species	Characters																													
	1	2	3	4	5	6	7	8	9	10	11	12	13	14	15	16	17	18	19	20	21	22	23	24	25	26	27	28	29	30	31
Heterodontosaurus tucki	0	0	0	0	0	0	0	0	0	0	0	0	0	0	0	1	0	0	0	0	0	0	0	1	0	0	0	0	0	0	0
Hypsilophodon foxii	0	0	0	0	0	0	0	0	0	0	0	0	0	0	0	0	0	0	0	1	0	0	0	0	0	0	0	1	0	0	0
Protoceratops andrewsi	0	0	0	1	0	0	1	0	0	0	1	1	1	0	0	1	0	1	0	1	0	1	1	1	0	0	0	0	0	0	0
P. mongoliensis	1	0	0	1	1	1	1	1	1	0	0	1	1	1	0	0	1	1	0	0	1	1	1	0	1	0	1	1	0	1	1
P. sinensis	1	1	1	1	1	1	1	1	1	1	0	1	0	0	1	1	1	1	1	1	0	0	0	0	0	0	0	0	1	1	0
P. meileyingensis	1	1	0	1	1	1	1	1	1	0	0	1	0	1	0	0	1	1	1	0	1	1	1	1	1	0	?	0	0	?	0
P. xinjiangensis	?	?	?	?	?	?	?	?	?	?	?	1	0	1	0	1	1	1	0	?	?	0	1	0	1	1	?	1	0	?	?
P. neimongoliensis	1	1	0	1	1	1	1	1	1	0	1	1	0	0	0	0	0	1	0	1	1	0	?	?	0	0	1	1	0	0	1
P. ordosensis	1	1	?	1	1	1	1	1	1	?	0	1	?	0	?	1	?	1	0	0	?	1	1	?	0	0	?	?	?	?	1
P. mazongshanensis	1	0	0	1	1	1	1	1	?	0	?	1	1	1	0	1	?	1	0	?	1	1	1	1	0	1	?	?	0	?	?
P. sibiricus	1	0	1	1	1	1	1	1	1	1	1	1	0	0	1	1	1	1	1	1	0	1	0	0	1	0	0	1	0	0	1
Psittacosaurus sp.†	?	?	?	?	1	?	1	1	?	?	?	1	0	?	?	1	?	1	0	?	?	1	?	0	0	0	?	1	0	1	0

†from Yixian Formation, China (Xu & Wang 1998; Mayr *et al.* 2002).